S.E.M. STEREOPAIR STUDY OF MARMOSET ORAL MICROVASCULATURE: USING CORROSION CASTS TO ASSESS THE GINGIVAL AND PDL VESSELS

A PROJECT SUBMITTED IN PARTIAL FULFILMENT OF THE REQUIREMENT FOR THE DEGREE OF MASTER OF DENTAL SURGERY

BY

CHRISTOPHER MARK STANLEY

Bachelor of Dental Surgery (The University of Adelaide)
Bachelor of Science in Dentistry (Honours)
(The University of Adelaide)
Graduate Diploma in Health Administration
(South Australian Institute of Technology)

DEPARTMENT OF DENTISTRY
THE UNIVERSITY OF ADELAIDE
SOUTH AUSTRALIA

1991 - 1993

TABLE OF CONTENTS

Page

Page

Page

LIST OF FIGURES

FIGURE SUBJECT Page

LIST OF TABLES

SUMMARY

The three-dimensional microvasculature of the marmoset PDL and gingival tissues is still imperfectly understood. Most studies in the past have been limited to two-dimensional histologic or TEM studies. The resolution of the SEM combined with stereopair recording of corrosion casts provides for three-dimensional interpretation of these structures.

The primate has been used in this study as a substitute for the human model. It is considered to provide an analogue to human dental structures anatomically and in function (**LEVY**, 1971; **WILSON** and **GARDNER**, 1982).

The aims of the current study were to record the normal microvasculature of the oral structures including the PDL in the cotton ear marmoset (*Callithrix jacchus*) using corrosion casts. The microvasculature was assessed using the imprint patterns described by **HODDE et al.** (1977), **HODDE** and **NOWELL** (1980), and **MIODINSKI et al.** (1981); the vessel diameters and branching patterns as described by **RHODIN** (1967, 1968); and the description of arterioles and venules as suggested by **LEE** (1988).

Eight female cotton ear marmosets had previously been perfused with methyl methacrylate through cannulated carotid arteries by **LEE** (1988). There were four mature animals (4-7 yrs) and 4 young animals (18-24 mths). The hard and soft tissues of the jaws were then dissolved away leaving a replica of the microvascular system.

The unexamined anterior segments were used for the current study. The surface microvasculature was recorded in the SEM using steropairs. Once this was completed, individual casts with SEM stubs still present were immersed in small containers of double distilled water. Entrapped air bubbles were reduced through evacuation and the water frozen.

Viewing through a dissecting microscope, the ice was cut away from the side of the tooth sockets using a mini-motor and diamond cutting wheel. A safety razor blade was used to do fine trimming through the socket wall to expose both PDL and pulpal vessels down to the tooth apex. The casts were then thawed, rinsed and allowed to dry in a dust proof cabinet. They were recoated with carbon, gold/palladium and viewed in the SEM. The kV ranged between 5 to 15 kV. SEM stereopairs were recorded using a 6^{o} angle of tilt. The distal socket walls were not viewed in the current study.

The circular plexus in the anterior region consisted of a single vessel that circled the tooth at the level of the gingival attachment. The crevicular gingival network varied considerably at different sites around the socket and in the different age groups of animals studied. Variation in the crevicular gingival network was also seen between the maxilla and mandible in the same animal and between animals in the same age group. The vestibular gingival network showed site and morphological variation.

It was considered that the formation of the more complex glomerular-like crevicular loops seen in the mature animals may be in response to chronic inflammation of the gingival tissues. **LEE** (1988) did not record the condition of the gingiva around the teeth of the marmosets photographically prior to the animals being sacrificed. This made the interpretation of the findings more difficult as an association could have been made between the extent of the glomerular-like crevicular loops and the gingival condition.

Significant vascular arrangements found in the anterior PDL of the cotton ear marmoset included the following:

1. An arterial supply to the mandibular labial and lingual gingiva which originated in the apical PDL.

2. Groups of vessels were seen communicating between the mandibular labial PDL in the apical region and the labial alveolar

mucosa. Examining the endothelial imprint pattern of these vessels and noting their progress in the PDL and alveolar mucosa has led the current author to conclude: (a) There was an arterial supply to the mandibular PDL from the labial alveolar mucosa. (b) There was venous drainage from the mandibular PDL to the labial alveolar mucosa.

3. Large venules, ranging up to 100 μm in diameter, were seen coursing down the mesial mandibular PDL of the anterior tooth sockets, or in the bone directly adjacent to the mesial mandibular PDL. Between the middle and apical PDL thirds they merged and appeared to drain through the labial plate of bone to the labial alveolar mucosa and down into the gingival sulcus. These large venules were not seen on the labial and lingual sides which suggests that vessel type and vascular volume may vary around the tooth socket. Studies which have evaluated vessel type and vascular volume from one side of the tooth socket may not necessarily represent the other sides.

4. Different patterns of pulpal venous drainage into the apical PDL vessels were seen. The fanning out of pulpal vessels below the apical foramen was not seen in all of the sockets examined.

In conclusion, an understanding of the normal vascular morphology is necessary before changes resulting from orthodontic tooth movement and pathological conditions can be understood. The corrosion casting technique provides a means whereby the three-dimensional vascular structures of various organs and tissues can be visualized and described.

SIGNED STATEMENT

The corrosion casts of the cotton ear marmoset used in this investigation, were originally processed by **LEE** (1988), while looking at the vasculature architecture of the palate, gingiva and PDL of the posterior teeth. The current research project has looked at the unexamined anterior segments which were not included in the previous thesis. Apart from the above, this thesis contains no other material which has been accepted for the award of any other degree or diploma in any University, and to the best of my knowledge and belief, contains no material previously published or written by another person, except where due reference is made in the text of the thesis.

CHRISTOPHER MARK STANLEY

NAME: Dr Chris Stanley COURSE: M.D.S.

I give consent to this copy of my research report, when deposited in the University Library, being available for photocopying and loan.

SIGNATURE: ..... DATE: 18-2-94

ACKNOWLEDGEMENTS

I would like to thank Dr David Lee for the initial processing of the oral microvascular corrosion casts of the Cotton Ear Marmoset. His technical expertise helped ensure the successful completion of this project.

To my two sons Aidan and Joshua and loving wife Dell, a special thank you is extended again for encouraging me and putting up with me while undertaking this course.

CHAPTER 1

INTRODUCTION

The study of the microvasculature of the palate, gingiva and periodontal ligament (PDL) of various animal species has involved using different techniques. The corrosion casting technique produces a three-dimensional replica of the blood vessel lumen. With the superior magnification, resolution and depth of focus of the scanning electron microscope (SEM), major advances have been made in the last 15 to 20 years. **LAMETSCHWANDTNER et al.**, 1990, have reviewed the literature and provide a comprehensive list of SEM investigations using the corrosion casting technique.

SEM micrographs can be taken in such a way as to allow their prints to be mounted for stereopair viewing. This technique provides a three-dimensional picture of the vascular bed, and assists in the visualization of the distribution, orientation, and connection of the vascular elements within a specimen of tissue (**HOWELL**, 1975).

Work carried out at The University of Adelaide, Dental Department into the microvasculature of the palate, gingiva and PDL and using the corrosion casting technique include: **WONG** (1983), who studied the mouse molar PDL microvasculature; **WEEKES** (1983), who recorded the microvascular architecture of the rat molar PDL; **WEEKES** and **SIMS** (1986c) who investigated the gingival vascular architecture of the common marmoset; **SIMS et al.** (1988) who looked at the glomeruli in the molar gingival microvascular bed of the germ-free rat; and **LEE** (1988) who recorded the microvasculature of the marmoset's palate, gingiva and PDL from the posterior segments.

The current author has used the corrosion casts of marmosets which were originally processed by **LEE** (1988). The microvasculature of both the gingiva and PDL of the unexamined anterior segments were recorded in the study.

1.1 MATERIALS AND METHODS

Eight female cotton ear marmosets (*Callithrix jacchus*) were initially selected by **LEE** (1988). In the permanent dentition of the marmoset all the incisor, canine and premolar teeth had single roots. The mandibular molars had two roots and the maxillary molars three roots (**SHAW et al.** 1954).

LEE (1988) divided the animals into two equal groups according to their age. Animals in the mature group were aged between 4 to 7 years, while animals in the young group were aged between 18 to 24 months.

Corrosion casts were made of the jaws using the following technique: The animals were weighed and then anaesthetized by intramuscular injection into the thigh quadricepts with Saffan (alphaxalone alphadone acetate, 19.5 mg/kg body weight). The two carotid arteries and the inferior vena cava were exposed and cannulated. A blood washout solution was injected into the cannulas inserted in the carotid arteries and drainage was via the inferior vena cava. Polyvinyl-pyrrolidone (PVP-40) in the blood washout provided a blood colloid osmotic pressure of 25 mm of Hg. Sodium nitrite and papaverine HCL acted as vasodilators, while heparin (40 IU) was used as an anticoagulant.

Once the blood washout phase was complete, a 20 ml syringe was filled with 1% gluteraldehyde fixative prepared in 0.1M phosphate buffer and perfused into the carotid arteries. The washout solution was then used to flush out the remaining fixative. Mercox casting resin with a viscosity of 36 centistokes was pressure perfused via the cannulated carotid arteries. The animals were then

immersed in a 50 °C water bath for 24 hours to ensure the resin was completely polymerized.

The animals were beheaded, the jaws removed and immersed in 10% HCL to enable the hard tissues to decalcify. Once this was complete, the tissue corrosion technique described by **HODDE** (1977) was followed. The specimens were rinsed on alternate days with warm distilled water and on alternate days with fresh 10% KOH. Complete tissue corrosion took from a couple of weeks to several months.

Once tissue corrosion was complete, the specimens were rinsed in double distilled water, dried, and mounted on SEM stubs using double sided adhesive and silver colloid. The specimens were coated with osmium vapour to make them conductive to electrons. This was suggested by **MURAKAMI et al.** (1973). A vapourized layer of carbon and gold/palladium was also used to help increase the electrical and thermal conductivity of the casts and prevent charge build-up during examination in the SEM.

In the current research project the surface vascular morphology of the anterior tooth segments was recorded. Once this was completed, the casts were sectioned through the tooth sockets sagittally and coronally so that different aspects of the PDL could be studied. In **LEE**'s (1988) study the cleaned casts were immersed in distilled water and frozen. They were sectioned with razor blades by carefully sawing through the ice. The ice helped to hold the delicate casts together during sectioning. Other methods to allow for sectioning were examined in the current study.

The specimens were examined in the Philips SEM 505. Accelerating voltages were kept low (usually around 5 kV) to minimize thermal and charging damage. Stereopair micrographs were taken in the SEM using a 6° angle of tilt to provide stereopair three-dimensional images of the microvascular replica.

Ilford FP4 120 mm black and white film was used and prints were made using Ilfospeed grade 3 and multigrade glossy paper with a Durst laborator 54 enlarger. The prints of the micrographs were examined in pairs using the Stereo Aids viewer (Rd No 70.485).

CHAPTER 2

AIMS OF THE INVESTIGATION

The aims of the investigation were:

1. To use the corrosion casts which were previously processed by **LEE** (1988). These corrosion casts show the microvascular architecture of the cotton ear marmoset's (*Callithrix jacchus*) palate, gingiva and PDL. The current study will examine the anterior segments which were not assessed in the previous study by **LEE** (1988) and include the gingiva, mucosa, PDL and col areas of the incisor and canine teeth.

2. To develop a satisfactory technique to section the corrosion casts through the tooth sockets so that the microvasculature of the PDL can be examined from the cervical region down to the apex.

3. To compare the oral microvascular architecture of the anterior segments of the cotton ear marmoset with those described by **LEE** (1988) for the posterior segments. To compare the oral microvascular architecture of the cotton ear marmoset to other animal species.

CHAPTER 3

REVIEW OF THE LITERATURE

The physiology and function of the oral microvasculature of various animal species has been studied for many years. In an attempt to understand the three-dimensional spatial arrangement of these structures, a variety of techniques have been developed. Most of these techniques have involved perfusing solutions through the vascular system and then viewing the tissue using a light microscope.

In the 1960's numerous authors examined the distribution of blood vessels within the PDL of various experimental animals. These included mice, rats, monkeys, hampsters, cats and dogs and included authors such as **BOYER** and **NEPTUNE** (1962); **KINDLOVA** and **MATENA** (1962); **KINDLOVA** (1963, 1965, 1967a, 1967b and 1970); **CARRANZA et al.** (1966); and **FOLKE** and **STALLARD** (1967). All of these early researchers were limited by the use of light microscopy with its inherent lack of depth of focus.

3.1 METHODS USED FOR STUDYING THE MICROVASCULAR ARCHITECTURE OF VARIOUS ANIMAL SPECIES

A. VITAL MICROSCOPY

Vital microscopy involves the examination of superficial blood vessels "in vivo" under the light microscope. Deeper structures could not be viewed making the technique unsuitable for studying the vascular architecture and its connections in three-dimensions.

B. HISTOLOGICAL TECHNIQUES

CASTELLI (1963) used india ink injected into the carotid arteries of the *Macaca* rhesus monkey to examine the PDL vascular under the binocular microscope. **GARFUNKEL** and **SCIAKY (1971)** traced rat PDL vessels after perfusing them with india ink, using histological sections 100 to 280 μm thick. **EGELBERG** (1966) looked at blood vessels at the dento-gingival junction in dogs after perfusion with a carbon-gelatin mixture via the carotid arteries. Sections were obtained using a microtome and examined under a stereo-microscope by transillumination. He attempted to assess the three-dimensional architecture of the vasculature by using two-dimensional serial sections. Even though the contrast medium or dye effectively perfused the microvasculature, the methods described above were severely limited by the lack of depth of focus of the light microscope.

C. THE USE OF MICROSPHERES

A method similar to that described above, but where plastic microspheres of about 15 μm ($\pm$ 5 μm) were injected into the blood stream, was used by **FOLKE** and **STALLARD** (1967). They used Squirrel monkeys and attempted to look at the PDL microcirculation. The major problem with this technique was the particles were too large to pass through the smaller vessels.

D. MICRO-ANGIOGRAPHIC TECHNIQUES

Instead of a dye or contrast medium being injected into the blood stream, and the tissue then being sectioned and viewed under the light microscope, a radio-opaque solution was used. The specimen once injected was sectioned, the sections were then exposed to X-rays, with the resultant image being recorded on a photographic plate. **CASTELLI** and **DEMPSTER** (1965) used this technique. They perfused *Macaca* rhesus monkeys with various substances, one being a radio-

opaque substance which was viewed using a roentographic technique. The image was still two dimensional however, and there was superimposition of structures throughout the tissue onto the film. The results were also limited as the sections were viewed using a light microscope.

E. CORROSION CASTING

The corrosion casting technique involves the filling of the vascular system with a liquid that solidifies. The vascular system is perfused with the liquid either via an arterial or venous route. The surrounding tissue is then corroded away from the casting medium leaving a replica of the vascular tree. The tissue replica can be dissected either before or after the tissue corrosion stage. It is then dried, rendered conductive, mounted and examined in the SEM.

The concept of using corrosion casts (vascular corrosion casts) for anatomical study is several hundred years old (**HODDE** and **NOWELL**, 1980). The technique of filling anatomical hollow spaces with liquids that solidify dates back to the 15th century when Leonardo da Vinci (1452-1519) made wax casts of human cerebral ventricles and the chambers of the heart (**HODDE**, 1981).

The criteria required of a satisfactory casting injection media have been discussed by **NOWELL** and **LOHSE** (1974), by **GANNON** (1978) and have been sumarized by **HODDE** (1981) to include 10 criteria. **CHRISTOFFERSON** (1988) has extended these criteria and suggested that the ideal characteristics should include the following:

1. Be non-toxic for both the investigator and for the system to be cast.
2. Be of sufficiently low viscosity or particle size to pass through the smallest capillaries.
3. Be physiologically inert in the system cast.
4. Polymerize within 3 to 15 minutes after mixing.

5. Not shrink during curing.
6. Permit microdissection with the surrounding tissue intact.
7. Be resistant to corrosion procedures.
8. Be visible in the dissecting microscope after dissection.
9. Retain the structural configuration during drying.
10. Be electron conductive.
11. Be resistant to electron bombardment.
12. Replicate delicate topographical details of the vessel luminal surface.
13. Indicate the direction of blood flow in the system cast.

The two main types of casting material which have been used in the past have been reviewed by **HODDE** and **NOWELL** (1980) and by **HODDE** (1981). The first type comprises the rubber (latex) compounds such as Cementex, Vultex, Microfil and Geon 151, Geon 576 + 351. All except Microfil are latex based materials. Microfil is a silicone rubber. The second and more common type of casting material is the polymer resins. These are made up of monomers, catalysts, accelerators and plasticizers.

Nowadays although many casting materials are available, **LAMETSCHWANDTNER et al.** (1990) found that only a few are widely used. These include Mercox (CL colourless, B blue, R red), methyl methacrylate, modified Batson No 17, Araldite CY 223, and Tardoplast. These materials meet most of the requirements necessary for use in the SEM. Polymerization without shrinkage or distortion is not possible however, because polymerization always results in shrinkage due to the nature of the polymerizing resins.

i. Rubber Compounds

Rubber (latex) compounds have been used in the past by a number of investigators including **KINDLOVA** and **MATENA** (1959, 1962) who studied the blood circulation in the rodent teeth of the rat; **KINDLOVA** (1963, 1965, 1970)

who studied the vascular supply in the pulp and periodontium in the rodent teeth of the rat, and the blood supply in the marginal periodontium in the *Macacus* rhesus monkey; and **NOWELL** and **LOHSE** (1974) who looked at the vasculature of the small intestine in the beagle dog. **NOWELL et al.** (1970) reported the first satisfactory SEM viewing of corrosion casts made from a latex material called Cemetex. Before this stage only the light microscope was used.

HODDE (1981) noted that there were several disadvantages in using rubber materials.

1. Diluted latex casts require freeze drying or critical point drying to preserve the spatial interrelationship.

2. They do not consistently replicate luminal surface microstructures.

3. The elasticity which enhances gross dissection inhibits accurate microdissection of single vessels.

LEE (1988) suggested that the dried latex casts had the disadvantage in that they tended to droop, shrink and adhere and were not very suitable for use with the SEM. He also noted that the silicone rubber compounds did not survive the digestion process due to the fragility of the silicone polymer. This also made them unsuitable for SEM observation.

ii. Polymer Resins

MURAKAMI (1971) noted that preliminary polymerized methacrylic methyl ester for corrosion casting had been used since the early 1950's. He was the first researcher however to introduce acrylic resins for corrosion casting of blood vessels for use in the SEM using a methacrylate mixture of his own formula. These methyl methacrylate casts were able to withstand strong acid and alkali corrosion, were strong enough and had adequate dimensional stablility to maintain the vascular architecture and not collapse or droop under their own weight.

Several modifications have been made since then. These have included the rendering of the entire specimen conductive with osmium tetroxide-hydrazine vapour and in simplifying the rather laborious prepolymerizing process (**MURAKAMI et al.**, 1973). **MURAKAMI** (1975) lowered the viscosity by adding 30-50% monomeric methacrylate to the base resin. He also improved the dissectability of the brittle casts.

iii. Advantages and Disadvantages of the SEM Corrosion Casting Technique

LAMETSCHWANDTNER et al. (1990) described the advantages of the corrosion casting technique as follows:

1. The SEM images in combination with other methods are much more informative than reconstructions from serial sections and they also enable large areas to be viewed.

2. A quasi three-dimensional image of the vascular bed is possible by the high depth of focus of the scanning electron microscope.

3. Large specimens can be examined.

4. Excellent manipulation of the specimen in the SEM specimen stage is possible by tilting, rotating and shifting in all three planes of space.

5. Vessels can be identified by the luminal diameter and endothelial imprints on the casts. Arteries reveal ovoid endothelial nuclear imprints orientated parallel to the long axis of the vessel; veins have a shallower roundish endothelial nuclear imprints with no particular orientation.

6. Several authors have suggested that by measuring the large diameter (D) and small diameter (d) nuclear imprint patterns the mean ratio D/d clearly differentiates arterial ($D/d > 2.9$) and venous vessels ($D/d < 2$).

7. True capillaries (diam. $< 8\ \mu m$) have been shown to have D/d ratios changing from the arterial side to the venous side. The morphology and quality of endothelial imprint patterns however, greatly depends on the precasting and casting conditions as well as on the casting media used.

8. Sinsuoids can be discerned easily.

9. Localization and identification of vascular structures like circular constrictions, sphincters, venous valves and cushions is possible.

10. Localization and identification of imprinted vessel wall structures (myocytes) and of pericapillary structures (collagen fibres, pericytes) and other differentiations are possible.

11. Individual vessels can be selected and studied with respect to their origin, course, number of branches, branching angles and the direction of orientation.

12. Vascular routes can be traced, photographed and presented in stereopair images for three-dimensional visualization.

The disadvantages of the corrosion casting technique compared to other techniques are few. **LAMETSCHWANDTNER et al.** (1990) suggested that the greatest disadvantage of scanning electron microscopy of corrosion casts was their inability to indicate the direction of blood flow within the capillaries. The change in the endothelial cell nuclei imprint patterns from the arterial side to the venous side helped in determining the blood flow direction. However, direct communication (shunts) may occur within the arterial or venous systems and the direction of flow could change. They suggested that the addition of suitable particles to the injection medium could show indirectly the direction of blood flow however these particles are not yet available.

LEE (1988) noted that one potential problem was that as all of the surrounding tissues were corroded away the spatial orientation of the structures was made more difficult. The use of the corrosion casting technique in association with other techniques such as TEM, histology, intravital microscopy and tissue SEM was suggested by **GANNON** (1985) as a way to help overcome this loss of spatial orientation to the surrounding structures.

SOBIN and **TREMER** (1980) suggested that a disadvantage in the corrosion casting technique was that there were significant dimensional changes in the blood vessels. This occurred due to agonal constriction of vessels which altered the microvascular bed. They also found that vascular perfusion demonstrated the total

vascular bed rather than the functional vascular bed. The dynamic state of the vascular bed may only be captured at the time of perfusion by quick-freezing.

In summarizing this section, **LAMETSCHWANDTNER et al.** (1990) felt that there were three main disadvantages in relation to the corrosion casting technique which needed to be addressed by future research. These included the following:

1. Too little information can be obtained about the direction of the blood flow within the cast area.

2. No information about actual "open" vessels (vessels may be opened artifically by the injection).

3. Little knowledge concerning the effects (chemically) that the casting media exerts on the luminal surface and on the vessel wall.

iv. Terminology

In the past, many terms have been used to describe the corrosion casting technique. A medline search was carried out between the years 1966 to 1990 to determine the different terminology being used. Terms which have been used include the following: vascular corrosion casting; corrosion casting; vascular casting; vascular corrosion replica; microcorrosion casting; microvascular casting; microvascular corrosion casting; injection replica; plastic injection method; polymer casting; plastoid injected; and luminal casting.

LAMETSCHWANDTNER et al. (1984) suggested that the term "**Vascular Corrosion Cast**" be adopted to describe resin casts of the blood vessels and lymphatics. It was hoped that this terminology would be adopted and would replace the many other names given to the technique, however this terminology has not been universally accepted at this stage. The current author to be consistent with the terminology used by **LEE** (1988) has used "corrosion casting" in this project.

A listing of the authors using the different terminology are listed:

"Vascular Corrosion Casting"

SEYNK et al., 1971; LAMETSCHWANDTNER et al., 1980; OHTANI, 1983; LAMETSCHWANDTNER et al., 1984; HOSSLER et al., 1986; WEIGER et al. 1986; FAHRENBACH et al., 1988; HOSSLER and WEST, 1988; LAHNSTEINER et al., 1988; KIKUTA and MURAKAMI, 1989; KONERDING et al., 1989; HOSSLER and OLSON, 1990; LAMETSCHWANDTNER et al., 1990 and VAN-BUSKIRK et al., 1990.

"Corrosion Casting"

COOK and TOMPSETT, 1968; MURAKAMI, 1972; TOMPSETT, 1976; NERANTZIS et al., 1978; NOPANITAYA et al., 1979; OLSON, 1980; HILL and McKINNEY, 1981; IRINO et al., 1982; TAKEMORI et al., 1984; GAUDIO et al., 1985; CASTENHOLZ, 1986; NELSON, 1987; SCHMIDT et al., 1988; STEWART et al., 1988; INOKUCHI et al., 1989; and YOSHIDA et al., 1989; HODDE et al., 1990.

"Vascular Casting"

KRATKY and ROACH, 1984; FRYCZKOWSKI et al., 1985; GATTONE and EVAN, 1986; GATTONE and SALE, 1986; FRYCZKOWSKI, 1987; FRYCZKOWSKI et al., 1987; and KRATKY et al., 1989.

"Vascular Corrosion Replica"

OLSON et al., 1981.

"Microcorrosion Casting"

HODDE et al., 1977; ANDERSON and ANDERSON, 1978; JASINSKI and MIODONSKI, 1978; JASINSKI and MIODONSKI, 1979; MIODONSKI and JASINSKI, 1979; HODDE and NOWELL, 1980; KUS et al., 1981; SCHMIDT et al., 1982; SCHMIDT et al., 1983a, 1983b and 1983c; HOSSLER and OLSEN, 1984; DILLY, 1986; PANNARALE et al., 1986; GAUDIO et al., 1988; MACPHEE et al., 1988; YOSHIDA et al., 1988; and LEISER et al., 1989.

"Microvascular Casting"

ROGERS and GANNON, 1983; and SCHRAUFNAGEL and SCHMID, 1988a, 1988b).

"Microvascular Corrosion Casting"

OHTANI et al., 1983; BURTON et al., 1986; SCHRAUFNAGEL, 1987; BURTON and PALMER, 1989.

"Injection Replica"

MURAKAMI et al., 1974; **NOWELL** and **TYLER**, 1974; **MURAKAMI**, 1976; **OHASHI et al.**, 1976; **OHTANI and MURAKAMI**, 1978; **IWAKU** and **OZAWA**, 1979; **KAJIHARA et al.**, 1983; and **KAJIHARA et al.**, 1985.

"Plastic Injection Method"

YAMAMOTO et al., 1974; and **HANAI et al.**, 1975.

"Polymer Casting"

SCHENKMAN et al. 1985.

"Plastoid Injected"

CASTENHOLZ, 1983a.

"Luminal Casting/Replica"

MOTTI et al., 1986; **MOTTI et al.**, 1987.

3.2 THE IDENTIFICATION AND CLASSIFICATION OF BLOOD VESSELS

The current author noted in reviewing the literature that it is possible to provide a fairly accurate classification of blood vessels by using criteria such as vessel diameter and shape, the pattern of branching and anastomosis and, in the case of corrosion casts, the cellular pattern left on the casts of the endothelial cell nuclei and endothelial cell borders.

A. ENDOTHELIAL IMPRINT PATTERN

HODDE et al. (1977) noted that there were two distinct surface patterns on the corrosion casts taken from various parts of the head region of the rat. These regions included the brain, spinal cord, trachea, eye cup and inner ear. Although the tissues were corroded away in the preparation of the casts, the vessel endothelium had left a characteristic imprint which they used to determine which

were arteries and veins. In general, an imprint pattern was left on the surface of vessels greater than 6 to 7 μm in diameter.

HODDE and **NOWELL** (1980) noted these imprint patterns in micrographs taken by researchers of the early 1970's in rubber and polymer resin casts. The authors from the 1970's also noted that there was a variation between veins and arteries in respect to this imprint.

MIODONSKI et al. (1981) found two distinctly different patterns displaying the luminal surface relief of the vessel to be present in quite a large range of tissues and organs. They found that these patterns could be observed practically everywhere on the surface of the cast if it was completely filled and clean, and if the diameter of the vessel replica was greater than 8 to 10 μm. They described the patterns as follows:

> **1.** Practically, every cast of an arterial vessel exhibited along its whole length down to the capillary level a pattern in the form of sharply outlined ovoid depressions, of which the long axis is orientated like that of the vessel. These depressions, constituting a replica of the endothelial cell nuclei, were surrounded by narrow fissures corresponding to the boundaries of the individual, usually fusiform, endothelial cells.
>
> **2.** The pattern on the casts of the venous vessels takes the form of roundish depressions distributed rather irregularly, and also extending along the whole length of the cast down to the capillary level. These depressions, replicas of the endothelial cell nuclei, are rather smaller in diameter and are not so flat and sharply outlined as the impressions seen on arterial casts. They are also surrounded by narrow fissures demarcating the boundaries of the endothelial cells, which are usually of an irregular rhomboidal form.
>
> **3.** The surface of the casts of the capillary network was usually smooth, though rather indistinct replicas of the endothelial cells could be seen. As a rule these assume the appearance of narrow fissures demarcating the boundaries of individual endothelial cells.

B. BLOOD VESSEL ULTRASTRUCTURE

Attempts have been made by several researchers over the years to classify blood vessels according to their lumen calibre, wall thickness, endothelial cell morphology, the type of peri-endothelial cells present and from any other distinguishing features present.

An important early study was carried out by **BENNETT et al.** (1959) who classified capillaries on the continuity of the basement membrane, on whether they had fenestrations or perforations and on the presence or absence of pericapillary cellular investment. This classification is still commonly used by authors describing PDL vasculature.

BEVELANDER and **NAKAHARA** (1968) described the structure of blood vessels in the human PDL as being thin-walled with a highly variable lumen calibre. They were separated from surrounding fibroblasts and collagen fibres by a basement membrane.

SIMIONESCU and **SIMIONESCU** (1984) described capillaries as being the smallest ramifications of the vascular system with a luminal diameter of 5 to 10 μm, with a wall reduced to only endothelium, a basal lamina and a few pericytes.

RHODIN (1967, 1968) provided a comprehensive classification of arterial and venous vessels according to diameter and ultrastructural features while looking at the fascia of rabbit medial thigh muscles. This classification is still widely used today and can assist with the identification of vessels from corrosion casts. (Table 1)

VESSEL TYPE	LUMEN DIAMETER	ENDOTHELIAL NUCLEI IMPRINT PATTERNS
Small Collecting Vein	100 to 300 μm	Rounded nuclei, without microvillus protrusions and a more rounded base. Nuclei are surrounded by irregular cell borders.
Muscular Venule	50 to 100 μm	
Collecting Venule	30 to 50 μm	A gradual transition in nuclei imprint shape.
Postcapillary Venule	8 to 30 μm	
Venous Capillary	4 to 7 μm	There is a decreased endothelial cell imprint density.
Precapillary Sphincter	7 to 15 μm	
Terminal Arteriole	Less than 50 μm	Ovoid nuclei with micro-villous protrusions, orientated along the axis of the vessel. Nuclei are paralleled by their cell borders.
Arteriole	50 to 100 μm	

It should be noted that the precapillary sphincters taper off to form arterial capillaries (approx. 10 μm in diameter) within about 50 μm.

TABLE 1: CLASSIFICATION OF BLOOD VESSELS USING VESSEL LUMEN DIAMETER (RHODIN, 1967, 1968), AND ENDOTHELIAL NUCLEI IMPRINT PATTERNS (HODDE, 1981; MIODONSKI et al., 1981).

LEE (1988) in discussing the oral microvasculature of the cotton ear marmoset from corrosion casts noted that arteries and veins could be differentiated because of their vessel diameter, vessel shape, the pattern of branching and interconnections with other vessels. He concluded that: "Arterioles ran a straighter course, had few branches, and showed a constant diameter. Venules ran a more sinuous course, had more branches, and possessed a varying diameter."

The current study will rely on vessel diameter, vessel shape, the interconnections with other vessels, the pattern of branching and endothelial imprint pattern to assist with the classification of blood vessels. Caution should be taken when interpretating any results using vessel diameter alone as the state of constriction or dilation of the vessels at the time of examination is not known. Also it should be noted that in a living animal, vessel diameter is continually changing due to autoregulatory mechanisms. It is also possible that vessel diameter will vary from species (**WEIDEMAN**, 1984).

3.3 RECENT ADVANCES IN THE CORROSION CASTING TECHNIQUE

The use of the corrosion casting technique in combination with the SEM is becoming more and more popular. **LAMETSCHWANDTNER et al.** (1990) have carried out an extensive review of the literature and provided almost 30 pages of references where this technique has been used. They estimated to have only covered approximately 70% of the available literature. This is a significant article.

Along with the greater number of researchers using this technique, a larger number of regions, tissues and organs have been studied. **LAMETSCHWANDTNER et al.** (1990) provides 3 tables at the conclusion of their review which list: **(1)** Regions, tissues and organs that have been studied. **(2)** Pathological cases. **(3)** Experimental conditions. In the first table, 53 headings were provided with numerous authors under each heading. Pioneer work into invertebrates is now being undertaken. Still no uniform nomeclature exists and greater confusion is occurring in relation to the following:

1. The need, location and type of anticoagulant used to prevent blood clotting.

2. The application of a vasoactive and spasmolytic substance and the site of administration.

3. The kind of anaesthetic used, the dosage, the application, and time lapse between application and casting procedures.

4. The solutions used to rinse the circulatory system free of blood (concentration, pH, molarity, osmolarity), the temperature at which the solutions are injected, the flow rate, hydrostatic pressure, the volume and duration of rinsing. Solutions mentioned included 0.015 M NaCl, phosphate-buffered saline, Paldy buffer, Ringers solution, Tyrode solution, phosphate buffer. Most of the solutions were injected at temperatures between 37 °C to 40 °C, however temperatures ranging from 20 °C to 55 °C were reported.

5. The perfusion pressures for rinsing, fixing and casting show a wide range of variation. The duration for injection also shows considerable variation. It should be noted that the longer and wider the vascular pathway to the target site and the higher the viscosity of the injection media, the less resin will flow.

6. The necessity to prefix the blood vascular system before casting is still disputed. The following fixatives are reported: glutaraldehyde (0.5% up to 6.0%), formaldehyde, and paraformaldehyde with buffer solutions such as cacodylate, phosphate and Sorensen buffer being mentioned. The duration of fixation varies from 1 to 7 minutes, the pH varies, osmolarity and temperatures of the fixative also vary.

7. The type of resin used and the appropriateness of that resin for a particular specimen of tissue is still poorly understood. Data mentioned by the manufacturers in relation to particular types of casting resins are also often incomparable. Resin viscosity is often measured under different conditions and is therefore not directly comparable. It is suggested that "the viscosity should be as high as there is still a total filling of the terminal vascular system".

8. The time between mixing of the casting medium and the end of polymerization is still unclear. It has been suggested that the specimens be left in water baths ranging in temperature from 40 °C to 80 °C to help gain full polymerization. Time duration ranged from 30 minutes to 24 hours.

9. The duration of tissue maceration (corrosion), the strength and temperature of the agents used were also variable. Alkali maceration solutions included 10%-30% NaOH, 10%-40% KOH, sodium hypochlorite, collagenase and trypsinase. Acids included HCl, bichromate sulphuric acid, chromium trioxide, 30% hydrogen peroxide, and HCOOH). Temperatures varied from 50 °C to 80 °C. Depending on the size and nature of the specimen the maceration time varied from several hours to several weeks.

10. Solutions used for decalcification (2% HCL, 3% sodium peroxide), for cleaning (5% formic acid, 5% sodium hypochlorite, 5%-10% trichloro-acetic acid, detergents) and the role of ultrasonics.

11. The type of drying technique to be employed. For example, whether the specimen should be air dried, freeze dried, or critical point dried.

12. The method used to dissect the specimen can also be confusing. For example, the specimen can be sectioned after polymerization of the casting resin is complete and before tissue maceratioin (corrosion); during rinsing of the cast in distilled or tap water; while they are embedded in frozen distilled water; while embedded in gelatine; after they are dried; after they are mounted; repeatedly after examination of superficial layers; within the scanning electron microscope.

13. The type of conductive coating used also varies considerably. For example, the impregnation of the cast with heavy metal vapours alone, or in combination with vapourized hydrazine-hydrate; the osmium-hydrazine-hydrate method; sputtering with gold, with gold-palladium or with platinum-palladium; evaporation with gold, carbon-gold, gold-palladium, platinum-palladium or silver-gold.

Finally, in the review by **LAMETSCHWANDTNER et al.** (1990), recent developments have been discussed. The measuring of various variables including vessel length, diameter, branching angles, intervascular distances and interbranching distances have enabled researchers to calculate the rheology within the cast vessels. Quantification of variables can be done using the following methods:

1. Modern image systems have been developed which can quantify all types of cast structures.

2. Grey level image analysis has been developed whereby the SEM image is digitized with structures that are in focus being assigned white and those not in focus black. The ratio of the total area measured to the black area is an index of the vascular density.

3. Point counting methods using the principles of stereology may have an application in corrosion cast studies. In these particular cases a cut cast or a flat cast surface tend to work best. Stereological test grids of the appropriate dimensions can either be laid directly over the SEM screen or over micrographs. Calculations can be made using stereological formulas of different types of variables.

4. Stereophotogrammetry requires a very precise tilting stage of the SEM and also a specific stereoscope equipped with a manual or computerized parallax measuring system.

5. Planimetry involves using micrographs or projected negative material. Computer equiptment connected to a digitizing tablet is used in combination with specific software programmes to carry out various calculations.

Quantification can also be carried out by weighing the corrosion casts or by measuring vascular structures. Where the density of the resin is known, the volume

of the vascular bed can then be calculated using the formula v = w/d whereby d = the density of the casting medium used, w = weight of the cast, v = volume of the vascular bed cast (**LAMETSCHWANDTNER et al.**, 1990).

Cast preparations without maceration and their treatment by ultrasound have been described. Advantages of this method include: visualization of tissue structures in the middle and outer vascular wall (myocytes and pericytes, basement membrane, adventitial tissue); preservation of the relationship between the cast vessel and the surrounding tissue (**CASTENHOLZ** 1983a, 1983b).

HODDE et al. (1990) described a new procedure of cleaning the corrosion casts with sodium hydroxide and Triton X-100 (v/v; Sigma, St Louis, MO) detergent. They noted that alternate 24 hour washes in 7.5% sodium hydroxide followed by Triton X-100 and the addition of Triton X-100 detergent to the sodium hydroxide resulted in a reduction in the time taken to clear the casts from tissue. A 5% solution of Triton X-100 was equally as effective as a 20% solution.

Finally, an exciting new area for possible research using the corrosion casting technique is in the detection of antigen uptake sites (**SCHENKMAN et al.**, 1985).

3.4 ORAL MICROVASCULATURE

There is almost a complete lack of detailed information about the oral microvasculature in man. All of the early reported work was carried out on cadavers, mainly of the elderly or the very young. As a result of the unavailability of human material, animal models were sought that would provide clues as to the structure and function of the oral microvasculature in man.

A. ORAL MICROVASCULATURE IN MAN

Detailed studies of human oral microvasculature including that of the PDL have been few. Early researchers included **HAYASHI** (1932); **STEINHARDT** (1935); **FORSSLUND** (1959); **COHEN** (1960); **PROVENZA et al.** (1960); **CASTELLI** (1963); **PROVENZA** (1964); **BIRN** (1966); **GLAVIND** and **LOE** (1966); **SAUNDERS** and **ROCKERT** (1967) and more recently **BOUYSSOU et al.** (1970).

HAYASHI (1932) using serial sections of the jaws of cadavers injected with carmine gelatin provided a fairly comprehensive description of human oral vasculature. He found that the dental artery ran through the bone and gave off interalveolar branches near the base of the alveolus. The PDL was supplied either directly by dental arteries or indirectly by interalveolar branches of the dental arteries. The former arteries entered the PDL at the apical region and branched to supply the pulp and the periodontium. The interalveolar branches passed through the socket wall to enter the PDL and coursed coronally. These perforating branches anastomosed with one another, as well as with the periodontal branches arising directly from the dental artery to form longitudinal periodontal arteries.

CASTELLI (1963) in looking at the vascular supply of the human adult mandible from cadavers reported that the mandible received its arterial supply from the inferior alveolar artery. This provided vessels in the cortical bone of the mandibular body and alveolar-dental branches to the teeth and adjacent tissue. In the incisive area, anastomoses occurred between the inferior alveolar artery and vessels from the sublingual region in the area of attachment of the geniohyoid, genioglossus and anterior digastric muscles. The alveolar dental branches were branches of the inferior alveolar artery and consisted of eight to twelve main channels, averaging 280 μm in diameter with a varied number of finer branches. These arteries surrounded each alveolus and having passed upwards through the

alveolar walls, anastomosed with the capillary network of the gingiva. These arteries also supplied the pulp, alveolar bone, interalveolar septi and the PDL.

FORSSLUND (1959) and **SAUNDERS** and **ROCKERT** (1967) noted that interdental branches of the superior and inferior dental arteries perforated the alveolar crest to end in the capillary network of the gingiva. These small arteries anastomosed with arteries supplying the vestibular and oral mucosa.

FORSSLUND (1959) felt that the gingival capillary network was formed by the division of the perforating branches into finer vessels to form a plexus. Capillary loops originated from this plexus subepithelially. The gingival vascular network anastomosed with vessels in the floor of the mouth and in the lips and with the vessels in the PDL.

PROVENZA et al. (1960) assessed the extracted teeth and periodontium of two patients, one suffering from what they termed "third-stage periodontosis", the other suffering from a "periodontitis complex". The tissues were fixed, sectioned and stained with various agents and examined under the light microscope. Convoluted vessels which they termed "glomera" were found throughout the PDL being more abundant in the apical third (**PROVENZA**, 1964). These vessels were thought to act as a communication between the arterioles and venules.

B. ORAL MICROVASCULATURE IN MICE

Very little research has been carried out into the microvascular morphology of the oral tissues in mice. The inherent difficulty associated with perfusing the mouse due to its tiny size, has meant that other animal species have been selected.

CARRANZA et al. (1966) were perhaps the earliest authors to have documented results specifically relating to the PDL vasculature of mice. Their paper was a comparative study of the PDL vasculature in different animal species

using a histochemical technique for the demonstration of adenosinetriphosphatase activity to detect blood vessels. A number of animal species including rats, hampsters, guinea pigs, cats and dogs were used. Very few specific references were made in relation to mice in the paper and one often had to assume that the mouse PDL vasculature was similar to that of the rat.

WONG (1983) studied the microvasculature of the mouse molar PDL using corrosion cast SEM stereopair micrographs. He reported that mouse molar PDL microvascular patterns were similar for both the mandibular and maxillary molars. He found that the outer (capillary) circular and inner (venous) gingival vessels were linked by radially orientated anastomoses. The inner gingival vessels anastomosed with the PDL vessels. **CARRANZA et al.** (1966) on the other hand had found that anastomoses between gingival and PDL vessels were rare.

WONG and **SIMS** (1987) in summarizing the previous work of **WONG** (1983) described the microvasculature of mouse molar gingiva and PDL as follows:

> "The molar gingiva had a circular, outer capillary and inner venous system linked by radial anastomoses. The outer (7 μm) capillaries enclosed the three molars in a continuous horizontal loop coursing beneath the crestal epithelium; the inner (10-15 μm) venous vessels encircled each molar just below the epithelial attachment. Glomerular-like vascular formations with an arterial and venous stalk, were associated with the inner circular system and extended toward the circular epithelium.
>
> Axially aligned, post-capillary, PDL vessels (21 μm) anastomosed with the inner circular system, forming different patterns in the occlusal, middle and apical thirds. The apical pattern comprised an enveloping plexus of anastomosing venous vessels supplied by arterio-venous shunts; similar shunts were present throughout the ligament. The microvascular bed of the mandibular inter-radicular ligament was characterized by the presence of a large venous ampulla measuring 60 to 200 μm. Some regions of the ligament microvasculature drained via the medullary vessels into 50 μm diameter venules located interdentally deep to the molar apices.
>
> Volumetrically, the ligament microvascular bed was predominantly of post-capillary venules, and morphologically, a paired arterial and venous system was demonstrated." (Figure 1)

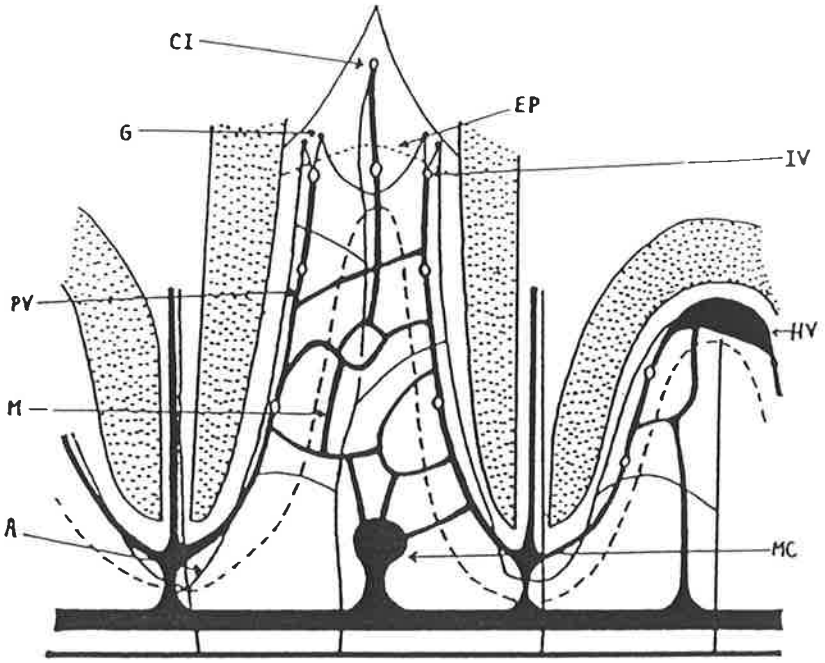

A = Arterial vessel.
CI = Crestal vessel of the interdental papilla.
EP = Crevicular epithelium.
G = Glomerular vascular structure.
HV = Huge reservoir-like interradicular vessel.
IV = Inner single circular vessel.
M = Medullary vessel.
MC = Medullary collecting vessel.
PV = Periodontal collecting vessel.

FIGURE 1: COMPOSITE VASCULAR PATTERN OF THE MOUSE SHOWING VESSELS IN THE PERIODONTAL LIGAMENT, INTERDENTAL, MEDULLARY AND INTERRADICULAR REGIONS. (WONG, 1983).

C. ORAL MICROVASCULATURE IN RATS

The microvascular architecture of the rat's PDL has been widely studied, perhaps more so than for any other animal, but still no researcher has been able to provide a definite categorization of the vessels from apex to gingival crevice. Illustrations to date only show selected isolated areas and do not provide an overall three-dimensional picture of the ligament. One disadvantage of the rat is that it has

a continually erupting incisor which does not fit into the human model. As a result of this, many researchers have concentrated their studies on the molar teeth, which are thought to resemble the human molar (**SCHOUR** and **MASSLER**, 1971).

The blood supply to the mandible and supporting structures including the teeth has been described as originating from the inferior dental artery (**KINDLOVA** and **MATENA**, 1962; **BOYER** and **NEPTUNE**, 1962; **HUELKE** and **CASTELLI**, 1965; **CARRANZA et al.** 1966). Branches of the lingual artery were also thought to supply the anterior mandibular teeth (**KINDLOVA**, 1965; **CASTELLI** and **DEMPSTER**, 1965).

Blood vessels supplying the gingiva, palate and PDL of the maxilla originated from the greater palatine vessels, superior alveolar vessels and vessels deep to the muco-buccal fold. **BOYER** and **NEPTUNE** (1962) found that the superior alveolar vessels supplied the periosteum and then penetrated it to reach the alveolar bone and subsequently supplied the pulp and PDL. The palatine and buccal cheek vessels were thought to supply the gingiva and soft tissues with branches perforating the bone. **CARRANZA et al.** (1966) found that periosteal vessels arising as branches of the mucosal vessels supplied the gingiva.

KINDLOVA and **MATENA** (1962) using latex corrosion casts, described the arteries of the lower molar PDL as having a pallisade formation, running axially to the neck of the tooth and being partly embedded in bone. The arteries and veins were mutually connected by a capillary network supplying the tissues of the PDL. On the interproximal sides the rows of loops of adjacent teeth intertwined. The veins passed through the PDL axially and also in the space between the ligaments, and toward the apex they coalesced into a plexus. At the peak of the inter-radicular septum they formed a rich network.

GARFUNKEL and **SCIAKY** (1971) described the arrangement of vessels in the PDL as being essentially the same for maxillary and mandibular molars.

They found two parallel vascular networks within the ligament, one close to the root and the other external to it. They were describing the mandibular molar ligament. However, they did not state where the external network was in relation to the bone or whether there was cementum formation or resorption associated with the internal network. **BERNICK** (1962) and **CARRANZA et al.** (1966) on the other hand reported that the blood vessels within the ligament were closer to the alveolar bone than to the tooth and this was supported by numerous authors including **NAKAMURA et al.** (1983), **WEEKES** (1983), **WEEKES** and **SIMS** (1986a). **BERNICK** (1962) found that although most of the vascular network was closer to the bone, there were branches that approached the tooth in areas of cellular cementum formation and root resorption.

WEEKES (1983) found a different microvascular arrangement within the various regions of the tooth socket (Figure 2). The morphological findings varied markedly from those of **KINDLOVA** and **MATENA's** (1962) paired arterial and venous description.

WEEKES and **SIMS** (1986a) described the different microvascular arrangements initially noted by **WEEKES** (1983) to be associated with:

1. The buccal and lingual walls.
2. The interdental septum.
3. The interradicular septum.

They noted that down the buccal and lingual walls, tracts of four to six vessels coursed occluso-apically with a few horizontal branches. They felt that this orientation helped to maintain the patency of the vessels during functional loading of the tooth. These vessels were mainly postcapillary-sized venules with a lesser number of capillaries being present. This pattern was similar in the interdental septum area although the vessels were more closely packed there. With the

interradicular septum, the postcapillary-sized venules ran within the ligament for only 100 to 400 μm before reentering the bone.

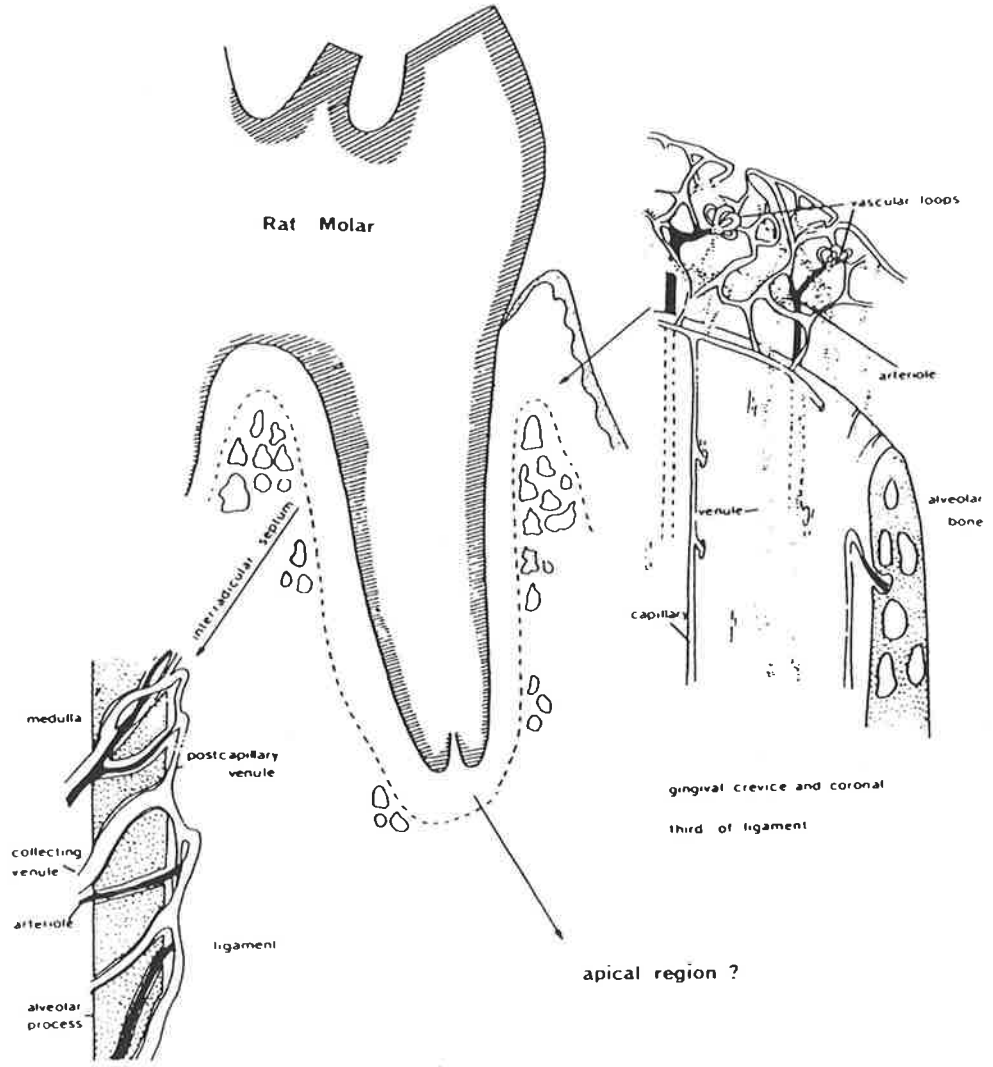

FIGURE 2: SCHEMATIC REPRESENTATION OF THE VASCULAR ARCHITECTURE AT THE GINGIVAL, CORONAL THIRD, AND INTERRADICULAR REGION OF THE RAT MOLAR LIGAMENT. (WEEKES, 1983).

WEEKES and **SIMS** (1986a) noted that anastomoses occurred infrequently between adjacent vessels within the ligament. However, communications with the alveolar plexus were common. Ligament vasculature arose mainly from the deeper gingival vessels except at the interradicular septum. Occasionally vessels that

originated from branches of the alveolar plexus, formed hairpin loops as they entered the plexus.

Loops were located in the apical region as well as in the cervical third of the PDL. These loops were postcapillary-sized venules, 100 μm long and 15 μm in diameter and in the apical region they were located over the interdental septa.

Arterioles, were rarely found in the PDL. In the interradicular septum, the arteriolar supply arose from the alveolar bone drained directly into the occluso-apically orientated postcapillary-sized venules without there being a capillary bed.

On a morphological basis it was felt that all vessels, except those overlying the interradicular septum, had a blood flow direction away from the gingiva and towards the apical PDL region. At the interradicular septum, the arteriolar supply was more dense on each side of the septum, and the venous elements were more prevalent over the crest of the interradicular septum. This arrangement indicated that the overall direction of blood flow in that portion of the ligament was predominantly from apical to occlusal.

WEEKES and **SIMS** (1986b) described the vasculature of the gingival connective tisssue as being characterized by a flat capillary plexus extending from the cemento-enamel junction up to the crest of the free gingival margin beneath the crevicular epithelium. Twisted, vascular loops on the buccal and lingual sides of the tooth originated from the middle third of this plexus. These loops were mainly postcapillary-sized venules with a twisted capillary ascending limb and a larger postcapillary-sized venule descending end.

In the interproximal col regions these loops had a more complex arrangement and resembled kidney glomeruli or intestinal villi. **GARFUNKEL** and **SCIAKY** (1971) using india ink perfusion on rats were unable to demonstrate these. **LEE** (1988) found these glomerular-like structures in multiple tiers in the

buccal gingiva of the maxillary canines of the marmoset, however he did not say whether these were age-related. **KINDLOVA** (1965) in looking at the *Macacus* rhesus monkey also found these glomerular-like structures to a greater extent in the posterior teeth than in the anterior teeth and considered them to be part of the PDL.

WEEKES and **SIMS** (1986b) described the arterial supply to the flat capillary plexus as coming from the gingival proper whereas the venous drainage was directed into the PDL plexus and deeper gingival vessels. The gingival capillary plexus was demarcated at its upper and lower limits by a circularly orientated vessel at each end. Discontinuity of the coronal vessel was noted.

NAKAMURA (1985) and **NAKAMURA et al.** (1987) in looking at the vascular system of the rat molar PDL in the SEM, found a basket-like arrangement of arteries and capillaries around the root apex. In the middle third of the PDL, the vasculature was less dense and showed few loops. Arterioles could be seen entering the PDL from Volkmann's canals in the alveolar bone. These ran towards the cervical PDL and alveolar crest.

SIMS, **SAMPSON** and **FUSS** (1988) found glomerular-like vascular structures in the germ free rat's gingival crevice, and on the buccal, and proximal aspects of the upper and lower molars. It was suggested that these structures appear to be a feature of normal healthy gingiva whereas earlier researchers such as **EGELBERG** (1966), **HOCK** and **NUKI** (1970, 1971 and 1975) thought that they were a response to inflammation.

D. ORAL MICROVASCULATURE IN MONKEYS

The use of non-human primates to study the oral microvasculature has also proved to be popular. As a substitute for the human model, **LEE** (1988) selected the marmoset in his study. These animals were relatively small, reached maturity within 12 to 18 months and had an estimated life span of 15 years. **LEVY et al.**

(1972a) described the dental apparatus as being similar to man, while **WILSON** and **GARDNER** (1982) showed that temporomandibular joint movements were also similar to those in man. The progression of periodontal disease and age changes were shown by **LEVY** (1971) and **LEVY et al.** (1972b), respectively, to be similar to man.

KINDLOVA (1965) examined the blood supply of the marginal periodontium in the *Macacus* rhesus monkey using latex corrosive preparations and histological sections. She described the vessels as being arranged in two networks, those which supplied the PDL and those which supplied the gingiva. Although the two networks anastomosed in many sites, the capillaries in the PDL were arranged in a manner different from those in the gingiva, and the capillaries which arose in the vicinity of the epithelial attachment pursued a course different from both. These gingival-PDL anastomoses were later confirmed by **SAUNDERS** (1967), **LENZ** (1968) and **CUTRIGHT** and **HUNSUCK** (1970a, 1970b).

The main vessels of the PDL ran parallel to the long axis of the tooth and were located adjacent to the bony wall. They sometimes grooved the alveolar bone and gave off branches towards the tooth that formed a flat irregular network of capillaries. Apart from the interradicular septum area of multirooted teeth this pattern was present throughout the PDL of all teeth (**KINDLOVA**, 1965).

KINDLOVA (1965) noted that in the coronal portion of the PDL, the flat irregular network of capillaries was further condensed into a narrow band. Glomerular-like coiled capillary structures emerged from this band and were more common in the posterior teeth and interdentally. "Tenuously looped" capillaries with a coiled arterial component arose coronal to these glomerular structures. She did not state whether all of the posterior teeth showed these glomerular-like structures or whether there was variation between the different teeth. She thought they were part of the PDL, an opinion with which other authors including **WONG**

(1983), **WEEKES** (1983) and **LEE** (1988) disagreed. **KINDLOVA** (1965) did not describe how she classified the blood vessels nor did she mention the height of the capillary loops or any vessel dimensions. (Figure 3)

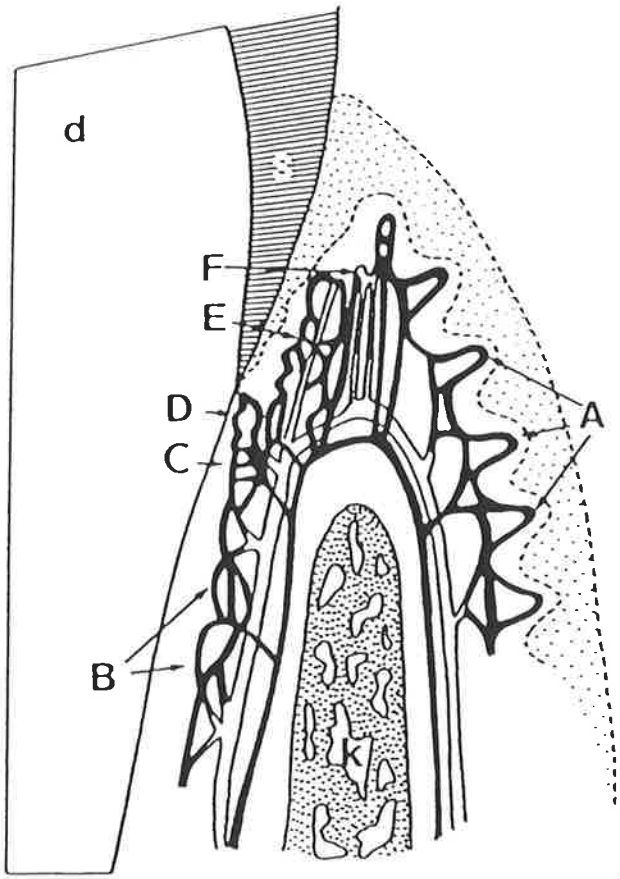

A = Subethelial capillary network of the gingiva.
B = Capillary network of the periodontal crevice.
C = Band of denser capillary network in the periodontal crevice.
D = Coiled capillaries representing glomeruli.
E = Capillary loops with the amply coiled arterial part.
F = Simple capillary loops.
s = Enamel.
d = Dentine.
k = Bone.

FIGURE 3: SCHEMATIC REPRESENTATION OF THE BLOOD SUPPLY OF THE MARGINAL PERIODONTIUM IN MONKEY. (KINDLOVA, 1965).

CASTELLI and **DEMPSTER** (1965) perfused *Macaca* rhesus monkeys with various substances. Three injection techniques were employed. The solutions used included india ink, Teichmann's paste coloured with cinnabar and a radio-opaque substance. The oral microvasculature was viewed histologically and with the use of a roentographic technique.

These authors noted that afferent arterioles to the PDL were less than 100 μm in diameter. In general, these vessels entered the PDL in the region of the apical two thirds of the root after passing through the cribriform plate. Once entering the PDL, these arterioles divided into capillaries forming a polyhedric plexiform pattern close to the cementum surface and orientated parallel to the long axis of the root. In the maxilla only, perforating arterial vessels from the gingiva were distributed to the labial aspect of the PDL, especially in the incisor region.

Venules presented as thicker, often irregular vessels which anastomosed with each other to form a mesh layer closer to the alveolar wall than the capillary layer. The veins of the PDL drained through the cribriform bony wall of the alveolus toward venous networks on the interradicular and interalveolar septa. Other veins increased in diameter as they coursed toward the root apex where they drained. Drainage in the coronal portion of the PDL and gingival crevice was seen to occur via anastomoses between PDL and gingival vessels.

India ink perfusion was used by **KENNEDY** (1969) to carry out a histological study of the PDL microvasculature in the squirrel monkey. Direct communication was seen occasionally between supraperiosteal vessels and PDL vessels. He found that in healthy animals, vascular connections between gingival and PDL blood vessels were seldom observed, confirming the observation made by **CARRANZA et al.** (1966), but conflicting with the report of **CASTELLI** and **DEMPSTER** (1965). The gingiva received its blood supply mainly from the supraperiosteal vessels as was also suggested by **FOLKE** and **STALLARD** (1967)

or any vessel dimensions. They did not find any relationship between the height of the loops and the possible function or physiology of the area.

LEE (1988) investigated the microvasculature of the palate, gingiva and PDL of the cotton ear marmoset using corrosion cast SEM stereopair micrographs. **LEE et al.** (1990) and **LEE et al.** (1991) have summarized many of these findings. The animals used by **LEE** (1988) were divided into two equal groups according to their age. The vascular architecture differed from region to region in the oral cavity, although bilateral symmetry was generally present with the left side being a mirror-image of the right. The principal findings of his study related to the maxillary and mandibular premolar and molar regions. (Figure 4)

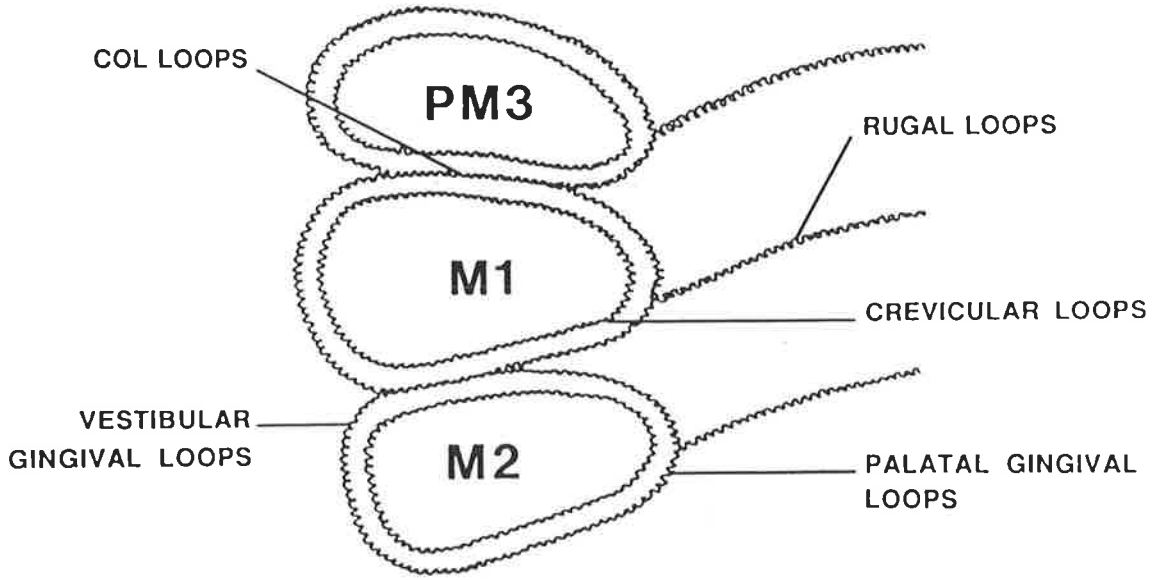

FIGURE 4: SCHEMATIC REPRESENTATION OF THE PALATAL AND VESTIBULAR LOOP SYSTEM OF THE MARGINAL GINGIVA OF THE MARMOSET. (LEE, 1988).

LEE (1988) described the crevicular vasculature of the marmoset's molars and premolars as being comprised of a plexus of vessels which encircled each tooth in the region of the junctional epithelium. A circular plexus consisted of a band of 1 to 4 vessels, varying from 10 to 25 μm in diameter. These vessels ran fairly parallel to each other and anastomosed with the crevicular loops above, and with nearby deep gingival and cervical PDL vessels. Drainage of all loops appeared to be into the ligament. (Figure 5)

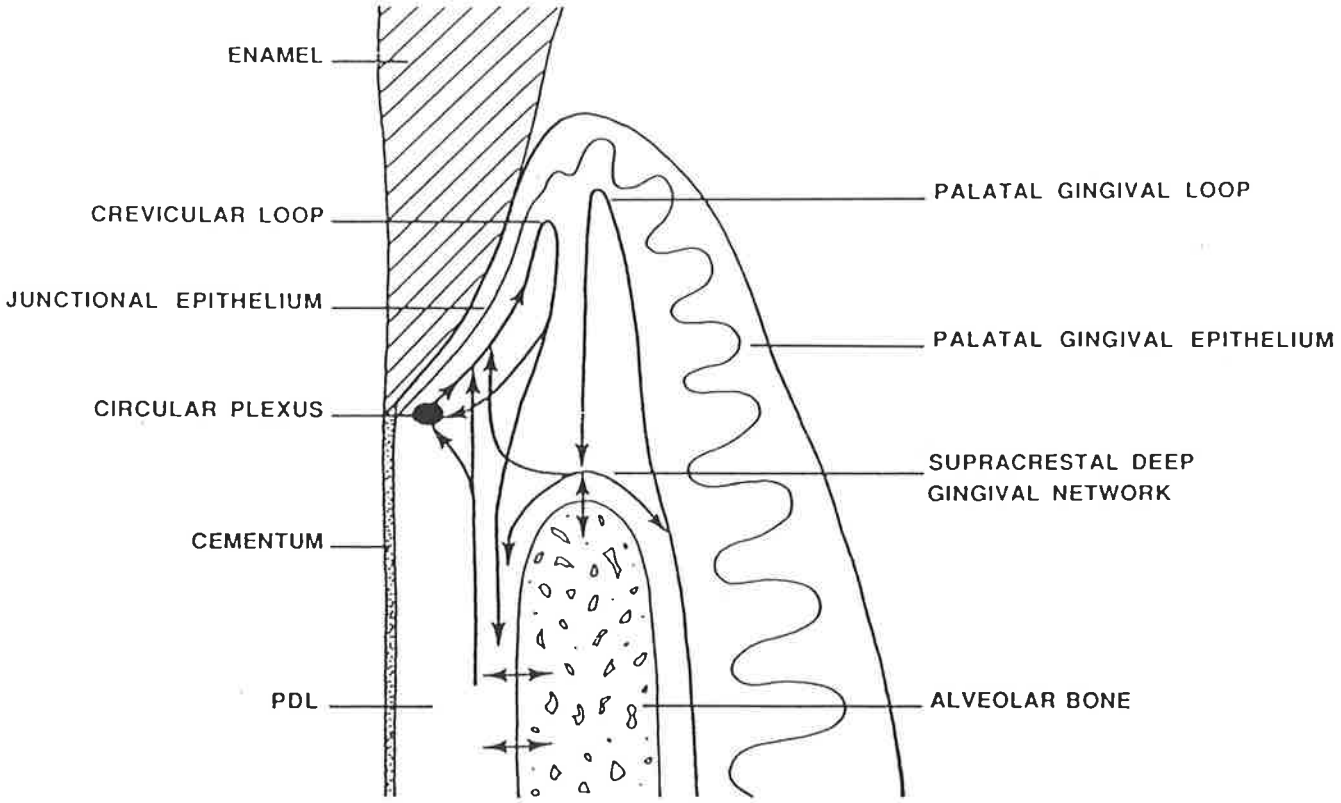

FIGURE 5: SCHEMATIC REPRESENTATION OF THE PRESUMPTIVE BLOOD FLOW IN THE PALATAL GINGIVA OF THE MARMOSET. (LEE, 1988).

Crevicular loops which varied from 10 to 30 μm in diameter and from 50 to 250 μm in height, were arranged in single or multiple rows around the posterior teeth above the level of the circular plexus. In general, they consisted of a larger diameter postcapillary-sized descending limb and a thinner ascending limb. These loops joined with capillaries in the circular plexus although some arose from deeper palatal or gingival vessels (**LEE**, 1988).

Oral gingival capillary loops surrounded the teeth to form a crest which corresponded with the gingival margin. These loops reduced in size from 60 to 120 μm down to 40 to 60 μm as they coursed towards the mucogingival junction. Some horizontal branching was seen between these loops, with anastomoses occurring at a deeper level. An arcade arrangement was found in the alveolar mucosa.

Deeper to the gingival capillary loops were larger vessels. Most were postcapillary-sized venules, 10 to 30 μm in diameter, which enlarged as they ran apically. Arterioles, 50 to 100 μm in diameter were less numerous and tapered off occlusally into smaller terminal vessels with diameters less than 50 μm. Vestibular and palatal loops merged in the interdental col area. Complex as well as simple loop structures were present in different regions around the tooth socket although **LEE** (1988) did not say exactly where.

The PDL vasculature of the premolar and molar teeth in the marmoset varied in different locations and at different levels. Apically directed postcapillary-sized venules drained from the circular plexus and crevicular loops. Terminal arterioles ran occlusally to supply the ascending limbs of the crevicular loops.

The PDL venules on the mesial and distal sides were arranged in a palisade formation with the vessels running occluso-apically. On the lingual side a more oblique orientation of vessels was seen. The arrangement on the labial side was not described by **LEE** (1988). Arterioles were seen to emerge from the alveolar bone and coursed occlusally. The venous network drained apically from the PDL to the

alveolar bone. Arterioles were found on either side of the venous network but were more common near the bone.

A capillary network linked PDL vessels to medullary vessels. These were less extensive than the venular arrangement. Hairpin-shaped capillary loops just apical to the circular plexus were occasionally seen and were mainly aligned apically. Annular constrictions were sometimes found at the base of the descending limb of these loops which suggested a sphincter-like function. In some loops the descending limb expanded rapidly to form a collecting-sized venule.

In the deeper part of the cervical PDL, the vessels had a plexiform arrangement with many anastomoses. The vessels in the middle third of the ligament mainly consisted of occlusoapically orientated venules 20 to 30 μm in diameter. They anastomosed with each other and with medullary vessels.

Vessels in the apical third of the ligament formed a basket-like arrangement around the apex. A network of postcapillary-sized venules was seen near the root surface with a capillary network adjacent to the alveolar bone. The vessels were closer together, were larger and anastomoses occurred more frequently. Anastomoses also occurred between the PDL vessels and the pulpal vessels at the apex. These vessels did not form a common trunk, but perforated the cribriform plate as small branches (**LEE**, 1988).

E. ORAL MICROVASCULATURE IN OTHER ANIMALS

The oral microvasculature of other animals such as dogs, cats, rabbits, opossums, hamsters and guinea pigs has been studied in the past. **WEDL** (1881) described the presence of coiled capillaries resembling renal glomeruli in the cervical part of the PDL of the cat, dog, hare, guinea pig and calf. He suggested that these structures function as coiled springs acting against the masticatory load.

SCHWEITZER (1909) suggested that the PDL vessels in man, monkey, dog, hare and sheep anastomose freely with those supplying the adjacent bone and gingiva. He stated that the main PDL vessels run close to the bony wall and ramify in the marginal periodontium.

Of the animals mentioned above, the dog's oral microvasculature has been examined most extensively. **EGELBERG** (1966) looked at the arrangement of gingival vessels at the dento-gingival junction after perfusion with a carbon-gelatin mixture. He found in clinically healthy gingiva, a plexus of blood vessels close to the crevicular epithelium. This plexus extended under the entire surface of the crevicular epithelium, from the gingival margin to the base of the crevice. Vessel diameters ranged from 7 to 40 μm. Capillary loops present in the oral epithelium were absent in the crevicular plexus except at the margins. The crevicular vessels were thought to be mainly of a venular type. A classification of vessel type in relation to vessel size was not described.

KISHI and **TAKASHI** (1977) studied dog PDL corrosion casts in the SEM. They found a dual plexus or bilaminar arrangement of vessels running occluso-apically. The layer closer to the bone consisted of arterioles and venules passing to and from the PDL. A rope, ladder-like layer closer to the tooth had a vertical arrangement of capillaries. Many hairpin-shaped capillary loops were present in the cervical portion of this layer. Above the alveolar crest both layers fused to provide a fine vascular plexus under the crevicular epithelium. In the apical third of the PDL numerous arterial-venous, arterial-arterial and venous-venous anastomoses were present.

KISHI et al. (1986a) also used corrosion casts to look at the gingival and mucosal microvasculature in dogs. They found capillary loops which were mainly hairpin in shape on the vestibular surface of the gingiva. The site and orientation of these were not described, they did not state which regions of the mouth were

examined, nor did they use stereopairs. They did note that the capillary network was denser in the alveolar mucosa and different in arrangement compared to that of the gingiva. In the alveolar mucosa capillary loops were short and few in number.

Finally, in relation to dogs, **NOBUTO et al.** (1987) used SEM corrosion casts and histological sections to look at the microvascularization of gingival wound healing. They described the normal mucosa of dogs as having a supraperiosteal plexus and an overlying subpapillary plexus of blood vessels. The supraperiosteal plexus and medullary vessels anastomosed via Volkmann canals with the supraperiosteal plexus and communicated with the PDL plexus at the alveolar crest. Hairpin capillary loops were found to go from the subpapillary plexus and extend into the connective tissue papilla. Loops in the free and attached gingiva were similar in height, but at the mucogingival junction the loops in the alveolar mucosa became suddenly shorter, displaying a flat, net-like structure.

COHEN (1960) looked at the vascular architecture of the mandible in cats under the light microscope after perfusing them with a carbon-gelatin mixture. He felt that the inferior dental artery was the principal nutrient artery to the mandible and that anastomoses existed between this artery and the periosteal blood vessels. He noted that the PDL was supplied by vessels from the apical region of the tooth, from the alveolar bone and from the gingival tissue.

BOYER and **NEPTUNE** (1962) perfused the blood vessels of rats, rabbits, opossums and hampsters with potassium dichromate and lead acetate. The tissues were embedded in plastic, sectioned and viewed under the light microscope. They concluded that essentially, the blood supply of the teeth of these animals showed a striking similarity, if minor differences in the shape of the teeth, mandible and maxilla were disregarded. The blood supply of the teeth originated from periosteal vessels, from vessels emanating from the medullary portion of the adjacent surrounding bone, from vessels which supplied adjacent or closely related

musculature, and from intrinsic named arteries, such as the superior alveolar or the inferior alveolar arteries.

CARRANZA et al. (1966) undertook a comparative study of PDL vasculature in mice, rats, hampsters, guinea pigs, cats and dogs. They found that the PDL of these animals had a similar distribution of blood vessels. They did not discuss the differences. However, the principal vessels in the PDL ran parallel to the long axis of the root and gave out branches that intertwined forming a PDL plexus. This plexus of blood vessels was closer to the alveolar bone than to the root surface. This feature was also confirmed by **FREEMAN** and **TEN CATE** (1971).

Blood vessels entered the PDL via the alveolar bone and ran occluso-apically. These vessels were more commonly seen in the middle and apical thirds. Connections were seen between PDL and pulpal blood vessels. However, connections between gingival and PDL blood vessels were rare. Vascular loops formed a circumferential plexus close to the epithelial cuff. The authors could not relate these loops to any circular band that was previously described by **KINDLOVA** and **MATENA** (1962) and **KINDLOVA** (1965).

3.5 RECENT DEVELOPMENTS IN RELATION TO ORAL MICROVASCULATURE

Unlike the rapid gains shown in the corrosion casting technique, interest in the oral microvascular distribution and structure of various animal species has almost ceased. Apart from the study provided by **LEE et al.** (1991) on the oral microvasculature of the marmoset, the current author has noted very few recent articles which deal with this topic. **BERKOVITZ** (1990) in his review of the PDL did not provide any new information in relation to its microvascular distribution and structure. Most of the references quoted on the PDL vasculature were either from

the seventies or early eighties and none were in relation to its microvascular distribution and structure.

NOBUTO et al. (1989a) used corrosion casts and the SEM to look at the microvasculature immediately beneath the epithelium in healthy dog gingiva. They described capillaries in the free gingiva as being arranged in an arcade-like fashion, whereas loop-shaped structures were found in the attached gingiva and a net-like structure in the alveolar mucosa. They felt that the morphology of the connective tissue reflected that of the capillaries within, presenting characteristic morphological differences depending on the area of tissue being observed.

NOBUTO et al. (1989b) attempted to look at the three-dimensional distribution of blood vessels within the gingival periosteum beneath the alveolar mucosa of adult mongrel dogs. Corrosion cast specimens of the vessels were observed from three-directions: from the mucosal side, the bone side, and from a horizontally cut surface. They observed each histological layer by removing the layers of the casts one-by-one from the epithelial side with forceps, under a stereoscopic microscope. The specimens were also frozen in ice while the horizontal cutting was carried out. They noted that a flat plexus of vessels distributed in the periosteum of the gingiva formed a coarse network structure and consisted mainly of arterioles and venules which were arranged in a relatively linear fashion. In the periosteum of the alveolar mucosa, a dense network arrangement consisted of arterioles, capillaries, and venules which formed a vascular bed. The mucogingival junction could be easily found even in the plexus of periosteum which was located beneath the gingiva and the alveolar mucosa. They felt that the difference in tissue specificity was reflected in the plexus of the periosteum.

KAI (1989) studied the microvasculature of dog PDL affected with chronic marginal periodontitis using corrosion casts. The following was noted:

1. The vasculature of the inner gingival epithelium which originally appeared as a flat, mesh-like network underwent conformational change and turned out to be a vasculature with glomerulus-like loops due to chronic inflammation.

2. No remarkable change was ever identified in the vasculature of the PDL surrounding the cervical portion of the tooth.

3. Certain parts of the PDL disappeared which, when combined with the occlusion indicated the occurrence of occlusal trauma.

KAWATO (1989) studied dog PDL microvasculature after tooth extrusion using corrosion casts. Results were obtained at 3 days, 7 days, 14 days, 21 days, 30 days and 60 days post-extrusion. Only the abstract was available in English and the amount of extrusion was not stated. The following changes were observed:

1. At 3 days post-extrusion, various types of vascular networks showing a looped pattern were seen along the direction of the tooth movement.

2. At 7 days post-extrusion, various types of vascular networks with a hairpin loop pattern along the direction of the tooth movement.

3. At 14 days post-extrusion, a much more extensive and developed hairpin loop pattern occurred.

4. At 21 days post-extrusion, the tooth side microvascular network showed abundant hairpin loops which anastomosed with each other.

5. At 30 days post-extrusion, the PDL vascular network showed an almost normal appearance.

6. At 60 days post-extrusion, the PDL vascular network completed its rearrangement and showed a normal appearance.

TORISU (1989) studied dog PDL and alveolar bone changes in relation to occlusal trauma using corrosion casts and the SEM. Occlusal trauma was experimentally induced by adding composite resin to the occlusal surfaces of the mandibular second and third premolars. The teeth showed increased mobility especially in the vertical direction and expansion of the PDL space occurred due to resorption of the alveolar process. The following changes to the PDL were observed:

1. After 14 days, a wide range of avascularized area was observed on the resin cast of the PDL.

2. After 30 days, the vasculature of the PDL underwent morphological change and turned out to appear as a mesh-like vascular network. The cervical region was circumscribed by a vasculature with glomerular-like loops.

3. After 60 days, the vasculature of the PDL facing the teeth appeared similar to that of a healthy periodontal membrane, whereas those next to the alveolar bone showed enlargement.

4. After 90 days, the vasculature in the PDL lost its original two-layered arrangement and was replaced by an irregular arrayed bundle-like vasculature.

5. After 180 days, bundle-like vessels arrayed as an ellipse pattern. The resorption process could be observed on the surface of the alveolar bone and interradicular septum.

AHARINEJAD et al. (1990) studied the microvasculature of the mandible and the mandibular molar teeth in 40 adult male and female albino guinea pigs. Corrosion casts and the SEM were used. Alveolar precapillaries had an average diameter of about 20 μm whereas PDL vessels averaged 30 μm and formed smaller and greater ring-shaped anastomoses. Periodontal precapillaries were tightly packed although they were less closely spaced on the lingual aspect than on the buccal. Pulp capillaries formed cylindrical structures which they called "capillary cords". Para-alveolar capillary convolutions with a "glomus-like" appearance were found lying between the alveoli and the PDL. They felt that these "glomera" contained arteriovenous anastomoses which may be involved in controlling the PDL blood flow during masticatory movements. Opening of the anastomoses would allow blood to flow to the venous side of the circulation without prior exchange processes with extravascular tissue so that blood pressure on the venous side would be increased.

AHARINEJAD et al. (1990) provided photographic evidence to support their hypothesis in relation to these arterial-venous anastomoses. However, no mention was made as to which side of the tooth socket was being viewed. The current author is not convinced that an arterial-venous anastomosis was present. The

branching pattern suggested that both vessels were venules with an adjoining venous-venous connection. The overall appearance of both vessels was similar, the endothelial imprint patterns were indistinct in the photographs presented as the 5 kV used was insufficient for accurate identification. The corrosion cast had been extensively damaged, had many contaminants and was also poorly cast with many vessels being missing.

AHARINEJAD et al. (1991) looked at the vasculature of the digestive tract (including the teeth) in 150 albino guinea pigs - Cavia porcellus, 50 Sprague Dawley rats, and 10 New Zealand white rabbits. Both sexes were included, with corrosion casts being viewed in the SEM. An extensive literature review was also provided in this article.

All diagrams concerning the PDL were of the guinea pig. Brief mention was made of the rat and rabbit PDL and the teeth examined were not specified. No mention was made as to whether there was any age or sex difference, whether there were differences between the maxilla and mandible or whether both were examined. Animal variability was also not mentioned.

The diagrams included appear to depict the arterial-venous anastomoses described previously by **AHARINEJAD et al.** (1990) although they were not consistent with the vessels viewed in the earlier article. Only one side of the socket was represented in this diagram and no mention was made as to whether these structures were present around the socket. No mention was made as to whether these arterial-venous anastomoses were found in every socket or whether this was a once off occurrence. They hypothesized that: "as pressure built up in the alveolar pocket, the collagen fibers of the PDL were compressed so that more blood could flow into the glomerula. The resultant blood-filled saccular spaces served as buffers counteracting the pressure built-up. Conversely, the arterial-venous anastomoses were thought to control flow in the PDL, as they channelled the blood towards the

venous side in their uncompressed state so that it was removed from the exchange processes in the interstitial spaces".

Finally under this section, **LEE et al.** (1990) in a delayed publication and as an extension to the paper by **LEE et al.** (1991) described the vascular architecture of the nasopalatine foramen, soft palate and gingival regions of the marmoset using SEM stereopair imaging of corrosion casts.

They suggested that the crevicular vasculature differed significantly in the anterior teeth compared to the molars and premolars. In the upper and lower canines and incisors the crevicular vasculature was made up of "complex anastomosing structures forming bulb-shaped formations resembling renal glomeruli". Height of these vascular structures ranged from 100 to 300 μm with maximum diameters being between 40 to 160 μm.

The location of these complex crevicular loop structures around the tooth sockets, the differences between the young and mature animals studied and between the maxillary and mandibular teeth, were not described. No mention was made as to whether other crevicular loop structures were found in the anterior sockets.

CHAPTER 4

MATERIALS AND METHODS

4.1 SELECTION OF A SUITABLE ANIMAL MODEL

The female cotton ear marmoset (*Callithrix jacchus*) was used in this study. **HILL** (1957), and **JAMES** (1960) described marmosets as being New World primates. They also described them as being platyrrhine (broad nosed) monkeys that belong to the suborder Anthropoidea, the infraorder Platyrrhini, the superfamily Ceboidea and the family Callithricidae.

The corrosion casts used in this investigation were originally processed by **LEE** (1988) while looking at the vascular architecture of the palate, gingiva and PDL of the posterior teeth. The unexamined anterior segments were examined in this study. **LEE** (1988) selected eight healthy young female cotton ear marmosets in his study and arranged them into two equal groups according to their age. By selecting these two groups it was hoped that an age comparison could be made. Unfortunately the palatal plexus in the older animals for some reason was incompletely cast and an age comparison of this area was not made. The two groups were as follows:

(a) Group I consisted of young adult females who were aged between 18 to 24 months.

(b) Group II consisted of older adult females aged from 4 to 7 years.

The cotton ear marmoset's have the following dentition:

(a) Deciduous dentition: $\frac{2}{2}I\text{-}, \frac{1}{1}C\text{-}, \frac{3}{3}M\text{-}.$

(b) Permanent dentition: $\frac{2}{2}I - , \frac{1}{1}C - , \frac{3}{3}PM - , \frac{2}{2}M - .$

In the permanent dentition the incisors, canines and premolars are single-rooted. In the mandibular arch the molars are two-rooted and in the maxillary arch the molars are three-rooted (**SHAW** and **AUSKAPS**, 1954).

The unavailability of unprocessed human PDL and gingival tissues to carry out extensive studies on its vascular system led **LEE** (1988) to look for a suitable alternative model. The alternative model would need to react to environmental factors in a similar way to man.

The cotton ear marmoset was selected as an alternative to the human model for the following reasons:

(a) The cotton ear marmoset is small and easy to handle and only weighs between 250 gms to 500 gms at maturity. They reach physical maturity reasonably quickly at between 12 to 18 months of age and have an estimated life span of 15 years in captivity (**LEVY et al.**, 1972a). They are readily available, are easy to breed in captivity and it could be argued are relatively inexpensive to acquire.

(b) **LEVY et al.** (1972a) described the dental apparatus of the marmoset as being comparable to that in man. They found that marmoset gingiva was also comparable to that in man in that it consisted of both free and attached gingiva, with a free gingival groove in between.

(c) **WILSON** and **GARDNER** (1982) from postmortem studies of the temporomandibular joint of the common marmoset showed that joint movements were similar to those in man. They consisted of hinge movements in the lower joint cavity and sliding movements in the upper joint cavity.

(d) **LEVY** (1971) and **LEVY et al.** (1972a) in studying the natural progression of periodontal disease in the marmoset felt that its behaviour was similar to that described in man. They noted that bacterial plaque and calculus form on the marmoset teeth as they do in man. They also found that the gingival tissues of the marmoset exhibited similar reactions to trauma as do gingival tissues in man. Also, chronic destructive periodontitis was similar in the marmoset and man.

(e) **LEVY et al.** (1970) and **LEVY et al.** (1972b) found that age changes in the periodontal tissues of both man and marmoset were similar.

4.2 CARE OF THE MARMOSETS BEFORE PROCESSING

LEE (1988) initially scaled and brushed the marmoset's teeth while the animals were under the surgical anaesthetic, Saffan. They were kept in an animal house under controlled conditions and fed a specially prepared diet.

The animal's teeth were cleaned on a regular basis initially using a toothbrush and 0.2% chlorhexidine digluconate. This solution was applied three times per week for the first three months in an attempt to maintain and improve their gingival condition. The gingival condition, especially with the older animals, did not improve and it was decided to abandon the cleaning routine about a month before the animals were sacrificed.

4.3 ANAESTHESIA USED

The animals were first weighed and then injected intramuscularly with Saffan (alphaxalone alphadone acetate, 19.5 mg./kg. body weight) into the thigh quadriceps muscle as suggested by **PHILLIPS** and **GRIST** (1975). **LEE** (1988) noted that some animals took longer than others to become anaesthetized, the depth of anaesthesia was tested by touching the cornea of the eye.

4.4 DISSECTION OF THE MARMOSETS

The technique used for obtaining corrosion casts has been described by others including **GANNON** (1978), **HODDE** and **NOWELL** (1980), **LAMETSCHWANDTNER et al.** (1984), and more recently by **LAMETSCHWANDTNER et al.** (1990). **LEE** (1988) described the technique he used as follows:

> **(a)** First, the selected animal was anaesthetized, the femoral vein being exposed by dissection and 40 IU of heparin were given through the femoral vein to prevent blood clotting.

(b) Next, the neck was dissected with the left and right carotid arteries being identified. A section of about 2 cm of each vessel was isolated and dissected free of fascia and fat with black silk sutures being loosely looped at the caudal and rostral ends.

(c) An incomplete oblique cut was made in one of these vessels and a cannula placed in a rostral direction. The cannula was secured tightly rostrally and caudally to the vessel. Back flow of blood was prevented by pressurizing to 60 mm./Hg the aspirating bottle that was attached to the cannula. The tubing was then clamped using haemostats and the procedure repeated for the other common carotid artery.

(d) A horizontal incision was made in the abdomen just below the xiphoid cartilage. This enabled the diaphragm to be dissected from the rib cage, the rib cage being cut with coarse scissors in the midaxial line up to the axilla on both sides. Haemostats were then used to hold the rib cage upwards and away from the vessels of interest.

(e) The inferior vena cava was identified with a 2 cm section of vessel dissected free of fascia and fat. An incomplete oblique cut was made and the vessel was cannulated. Black silk sutures looped loosely at the rostral and caudal ends were tightly tied. In this case the cannula allowed egress of blood to be carefully monitored.

(f) Finally, the heart was cleared of fascia and fat with black silk sutures being tied around the aorta and pulmonary arteries at the base of the heart. This restricted the flow of perfusate to the areas of interest and prevented it from going into the pulmonary and general circulations.

4.5 PERFUSION APPARATUS

The perfusion equiptment used by **LEE** (1988) to assist with blood washout and resin casting was a modification of the equiptment used by **GANNON** (1978). The system consisted of a one litre aspiration bottle that provided a controlled pressure unit with a spout at the bottom. An air pressure regulator allowed the aspirator bottle to be pressurized between 0 and 300 mm/Hg. The pressure in the bottle was measured using a mercury manometer attached to the system via plastic tubing.

A three-way stopcock was connected via tubing to the aspirating bottle. This enabled the system to be shut off when it was not required to perfuse from the aspirating bottle. The spout of the stopcock was connected to an 18 gauge needle

hub with the needle shaft being inserted into the beginning of a series of tubing that had reducing diameters. After several centimeters, the tubing divided at a Y-junction to give rise to two smaller diameter tubes. The tubing then reduced in diameter several times until quite small diameter cannulae were reached. The ends of these two cannulae were attached to the left and right common carotid arteries.

Once the animal's blood had been washed out, the 18 gauge needle hub was removed from the spout to allow a 20 ml syringe of either fixative or resin to be attached to the 18 gauge needle and the rest of the plastic tubing. (Figure 6)

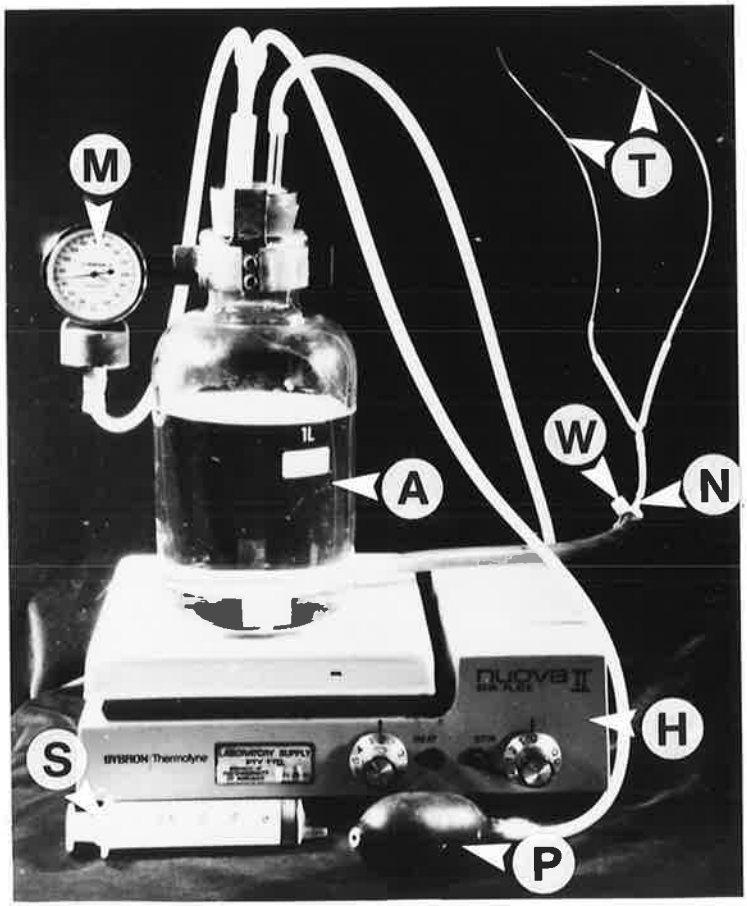

A = Aspirating bottle.
H = Magnetic stirrer and heater.
M = Mercury manometer,
N = 18G needle attached to a spout.
P = Air pressure regulator.
S = 20 ml syringe.
T = Tubing.
W = Three-way stopcock.

FIGURE 6: PERFUSION APPARATUS USED BY LEE (1988).
(Photograph supplied courtesy of David Lee)

4.6 BLOOD WASHOUT SOLUTION

A blood washout solution was made up prior to perfusing the marmosets via the common carotid arteries. A 300 ml solution was freshly prepared just before the animal was to be processed. The composition of one litre of the washout solution was described by **LEE** (1988) as follows:

(a) Double-distilled water	1000.00 millilitres
(b) Heparin (1000 IU/ml)	5.00 millilitres
(c) Papaverine HCL (12 mgm/ml)	0.10 millilitres
(d) PVP-40	58.74 grams
(e) Sodium Chloride	9.00 grams
(f) Sodium Nitrite	0.07 grams

The freshly prepared blood washout solution was filtered through a 0.22 μm Membra-Fil filter. This removed minute particles which could cause blockage to the small vessels and incomplete casting. Once the solution had been filtered it was heated in a magnetic stirrer to a temperature of between 37 to 40 ^{o}C.

GANNON (1978) described the function of polyvinyl-pyrrolidone (PVP-40) in the blood washout solution as providing a blood colloidal osmotic pressure of 25 mm/Hg. Sodium nitrite and papaverine HCL acted as vasodilators while heparin was used as an anticoagulant to prevent clot and thrombosis formation which would result in vessel blockage and incomplete casting.

4.7 VASCULAR CASTING RESIN

The Mercox casting resin was obtained from Japan. **LEE** (1988) prepared the resin by mixing 20.0 ml of polymethyl methacrylate Mercox resin with 0.5 gm of catalyst paste.

HODDE et al. (1977) described the resin as setting quickly under pressure and in the absence of oxygen. It had a viscosity of about 36 centistokes which could be measured with a modified Oswald's viscometer. Shrinkage occurred during polymerization and the surface remained sticky.

4.8 PERFUSION TECHNIQUE

The dissection and perfusion techniques were practised and modified by **LEE** (1988) by using rats and a number of dead marmosets. Once the technique had been mastered the eight cotton ear marmosets were anaethetized one at a time.

After each marmoset had been anaesthetized the carotid arteries and inferior vena cava were exposed and cannulated. As the pressure in the aspirating bottle was raised to about 240 mm/Hg the clamps on the tubing were slowly released thereby allowing the washout solution to perfuse through the animal's blood vessels. The site of cannulation was checked for leakage as the solution passed through the vessels.

The pressure in the aspirating bottle was increased to 300 mm/Hg and then maintained while the blood drained out of the inferior vena cava until only a clear egress was seen. The washout was continued for another 10 minutes to ensure that all blood was removed from the oral tissues and cephalic vascular system. The tongue and gingiva were observed to turn pale as the blood was forced out of the vascular system by the washout solution.

Once the blood washout phase was complete, a 20 ml syringe was filled with 1% glutaraldehyde fixative prepared in 0.1M phosphate buffer. It was inserted into the three-way stopcock with the tap being turned so that the fixative could be syringed into the vascular system. Care was taken not to introduce air into the tubing as this would cause blockages to the tiny blood vessels. Hand pressure was used to perfuse the fixative through the animal. It was noted that at this stage the

animal would go into spasm with its eyes turning yellow as the solution perfused through the tissues. Once all of the fixative was syringed into the vascular system the animal was perfused for another 10 minutes with washout solution.

The Mercox casting resin was mixed during the final phases of the blood washout. A 20 ml syringe was loaded with resin and connected to the 18 gauge needle hub attached to the three-way stopcock. The resin was then perfused through the animal with hand pressure taking care not to introduce air bubbles. Before all of the resin was syringed into the vessels, the inferior vena cava and common carotid artery inlets were clamped so that pressure was maintained in the system and so that the casting resin was not allowed to flow out of the vessels before it had time to set.

After perfusion of the casting resin was complete, the marmoset was then immersed in a warm 50 ^{o}C water bath. The marmoset was left in the bath for 24 hours to ensure that the casting resin was completely polymerized. This immersion also prevented dessication and shrinkage of the specimen and softened the tissue thereby making tissue maceration easier.

4.9 TISSUE CORROSION

The next step and the one that could span from a couple of weeks to several months was the process known as tissue corrosion. Once the resin had completely polymerized the marmoset was beheaded, the mandible and maxilla being dissected out and placed in 10% hydrochloric acid. **LEE** (1988) then changed the solutions daily for 3 to 4 days to enable the hard tissues to decalcify. Once decalcification was complete the specimens were rinsed in distilled water for 15 minutes and then placed in a freezer for at least 4 hours to allow for partial freezing. This would allow the specimen to be sectioned and excess tissue removed without causing damage to the cast.

Excess tissue was removed from the frozen specimens using sharp safety razor blades. The jaws were then sectioned sagittally across the midline and coronally across a premolar socket with the assistance of the saftey razor blades. The soft tissue was macerated by placing the specimens in fresh 10% potassium hydroxide (KOH) solution in a 37 ^{o}C oven for 24 hours.

The tissue maceration technique that was described by **HODDE et al.** (1977) was followed. The specimens were rinsed on alternate days with warm distilled water and on alternate days with fresh 10% solution of KOH. This alternate rinsing helped with the maceration process and was repeated until the tissue was removed from the resin casts. This process took from 2 weeks to several months.

Once it was thought that all of the tissue had been removed the casts were then rinsed in double-distilled water containing a few drops of detergent. The detergent was used to help reduce the surface tension of the water so that the corrosion casts did not distort by surface tension during the drying process. The corrosion casts were allowed to dry on filter paper in a closed container to prevent dust contamination.

Once dried, the corrosion casts were assessed under the stereo-dissecting microscope to determine their cleanliness, completeness and morphology. **GANNON** (1978) suggested that a knowledge of the anatomy of the specimen at the light microscope level facilitated the interpretation of the corrosion casts in the SEM. It also helped to orientate the specimen more quickly to the area of interest in the SEM.

4.10 MOUNTING OF THE SECTIONED CASTS

The corrosion casts were viewed under the stereo-dissecting microscope to determine the best way for them to be mounted on the SEM stubs (**LEE**, 1988).

One centimeter aluminium SEM stubs were selected and double sided adhesive tape stuck onto the mounting surface. The corrosion casts were then secured on to the SEM stubs using silver colloid conductive paste. The corrosion casts were orientated to facilitate SEM viewing and care was taken not to use excessive colloidal silver as it tended to spread over the cast and cover up the area of interest.

4.11 COATING THE CASTS WITH A CONDUCTIVE OSMIUM LAYER

For SEM examination the specimen needed to be conductive to electrons. In the case of the corrosion casts the resin was non-conductive to electrons. To overcome this problem, **LEE** (1988) treated the dry corrosion casts with vapourized osmium. This technique was initially suggested by **MURAKAMI et al.** (1973) and ensured that complete conductivity of the specimens was achieved thereby assisting in producing good, contrasted images in the SEM.

The conductive layer of osmium prevented charge build up on the specimen by facilitating the grounding of the primary electron beam. It also gave off secondary electrons that helped produce a good SEM image.

The mounted specimens were placed on a glass rack in a sealed glass jar and their positions noted. An ampoule of osmium tetroxide was then broken in the sealed glass jar which was housed in a fume cupboard. The glass rack containing the specimens was inserted into the glass jar and sealed there for 48 to 72 hours. The glass rack was then transferred to an unsealed jar in the fume cupboard for about 1 hour to allow the vapours of osmium tetroxide to subside.

4.12 COATING THE CASTS WITH A LAYER OF CARBON AND GOLD/PALLADIUM

HODDE and **NOWELL** (1980) described a technique whereby corrosion casts were coated with vapourized carbon and gold/palladium alloy intermittently for a total of 6 minutes. The specimens processed by **LEE** (1988) had this layer applied to them. They were coated evenly by continuously tilting and rotating the SEM stubs as the coating was applied. The layer helped prevent charge build up during examination in the SEM as well as increasing the electrical and thermal conductivity of the corrosion cast.

4.13 SECTIONING THE CORROSION CASTS

LAMETSCHWANDTNER et al. (1990) in their article described several techniques whereby corrosion casts could be dissected. A brief description of these dissection techniques is as follows:

(a) The corrosion cast can be dissected after the casting medium has hardened but before the tissue maceration stage. The organ or tissue of interest can be excised with some of the surrounding tissue. The tissues of interest can then be macerated and the cast cleaned.

(b) The corrosion cast can be dissected during rinsing in distilled or tap water using the stereo-dissecting microscope to view. The instruments used to do the dissecting were not discussed.

(c) The cast can be dissected after it has been frozen (ice embedded) using razor blades. The frozen cast could be cut using a band saw or for small specimens a mini wheel-saw placed in a cryomicrotome.

(d) They can be cut after they have been embedded in gelatine or after being frozen in liquid nitrogen.

(e) They can be dissected using a micromanipulator or freehand after they have been dried and/or after they have been mounted.

(f) Consecutive layers could be removed using very fine tweezers and small scissors. Adequate micrographs need to be taken before the next layer is dissected.

(g) Dissection within the SEM chamber using a micromanipulator.

(h) Dissection of the dried casts using razor blades. There is a high risk of damaging the casts with this technique.

(i) Using lasers to burn/vapourize through the cast material. The laser beam tends to melt the surface of the cast due to its inability to be focussed accurately.

Most of the specimens used by **LEE** (1988) were sectioned before the tissue corrosion phase using sharp safety razor blades. Many of the jaw specimens were sectioned sagittally across the midline and coronally across a premolar sockets. Occasionally when a tooth socket or some other part of the casting needed to be viewed from a different direction, the unmounted specimen was immersed in a small container of double distilled water. A drop of detergent was added as a wetting agent and the specimen frozen. Using razor blades the ice would be cut through with a slow sawing motion. The ice helped to prevent the fragile corrosion cast from being damaged during sectioning.

The current author was using the corrosion casts of **LEE** (1988) that in the majority of cases had already been mounted on SEM stubs using double sided adhesive and colloidal silver. These casts had been coated with vapourized carbon and gold/palladium alloy. Immersing them in double-distilled water resulted in small air bubbles being trapped in and around the casting. Attempting to freeze the casts caused these bubbles to expand resulting in fogging of the ice. Using a wetting agent and warming the water reduced this problem, although it was still difficult to accurately section the frozen specimen. A method therefore needed to be found whereby the air bubbles trapped around the immersed casts could be removed.

A. DISSECTING TECHNIQUES ATTEMPTED

i. Dissection Using Lasers

To try and improve the visibility of the specimen when cutting, the current author looked at the possibility of using the newly developed American Dental

Laser. These lasers used the pulsed YAG (neodymium yitrium-aluminium-garnet) system which generates an invisible infrared beam. A visible aiming beam, coaxial with the YAG system was provided by a HeNe (helium neon) laser. The pulse rate could be altered from 10 to 30 times per second to minimize the accumulation of heat to the tissue. Beam diameter was fixed at 300 μm. The power could be altered so that an average of up to 3 watts could be delivered. To avoid eye damage from the bright light of the dental laser, saftey glasses had to be worn. Even with the wearing of these glasses the light beam was very bright.

In an attempt to improve on the beam size available with the American Dental Laser, a larger CO_2 Sharp Plan Laser, with variable power output and beam diameter was tested. This laser was manufactured by Sharp and was being used in one of the local hospitals. It could be programmed so that the beam would follow a predetermined path. The beam diameter could be reduced to only 100 μm, and the pulse rate had a greater range over the smaller American Dental Laser.

ii. Dissection Using Fine Instruments

The technique was also examined whereby some of the specimen was removed using very fine tweezers and small spring scissors so that the area of interest could be viewed. The mounted specimen was placed into a small resin block in which a hole had been drilled in the centre. The casting resin block measured approximately 3 cm by 3 cm by 1 cm high. The specimen was then viewed under the stereo-dissecting microscope and the casting gently tweezered away until the area of interest could be seen. The resin block enabled the operator's fingers to be supported while the fine dissecting work was being carried out. The resin block also meant that the SEM stub was being held firmly thereby reducing the chance of accidentally dropping the specimen. Care was needed not to pull on the cast with the tweezers but to only break the casting away like breaking twigs

from a tree. The cast was gently blown with a rubber camera lens blower to remove any surplus pieces of casting that were broken off. (Figure 7)

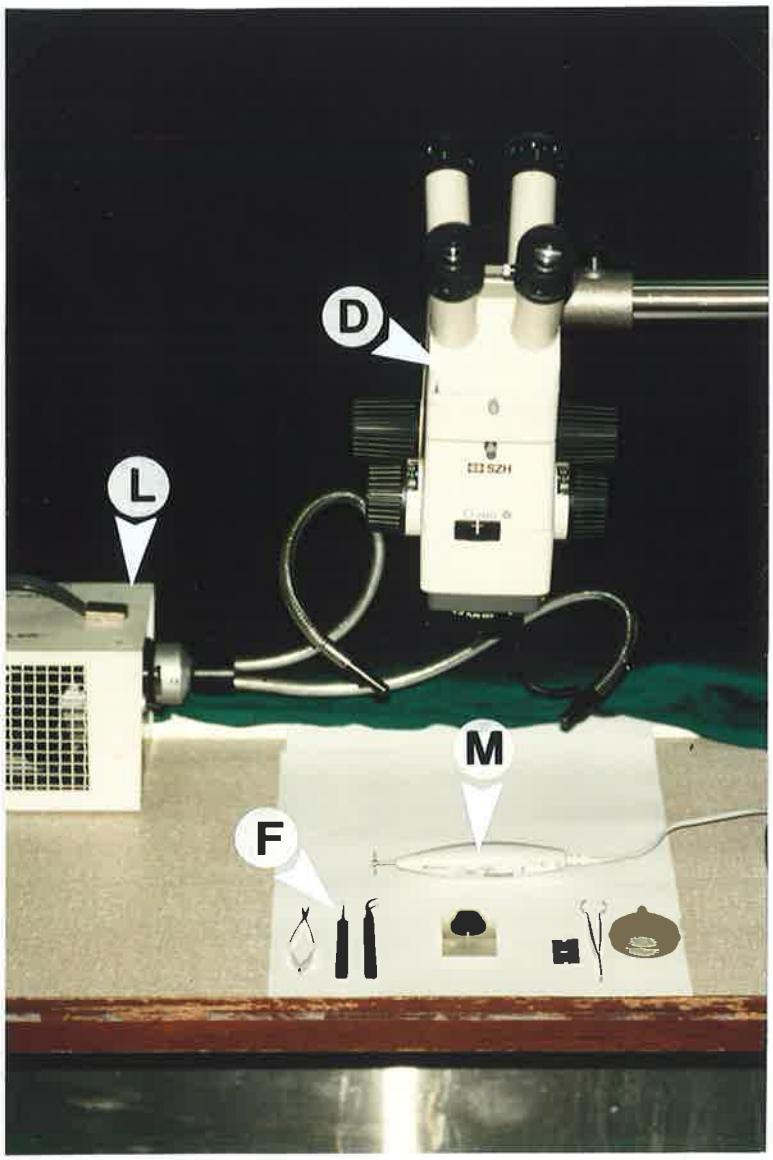

D = Dissecting microscope.
F = Fine dissecting instruments.
L = Fibre-optic light source.
M = Mini-motor and diamond cutting wheel.

FIGURE 7: DISSECTING MICROSCOPE, MINI MOTOR AND DIAMOND CUTTING WHEEL, FINE DISSECTING INSTRUMENTS.

iii. Dissection of Fozen "Ice Embedded" Casts using a Mini-Motor and Diamond Cutting Wheel

To gain further information in relation to the technique developed by **LAMETSCHWANDTNER et al.** (1990) whereby a "mini wheel-saw" was used to cut through ice embedded casts, the current author wrote to professor A. Lametschwantner (March 1992). In reply, it was suggested that to overcome the problem of air bubble entrapment when the cast was frozen, the cast immersed in double distilled water should first be evacuated. This may need to be repeated several times until all the air bubbles trapped around the cast were released.

The mini-motor used by Professor A. Lametschwandtner could be obtained from any hobby store. It was clamped in the cryomicrotome chamber so that the cutting wheel could be viewed through the stereo-dissecting microscope. The ice embedded cast was then passed across the cutting wheel.

The corrosion casts in the current project had already been mounted on SEM stubs which prevented them from being viewed while being cut using a mini-motor and cutting wheel fixed in the chamber of the cryomicrotome. It was decided not to attempt to remove the casts from the SEM stubs as this may have caused damage to the apical areas.

A mini-motor was purchased from a hardware store for use in the current study. It was originally designed for engraving. The cutting wheel selected to use with the mini-motor was approximately 2 cm in diameter and 200 μm thick. It was coated with diamond chips on both surfaces as well as on the cutting edge. The wheel was made of a very resilient metal and would normally be used for disking between teeth. (Figure 8)

To be able to section through the corrosion casts the current author held the frozen specimen in one hand and the mini-motor in the other. The diamond cutting

wheel could then be moved above the cast and into the correct position while viewing under the dissecting microscope before being lowered into the ice embedded cast.

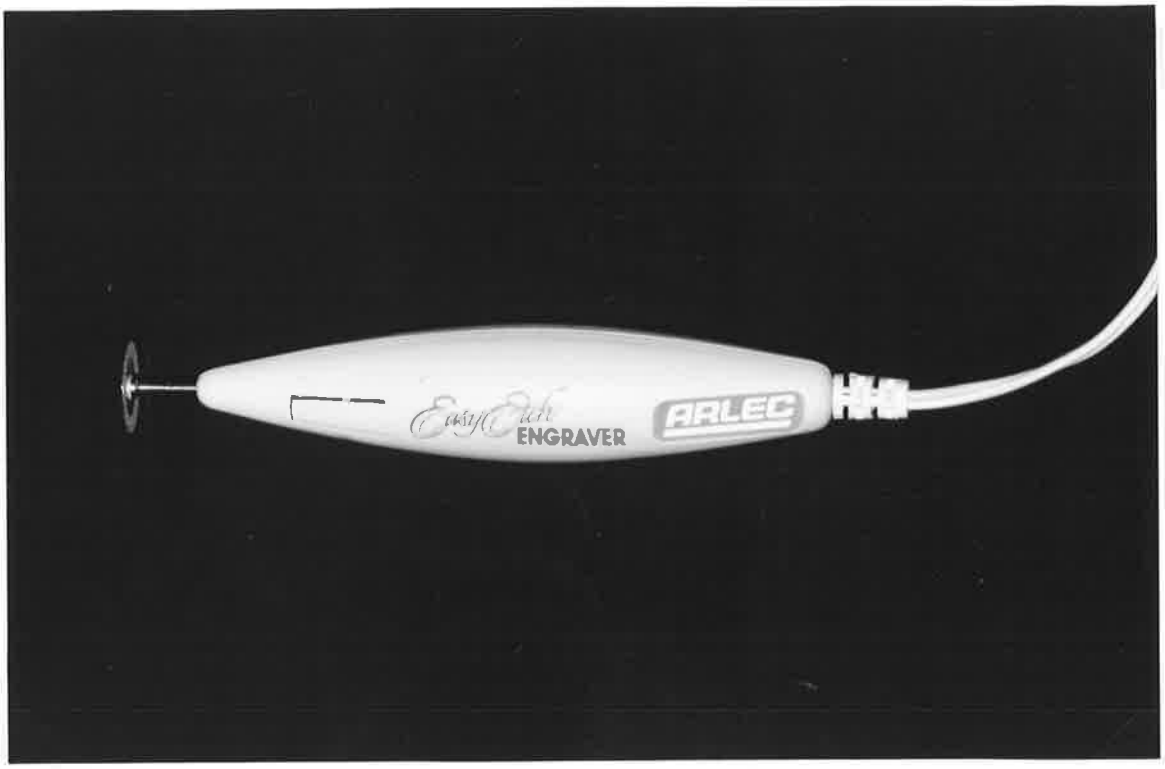

FIGURE 8: MINI-MOTOR AND DIAMOND CUTTING WHEEL.

iv. Dissection of Frozen "Ice Embedded" Casts using Razor Blades

The use of a razor blade to cut through the ice embedded cast was also investigated. Using the stereo-dissecting microscope the ice embedded cast could be cut through with a gentle sawing motion. The procedure was stopped intermittently to allow the melting ice to be refrozen. Care was required to cut through the ice

rather than to cause it to fracture as this would damage the cast. The advantage of this technique over the use of the mini-motor and diamond coated wheel, was that less tissue was removed and that visibility was better. Disadvantages were that cutting was slow and that there was a possibility of fracturing the corrosion cast.

v. Dissection using Other Techniques

The use of micromanipulators was not attempted in the present study. **YOSHIDA et al.** (1986) and **REISS** and **REALE** (1989) described the use of micromanipulators in the SEM. Here the surface layers of the corrosion casts were broken away using the micromanipulator so that vessels at a deeper level were revealed. The current author felt that the desired breakage of the cast to reveal underlying layers was unpredictable and would result in damage to areas of interest.

The use of gelatine as an embedding medium while the cast was being sectioned was also not attempted. **LEISER et al.** (1985) described a technique whereby gelatine was used. This embedding medium has poor visibility when set, and this would make sectioning through the tooth socket accurately, extremely difficult, if not impossible.

The use of razor blades to section through a dried cast was not attempted. The current author felt that the risk of damage to the cast far outweighed the advantage of increased visibility of not using an embedding medium.

Professor A. Lametschwandtner in a personal communication (1992) stated that no new dissecting techniques had been described in the literature. He suggested that fine wires were available which were coated with abrasive particles which may have some application in dissecting "ice embedded" frozen casts. The current author has not tested these wires at this stage and felt that it may be difficult to obtain a straight cut with them.

B. DISSECTION TECHNIQUE SELECTED

None of the previous techniques attempted by the current author proved satisfactory. The dissection technique eventually selected used frozen "ice embedded" corrosion casts. Air bubbles around the corrosion casts were removed through evacuation. The mini-motor and diamond cutting wheel were used initially to cut away the "ice embedded" corrosion cast. A safety razor blade was then used to trim away the tooth socket walls.

The dissection technique had to be varied depending on the tooth sockets present. In the case of the corrosion casts that had only the six anterior tooth sockets remaining, the ice was first removed distal to the canine sockets using the mini-motor and diamond cutting wheel. The canine sockets were still embedded in ice at this stage and protected from damage. The distal socket wall of the canine was then trimmed away using a safety razor blade and a slicing motion (Figure 9). As the distal wall was sliced away, the PDL and pulpal vessels could be viewed under the dissecting microscope. The wall of the socket was removed until the pulpal vessels could be viewed from the apical to the cervical portions. The "ice embedded" specimen needed to be refrozen several times during sectioning as the ice tended to melt fairly quickly.

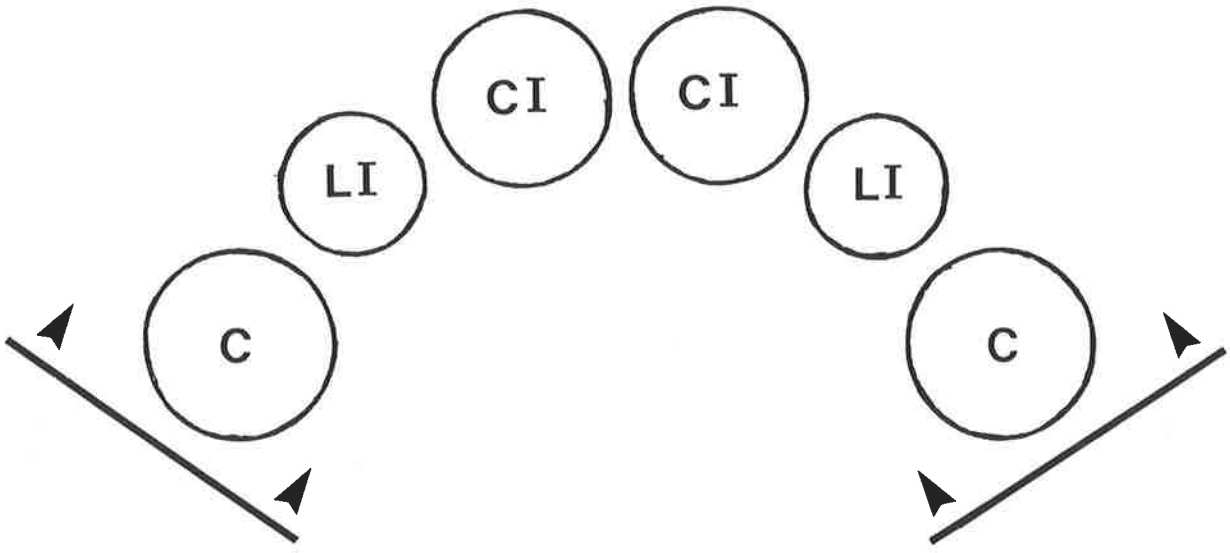

FIGURE 9: SECTIONING CORROSION CASTS OF THE ANTERIOR TOOTH SOCKETS.

"Ice embedded" corrosion casts of the maxilla and mandible were sectioned in two ways. Some of the corrosion casts were left intact and the labial (buccal) gingival vessels cut away using the mini-motor and diamond cutting wheel (Figure 10, planes a1 and a2). The labial (buccal) wall of the tooth sockets was then sliced away using the safety razor blade until the pulpal vessels from the cervical region down to the apex were seen. This enabled the palatal as well as some of the mesial and distal PDL, and pulpal vessels to be viewed. The angulation of the tooth sockets due to the proclination of the teeth, especially in the incisor regions made trimming down to the apex difficult.

Other "ice embedded" corrosion casts of the maxilla and mandible were sectioned into two portions using the mini-motor and diamond cutting wheel. A straight cut was made through the first premolar sockets so that there was an anterior and a posterior segment (Figure 10, plane b).

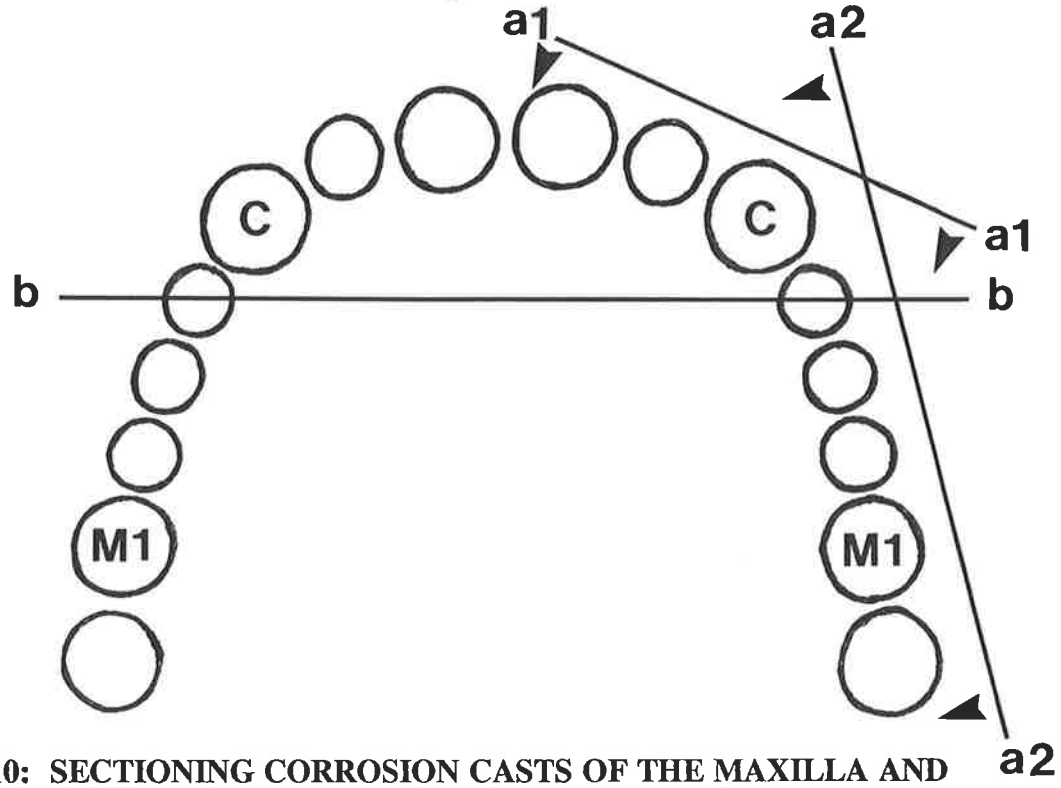

FIGURE 10: SECTIONING CORROSION CASTS OF THE MAXILLA AND MANDIBLE.

The anterior segment included the six anterior sockets and the mesial half of the first premolar sockets. It was left attached to the SEM stub. The posterior

segment, still embedded in ice, was removed by sectioning between the SEM stub and the apices of the posterior tooth sockets. Once thawed and dried the corrosion cast of the posterior tooth sockets was remounted onto a new SEM stub using silver colloid and double-sided adhesive. The "ice embedded" anterior segment was then sectioned in a similar way to that described on the previous page (Figure 9) so that the mesial PDL, as well as part of the labial and palatal PDL, and the pulpal vessels were in view.

Once the corrosion casts had been sectioned and the desired areas exposed, they were allowed to thaw. They were rinsed under double distilled water to remove cast remnants and silver colloid particles and allowed to dry in a dust proof cabinet. The casts were recoated with a layer of carbon and gold/palladium and viewed in the Philips SEM 505.

4.14 EXAMINATION AND RECORDING WITH THE SCANNING ELECTRON MICROSCOPE

The technique for taking stereopair SEM micrographs has been described by a number of authors including **BOYDE** (1973), **HOWELL** (1975), **WERGIN** and **PAWLEY** (1980) and **LOW et al.** (1981). SEM stereopair micrographs were taken in the Philips SEM 505 by the current author. An angle of tilt of 6^{o} was used to provide stereopair three-dimensional images of the corrosion casts.

Accelerating voltages were kept low and ranged between 5 to 15 kV while working distances varied between 12 to 30 mm. The low accelerating voltages helped to reduce the risk of charging and thermal damage thereby minimizing the risk of deformation of the casts. This reduced kilovoltage was suggested by **LAMETSCHWANDTNER et al.** (1984) and was also used by **LEE** (1988). The final condenser aperature was set at 20 μm.

Ilford FP4 120 mm black and white film was used with the SEM photographic equipment. This equipment allowed the magnifications of the specimen to be recorded on the film with a small scale bar.

4.15 DEVELOPING AND PRINTING

Ilford Microphen Developer and Ilford Hypam Rapid Fixer were used to process the Ilford FP4 black and white film according to the manufacturer's instructions. The negatives were then placed under running water for 15 minutes and rinsed in deionized water. After drying in an air-dryer for 2 hours, the negatives were stored in separate plastic envelopes. Ilfospeed grade 3 and multigrade glossy paper were used with the Durst Laborator 54 enlarger to make 10 cm by 12 cm prints from the negatives.

Ilfospeed Paper Developer and Ilford Hypam Rapid Fixer were used to process the prints according to manufactures instructions. The prints were washed thoroughly for 15 minutes and then dried in an air dryer and stored in paper envelopes.

4.16 VIEWING OF THE STEREOPAIR PHOTOMICROGRAPHS

To enable the images to be visualized in three-dimensions, a Stereo Aids viewer was used. **CHATFIELD** (1978) and **LOW et al.** (1981) have described how stereopairs can be used to gain more information than can be obtained from similar material viewed singly at a higher magnification.

LEE (1988) suggested that the magnification factor should be ignored as the prints had been enlarged and that the scale bar was useful in giving an indication of the magnification.

4.17 DATA IMPRINT ON PHOTOMICROGRAPHS

The photomicrographs which have been included in this report were taken on the Philips SEM 505. Because of technical problems with the ETEC Autoscan SEM, it was decided to use only the Philips SEM 505 until the ETEC had been recalibrated. All of the images viewed were recorded using stereopair photomicrographs. These photomicrographs need to be rotated either 90^{o} clockwise or anticlockwise to observe them in three-dimensions using a stereopair viewer. Only the photomicrographs that could be easily orientated by the reader who does not have a stereopair viewer were included for stereopair viewing.

The photomicrographs had a data imprint included with them. The important features of this data imprint are as follows:

(1) A bar graph for a particular magnification. Below this bar graph and to the left of the data imprint, a magnification has been indicated. eg. 1 mm, 0.1 mm

(2) The accelerating voltage used in kV (to one decimal place). eg. 5.0 kV

(3) To the far right of the data imprint, the specimen code has been included. eg. MAR-224 represent marmoset 224.

CHAPTER 5

RESULTS OF THE INVESTIGATION

The corrosion casts used in the current study although being more than 3 years old, were still in very good condition. Some of the original material had been destroyed during sectioning by **LEE** (1988). However, there was still adequate material left to assess the anterior segments.

Gross anatomic features and a knowledge of the microanatomy of the area were used to help describe the relationship of the vessels to surrounding structures such as the alveolar bone, root surface, the mucosa and gingival tissues.

5.1 ENDOTHELIAL IMPRINT PATTERN, VESSEL DIAMETER AND VESSEL SHAPE

The endothelial imprint patterns as described by **HODDE et al.** (1977), **HODDE** (1981) and **MIODONSKI et al.** (1981) proved useful in the identification of both arterioles and venules when looking at the corrosion casts at higher magnification.

The description of **LEE** (1988) that "arterioles ran a straighter course, had few branches, and showed a constant diameter compared with venules that ran a more sinuous course, had more branches, and possessed a varying diameter", was also extremely useful. This combined with the classification of blood vessels using vessel diameter by **RHODIN** (1967, 1968) enabled quite an accurate assessment of the types of vessels present.

The current author had difficulty in classifying venules with internal lumen diameters greater than 50 μm. **RHODIN** (1967, 1968) classified venules with an internal lumen diameter between 50 to 100 μm as being muscular venules. These were from rabbit thigh fascia and had one to two layers of smooth muscle cells.

PARLANGE (1991) did not describe muscular venules in the PDL of the cotton ear marmoset while looking at the maxillary anterior segment, even though venules with an internal lumen diameter greater than 50 μm were seen. She classified venules with an internal lumen diameter ranging from 32 to 80 μm as being collecting venules. These vessels did not have a muscular layer.

The findings of **PARLANGE** (1991) suggested that the model used by **RHODIN** (1967, 1968) to classify blood vessels in rabbit thigh fascia may not be applicable when describing the vasculature of the PDL in the maxillary anterior segment of the cotton ear marmoset. **LEE** (1988) did not describe venules greater than 50 μm in diameter while looking at the vasculature of the PDL in the maxillary and mandibular posterior segments of the cotton ear marmoset. Muscular venules may be present in the PDL of the mandibular anterior segments of the cotton ear marmoset and further research is required in this area.

As the corrosion casting technique had removed the blood vessel wall during processing, the current author was unable to determine whether venules that had an internal lumen diameter greater than 50 μm as being either muscular or collecting venules. To be consistent with the classification of **RHODIN** (1967, 1968) and the findings of **PARLANGE** (1991), venules with an internal lumen diameter ranging from 30 to 50 μm in diameter were descibed as being collecting-sized venules by the current author. As both the maxilla and mandible were examined in the current study, venules with an internal lumen diameter greater than 50 μm were not given any specific name although one suspects from **PARLANGE's** (1991) work that these were also collecting venules.

5.2 RECORDING OF INFORMATION

To allow the morphology of various structures to be described in relation to a particular location around the tooth socket, the current author divided the tooth into 8 segments. The tooth socket was first divided into labial (buccal), palatal (lingual), mesial and distal segments and then these segments were divided into halves. The segments were called L1, L2, P1, P2, M1, M2, D1, and D2. The following diagram is a representation of this subdivision. (Figure 11)

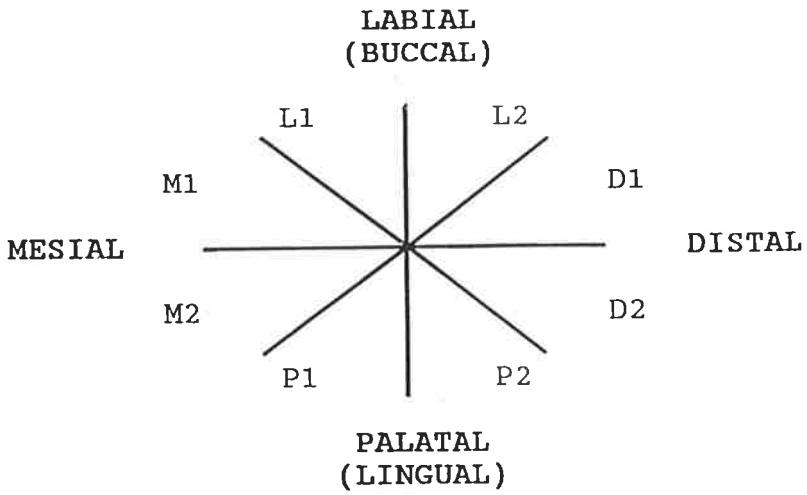

FIGURE 11: SEGMENTAL DIVISION OF TEETH.

To be consistent, the current author continued with the terminology used by LEE (1988) to describe the different types of capillary loops and their location. (Figures 4 and 5)

5.3 SECTIONING THE CORROSION CASTS

A. USING LASERS

The American Dental Laser cut through the corrosion cast by vapourizing the resin with extreme heat. The Dental Laser had a wide beam and produced a cut through the corrosion cast ranging from 300 to 700 μm (Figure 50). The beam

needed to be passed over the cast a number of times so that the tissue was cut through completely. The accuracy of doing this was difficult and often the cut was widened. The beam would only penetrate a shallow distance and therefore the only way deeper structures could be reached was if the tissue was cut away from the side of the cast.

The laser beam was also extremely bright and after a period of time the corrosion cast was difficult to see once the laser beam had been stopped. Care was required not to have the output too high as the silver colloid adhering the corrosion cast to the SEM stub was highly inflammable. In fact one of the trial corrosion casts caught on fire with the cast being completely destroyed.

The larger CO_2 Sharp Dental Laser had the advantage over the American Dental Laser in that the beam size could be reduced to only 100 μm. It also had a variable power setting and pulse rate. Setting it on the lowest power output still caused too much heat generation with the subsequent combustion of the cast. The laser was mainly designed to burn through tissue and was unsuitable for cutting through the delicate resin structures of the corrosion cast.

B. USING FINE INSTRUMENTS

Difficulty was experienced when attempting to remove the surface of the corrosion cast to get to deeper structures using fine tweezers and small spring scissors. Breakage of the fine vessels was fairly predictable, however larger vessels often were difficult to break cleanly with subsequent damage to the surrounding cast.

Any technique where there is any chance of breakage or damage to the area being viewed should be reassessed. If another technique is available which has less risk of damage to the corrosion cast, then this technique should be used in preference.

C. USING "ICE EMBEDDED" CASTS WITH THE MINI-MOTOR AND DIAMOND CUTTING WHEEL

Cutting through the "ice embedded" corrosion casts using a diamond cutting wheel in combination with the mini-motor was very effective. Evaluation of the corrosion cast in the SEM showed a clean, sharp cut through the cast. The thickness of the cut was slightly more than 200 μm with no damage to the surrounding cast. The cut was made quickly through the ice to avoid increased heat generation. The cutting wheel was passed through the ice only once to avoid increasing the width of the cut and the risk of damage to the surrounding cast.

Cutting through the tooth sockets using this technique also gave a good result as there was minimal damage to the surrounding corrosion cast. The accuracy of the cut to include the root apex was unpredictable however and often the cut would be either side of the apex. When viewing under the dissecting microscope the cutting wheel would produce a smear of ice particles while cutting which tended to make viewing difficult. Also the cutting wheel tended to obscure the tooth socket as the cut was being made.

D. USING "ICE EMBEDDED" CASTS WITH RAZOR BLADES

Visibility was greatly improved when safety razor blades in combination with the dissecting microscope were used compared to using the mini-motor and diamond cutting wheel. There were two main disadvantages in using this technique over the technique finally adopted. The first was that there was a risk of the ice splitting in the wrong place while the razor blade was moved backwards and forwards in a sawing motion. This splitting actually happened on several occasions, and although the technique could possibly have been improved upon to reduce this by either heating the razor blade or by varying the pressure applied, any possibility of damage to the corrosion cast would be unacceptable.

The second major disadvantage of this technique was the difficulty encountered in cutting through the socket accurately to include the tooth apex. It is difficult if not impossible to see the location of the pulpal vessels near the apex of the tooth socket when viewing from the occlusal. If the cut is going crooked, it is very difficult to correct. Therefore, including the apical vessels is often achieved by chance which is less than desirable.

E. DISSECTION TECHNIQUE SELECTED

The technique of removing the distal or labial socket wall by first cutting away the ice using the mini-motor and diamond cutting wheel and then by fine trimming using a safety razor blade gave consistently good results. By viewing the tooth socket from the side, localization of the apical vessels including those of the pulp could be achieved most of the time.

Problems were encountered when attempting to cut away the labial side of the sockets especially when half of the maxilla or mandible was present. Because the teeth tended to protrude from the jaws, trimming nearer the apex became more difficult as visibility was limited. It was difficult to see the apex and over trimming could easily occur. The technique however was far more reliable and less likely to cause damage than any of the other techniques attempted.

5.4 ORAL VASCULATURE

In general, the oral vasculature showed a wide degree of animal variability not only between the young and mature animals but also between animals in the same age range. Variability also existed between the maxilla and mandible. This variation will be described in the photographs included in this chapter. Figures 4 and 5 provide a diagramatic representation by **LEE** (1988) of the gingival loop systems and the presumptive blood flow in the palatal gingiva, respectively.

Figures 12 and 13 are low power occlusal views of the vasculature of the maxilla and mandible.

A. PALATAL AND LINGUAL VASCULATURE

The surface vasculature of the hard palate could only be assessed in the young animals as incomplete casting in this region occured in the mature animals. In the young animals the surface vasculature consisted of a capillary loop network extending from the rugal crests to the rugal troughs. From the midline of the canines, premolars and molars, the rugae curved gently to extend into the midline of the palate. The capillaries formed simple hairpin loops which were generally orientated sagittally. Loop diameters ranged between 8 to 12 μm with a height ranging from 70 to 250 μm. For the maxillary lateral incisors, small rugal crests extended from the nasopalatine foramen to the midline of the lateral incisors. No rugae were found associated with the maxillary central incisors (Figure 12). Deep to the capillary loops was a predominantly venous network consisting mainly of postcapillary-sized and collecting-sized venules with arterioles being few in number and often found deep to the venous network.

The surface vasculature of the lingual gingival region of the mandible was similar for both the young and mature animals. It consisted of simple hairpin loops which were orientated from the tooth sockets towards the lingual sulcus. Loop height ranged from 50 to 120 μm with diameters being from 8 to 10 μm. As the lingual sulcus was approached, the loop structure changed to a network of capillary vessels similar to those found in the labial alveolar mucosa. Deep to this capillary network was a mainly venous network of postcapillary-sized and collecting-sized venules which appeared to drain from the region of the tooth sockets towards the lingual sulcus and tongue. Again arterioles were few in number.

B. GINGIVAL VASCULATURE

The gingival vasculature in the anterior region was made up of the crevicular vasculature. This extended occlusally from the circular plexus which was at the level of the epithelial attachment to the crest of the tooth socket (Figures 14, 15, 19). Around the tooth socket at the crest were located the palatal/lingual, col and vestibular gingival vessels. Intercommunication between the oral gingival vasculature and the crevicular vasculature was common both near the surface and at a deeper level. Blood flow occurred either inwards towards the crevicular plexus and PDL or outward toward the gingival network. On the labial surface, below the vestibular gingival vessels, the labial gingival and alveolar mucosal vessels were located.

i. Crevicular Vasculature

The circular plexus in the canine and incisor regions consisted of a single vessel which encircled the tooth socket at the level corresponding to the epithelial attachment. It was located adjacent to the junctional epithelium and had an internal luminal vessel diameter that ranged between 10 to 30 μm, although the diameter was usually between 10 and 15 μm.

An internal luminal diameter of 30 μm was seen only in the labial portion of an upper right central incisor (Figure 14). The endothelial imprint pattern, morphological features and vessel connections here indicated it was venous in nature. The diameter of the vessel reduced rapidly to approximately 10 to 15 μm in the mesiolabial and distolabial regions of the tooth socket.

The circular plexus communicated occlusally with the crevicular vasculature and less frequently below with the cervical PDL. The circular plexus had no distinct imprint pattern, except in the example mentioned in Figure 14, and it is presumed

that blood flow was normally from the crevicular vessels to the circular plexus and then apical to the cervical PDL.

Occasionally arterioles drained into the circular plexus from the cervical PDL at various sites around the tooth sockets, although the sites were not consistent between the teeth. Arterioles feeding directly into the circular plexus from the cervical PDL suggested that blood may flow around the circular plexus from the cervical PDL and possibly occlusally into the crevicular loops. Most arterioles in the cervical PDL, however, bypassed the circular plexus to supply the ascending capillary loops of the crevicular plexus directly as well as the labial and palatal gingiva. Communication between the circular plexus and venous vessels in the cervical PDL was also observed (Figure 15).

The circular plexus showed variability in vessel form around the tooth sockets, although no consistent pattern could be established either with respect to the different age groups of animals, between the maxilla and mandible or between the various tooth sockets examined. This variability in vessel form included a "wavy appearance" in which the vessel had an irregular course. Numerous constrictions could be seen as the vessel coursed around the tooth socket (Figures 14, 15).

Other variations in the circular plexus included discontinuity around the tooth socket, whereby loop structures, presumably crevicular loops, would emerge at the level of the circular plexus, or where there appeared to be complete absence of the circular vessel. The absence of the circular plexus may in fact be an area of incomplete casting.

The level of the circular plexus in several of the tooth sockets changed rapidly, whereby the level of crevicular gingival attachment was lower on the mesial and distal sides of the tooth socket compared to that on the palatal (Figure 19). Periodontal pocketing may have occurred here.

A meshwork of capillaries and postcapillary-sized venules with short communicating links were often found occlusal to the circular plexus in the crevicular gingival region. These vessels ranged in diameter from 10 to 25 μm (Figures 14, 15). Variation in this arrangement was seen whereby the crevicular loops were directly occlusal to the circular plexus with the meshwork of capillaries and postcapillary-sized venules being absent (Figure 20).

The crevicular vessels varied in both complexity and form (Figures 14 to 22). Simple hairpin loops (Figure 14) with similar diameter, 10 to 15 μm, ascending and desending limbs, and with a height ranging from 50 to 250 μm were found in the palatal region of both the young and mature animals (Figure 19). They were more commonly found in the young animals at other sites around the socket (Figure 14). These loop structures communicated with both the circular plexus and with deeper vessels running up from the cervical PDL.

Crevicular loops were also seen which had a smaller diameter, 8 to 12 μm, ascending limb and a larger diameter, 15 to 40 μm, postcapillary-sized descending limb (Figure 15). A simple hairpin loop joined these limbs and their height ranged from 100 to 350 μm. The loops were arranged around the tooth socket in single or multiple layers. Communication occurred between the loop structures via a system of capillaries (Figure 15). It was thought that blood ascended via the smaller diameter limb and drained via the larger diameter limb, however the reverse may also have occurred. These loop structures were commonly found in the labial portion of the tooth sockets in the young animals. They were also present in both the upper and lower anterior sockets. In the mature animals they were interspersed with more complex structures which the current author has termed "knot-like".

More complex knot-like loop structures were very common particularly in the mature animals (Figures 16, 17). Several limbs of relatively equal diameter could be seen. They ranged in height from 80 to 450 μm around the tooth sockets

and had a diameter ranging from 10 to 25 μm. In general, these structures were more common in the mature animals and more common on the mesial and distal sides of the tooth sockets. They were found in both the maxillary and mandibular anterior sockets.

One of the young animals showed proliferation of these knot-like structures. They extended completely around the crevicular region of the anterior tooth sockets as well as into the interproximal papilla area and onto the labial gingival surface (Figures 30, 31).

More complex crevicular loop structures which had a bulb-like appearance resembling "renal glomeruli" were present in the mature animals (Figures 18 to 22). Intercommunication between these structures was seen with two or more limbs leading from these glomerular-like crevicular complexes. The direction of blood flow could not be ascertained. All limbs appeared to be venous in nature.

The glomerular-like crevicular structures were not found in the young animals although the knot-like structures were present in both age groups. The most complex and extensive formations were found in both the maxillary and mandibular canine sockets in the labial, mesial and distal portions of the tooth socket (Figures 19, 21). The height of the glomerular-like crevicular structures ranged from 100 to 350 μm, the maximum cross sectional diameter ranged from 35 to 170 μm. (Figures 20 to 22).

A transition in complexity occurred from the knot-like formations to the more complex glomerular-like crevicular structures, and possibly from the simple hairpin loops (Figures 17, 18). In Figure 17, small knot-like crevicular structures were seen. These had several limbs and communication between the knot-like structures occurred. The tooth socket illustrated was the maxillary right central incisor and the location was the distolabial region of the socket. In Figure 18, the formation of small glomerular-like structures had occurred. Also present in this

figure were knot-like structures, but in a more advanced stage. The tooth depicted here was a maxillary left central incisor from the same animal as that in Figure 17. The location was the labial surface of the socket.

Around the labial crevicular region of the maxillary left canine socket of the same animal as described in the previous paragraph, extensive glomerular-like crevicular structures were seen (Figure 21). These should be compared with Figure 15, where the labial crevicular region of the upper right canine of a young animal was depicted. The structures here showed simple hairpin loops which had a smaller diameter ascending limb and a postcapillary-sized descending limb. None of the more complex glomerular-like crevicular structures were present in this animal in any of the anterior tooth sockets. Knot-like crevicular structures had formed in the distolabial portion of the maxillary right canine and around the labial, mesial and distal surfaces of the maxillary left canine.

The inner, larger diameter vessels of a glomerular-like crevicular loop structure were seen in Figure 22. The outer capillary network was reduced here, possibly because it had not cast, and this has allowed the inner structures to be viewed. There appeared to be an ascending and a descending limb which formed a horseshoe shape and with nearly equal diameters ranging up to 35 μm. A capillary network emerged from these larger vessels and formed a bulb-like arrangement around the periphery. The direction of blood flow could not be determined and may in fact change.

The two glomerular-like crevicular loop structures shown in Figure 22 were located on the distolabial side of a maxillary left lateral incisor socket. There were no other complex glomerular-like crevicular loop complexes found around this socket. The canine sockets of this animal appeared to be more susceptible to the formation of these complex loop structures compared to the incisors. More animals need to be assessed to confirm this arrangement.

The initial site of formation of the glomerular-like crevicular loop complexes was interproximally, either on the mesiolabial or distolabial surface (Figure 11). Several sockets showed the formation of these complex loop structures only in these regions (Figures 22, 34).

The height of the crevicular loops, whether they were simple or complex, reduced from the mesial and distal sides of the tooth socket towards the palatal (Figures 19, 20). On the palatal side of the socket, except for one of the young animals, only simple loop structures were found, although in some of the mature animals there was a difference in diameters between the ascending and descending limbs.

Knot-like and glomerular-like loop structures in some of the mature animals appeared to extend onto the labial gingival surface, and occured for both the maxillary and mandibular anterior teeth (Figures 23, 24, 25, 27, 28). The knot-like loop structures were found closer to the vestibular gingival vessels. A distinct gap extended between these knot-like loops and the horizontal bands of vestibular gingival vessels (Figure 25).

Finally under this section, it was noted that knot-like and glomerular-like crevicular loops occurred in some of the mature animals in the posterior regions (molars and premolars). These structures were far less numerous than those found in the anterior regions.

ii. Labial Gingival Vasculature

The labial gingival vasculature consisted of vestibular gingival loops and labial gingival loops (Figures 24, 26). The vestibular gingival loops encircled the crest of the tooth socket around the labial surface. They were found in the area of free gingival attachment. Directly below these were the labial gingival loops which

occupied the region of attached gingiva. These merged with the alveolar mucosa vessels as the sulcus was approached (Figure 24).

In the anterior segments, considerable variation in both the quantity and location of the gingival vasculature was noted. In the younger animals, the vestibular gingival network was at the crest of the tooth sockets (Figure 26).

In one of the mature animals, the vestibular gingival loops in the maxillary anterior segments extended down the labial gingival region from just below the crest of the sockets (Figures 24, 25). Here the vestibular gingival loops were arranged in bands which ran horizontally around the labial side. In this animal knot-like and glomerular-like loops extended from the crevicular region onto the labial gingival surface. A distinct gap between the vestibular gingival loops and these knot-like loops was also seen (Figure 25). Compare this illustration with Figure 26, where the vestibular gingival loops were at the crest of the tooth socket in a young animal.

Below the vestibular gingival vessels were the labial gingival loops (Figures 24 to 26). These loops had an occluso-apical orientation and projected out towards the lips with a height ranging from 50 to 100 μm. The loops showed simple hairpin bends and drained into a deeper venous system and towards the gingival sulcus. Larger postcapillary-sized venules, 10 to 30 μm in diameter, collecting-sized venules, 30 to 50 μm in diameter and larger venules, 50 to 100 μm in diameter, as well as a small number of terminal arterioles that were less than 50 μm in diameter, coursed in an occluso-apical direction at this deeper level (Figure 32).

As the sulcus was approached the gingival loops changed from being orientated occluso-apically (Figures 24, 27). A junction was seen between the labial gingival loops and the alveolar mucosa capillary network. This was thought to be the muco-gingival junction. Small capillary loops were found in the first millimeter or so after the junction. These loops projected towards the lip. Below this level as

the labial sulcus was approached, the capillaries appeared to be arranged in wide arcades. This was the area where the alveolar mucosa was found. (Figures 24, 27, 32).

In the lower anterior segments considerable variation was also found in relation to the labial gingival vasculature. Gingival clefts (depressions) could be seen encircling the labial gingival region around the tooth sockets (Figures 27, 28). These clefts were only found with this mature animal and extended into the interproximal col region. They were found around the labial gingival surface of both the mandibular incisor and canine teeth.

Capillary loops were not found in association with these clefts. However vessels ran in a semi-circular direction from the mesial col region around the labial gingival surface towards the distal. The clefts were from 100 to 300 μm wide, but the depth was not determined (Figure 28). The capillary network appeared to drain to deeper vessels as well as towards the labial sulcus. In the canine socket glomerular-like loops were seen extending onto the labial surface (Figures 27, 28). This can be compared with Figures 24, 25, where glomerular-like loops were seen extending onto the labial gingival surface in an upper canine. Also with this lower canine, the width of the band of labial gingival loops (attached gingiva) appeared to be reduced considerably below these clefts. The wide arcades of vessels directly below the clefts were consistent with the vessels seen with the alveolar mucosa. (Figure 27).

In the same animal as described above, cords of labial gingival loops ran occluso-apically in the gingival region between the mandibular central incisors (Figure 29). This arrangement was in contrast to the usual feature of single capillary loops projecting towards the lips and having an occluso-apical orientation (Figures 24, 26). These cords ranged between 100 to 150 μm in height and were

separated by gaps of between 80 to 100 μm. Intercommunication between the cords of vessels was at a deeper level.

Variability with the labial gingival vasculature was also seen in Figures 30 to 32. These figures showed the labial gingival vasculature in the mandibular anterior segment of a young animal. Figure 30 illustrates extensive proliferation of knot-like loop structures extending from the crevicular region onto the labial gingival surface, interproximally and even palatally. Figure 32 is a higher power view of the labial gingival and interproximal region. Extensive proliferation of the knot-like loop structures can be seen. The more complex glomerular-like loop structures were absent suggesting that the complexity of these loops increased with time.

It is interesting to note that the labial gingival loops representative of attached gingiva appeared to be completely absent in the lower anterior region with this young animal. Figure 32 shows the wide arcades of capillary vessels representative of the alveolar mucosa extending up to the tooth socket.

iii. Interproximal Col Vasculature

The col region is another area where considerable variability existed. This variability was dependent on whether there was spacing between adjoining teeth, whether it was in the upper or lower arches and on the morphology of crevicular loop structures present (Figures 23, 27, 30, 33, 34).

In Figure 33, an occlusal view of the col region between a mandibular right canine and first premolar socket has been shown. The crevicular loops had a simple hairpin configuration (young animal), and curved occlusally towards the centre of the col region. It was difficult to differentiate between the col vessels and crevicular vessels as no distinct gap was present which separated these vessels. What appeared

to be a gap between these vessels was not continuous throughout the col area. A central ridge of vessels also appeared to be present and coursed labio-lingually.

Figure 34 illustrated the col region between a maxillary right lateral incisor and canine socket in a mature animal. Glomerular-like loops were seen extending up the distal wall of the lateral incisor and mesial wall of the canine. In the col area, finer capillary loop structures coursed labio-palatally. A distinct gap between the col vessels and the crevicular vessels could not be seen. The space between the teeth was fairly wide here and the palatal vessels may have extended interproximally into the col region. In one of the young animals (Figure 13), a large space approximately 1.5 mm wide was present between the mandibular left central and lateral incisors. The lingual gingival loops appeared to run between these two teeth.

Variation in the col region could also be seen (Figures 23, 27 and 30). Figure 23 showed a very narrow col area between a maxillary right lateral and central incisor. The crevicular loops from adjoining sockets appeared to be merging in the col region here. In Figure 27, a gingival cleft was seen extending into the interproximal col region between a mandibular left lateral incisor and canine. Figure 30 showed proliferation of knot-like loops into the col region of a young animal. It was difficult to distinguish col vessels from crevicular vesels. A distinct gap could not be seen between these vessels.

C. PERIODONTAL LIGAMENT VASCULATURE

Sectioning of the corrosion casts enabled the PDL vasculature to be viewed from the cervical third to below the apex (Figure 35). In this project the distal PDL wall of the anterior sockets was not viewed and variation in vessel morphology may have occurred at this site relative to the other locations around the tooth sockets.

Postcapillary-sized venules and collecting-sized venules were the most numerous vessels seen in the cervical and middle thirds of the PDL, although larger venules ranging from 50 to 100 μm in diameter were also present (Figure 37). The apical PDL was highly vascular. The venous vessels formed a basket-like arrangement around the apex of the tooth socket with numerous communications being present. Vessel diameters were variable with the collecting-sized venules being the most numerous. The vessels coursed occluso-apically as well as around the tooth socket. Numerous arterio-venous and venous-venous anastamoses were present (Figure 41). The arterial vessels supplying the PDL were considerably fewer in number than the venous vessels. They ran predominantly from the apex toward the cervical third, although vessels did emerge through the surrounding bone and from the gingiva to supply the cervical third of the PDL.

i. Cervical Third of the PDL

Around the anterior tooth sockets the cervical PDL vessels communicated with the circular plexus. More frequently these cervical PDL vessels ran at a deeper level to the circular plexus to communicate with the crevicular vessels (Figures 15, 20). No specific site preference could be seen around the sockets for these communications. Postcapillary-sized venules were the most frequent vessels found and also appeared to drain into the cervical PDL from the surrounding free gingival vessels.

Capillaries in the cervical PDL were less numerous than the postcapillary-sized venules. They linked larger diameter venules and also communicated with the medullary network. The capillaries ran both horizontally and occluso-apically to form an intercommunicating network of vessels.

Arterioles in the cervical PDL were considerably fewer in number compared to the venules. They branched less than the venules and ran mainly coronally until

reaching the circular plexus. Communication with the circular plexus was infrequent. Running at a deeper level to the circular plexus they would supply the crevicular vessels and surrounding gingival vessels.

In the cervical PDL third of the lower anterior tooth sockets, arterioles were more numerous on the mesial and distal sides compared to the upper anterior tooth sockets. Groups of arterioles were seen running coronally and then changing direction at the level of the circular plexus to supply the lingual and labial gingiva as well as the crevicular vessels. Terminal arterioles here ranged in diameter from 15 to 25 μm (Figure 36).

In the cervical PDL directly below the circular plexus, loop structures were often seen in the palatal (lingual) portion of the tooth sockets (Figure 37). They were less often seen around the other sides of the sockets and were seen in both the incisor and canine sockets. Animal and socket variability occurred with these loop structures. However they were found in both the young and mature animals and in the maxillary and mandibular sockets (Figures 37, 38).

In Figure 37, a band of these loop structures, 150 to 300 μm wide, were seen running around the mesiopalatal cervical PDL directly below the circular plexus. The socket was from a maxillary left lateral incisor and the animal was young. They projected from the bone towards the tooth and had an ascending and descending limb with a simple hairpin bend. Loop diameters between the limbs were similar and ranged between 12 to 15 μm. Length of the loop structures varied between 100 to 150 μm. Directly apical to these loop structures, postcapillary-sized venules emerged from a deeper level. Diameters ranged between 10 to 15 μm and increased rapidly as the vessels coursed towards the apex. These vessels formed larger diameter collecting-sized venules of 30 to 50 μm, and even larger venules up to 80 μm in diameter as they coursed apically with lateral branches being present. Arterial vessels appeared to be at a deeper level to these venules.

Cervical PDL loop structures in a mature animal varied from those described for the young animal in Figure 37. In Figure 38, the cervical PDL loop structures had a larger diameter limb ranging from 20 to 60 μm, and smaller diameter limbs ranging from 10 to 15 μm. The socket in Figure 38 was also from a maxillary left lateral incisor, although these loops were found with the maxillary canine and central incisor sockets of the same animal. Often more than one smaller diameter limb was seen associated with a larger diameter limb. They made a sharp hairpin bend as they approached the tooth and then coursed back down the side of the larger diameter limb towards the bone. Blood flow was presumed to be from the smaller diameter vessels into the larger diameter vessel. Endothelial imprint patterns indicated the larger diameter vessels were venous in nature. Endothelial imprints were not distinct for the smaller diameter vessels.

Animal variability was also seen in the palatal cervical PDL as illustrated in Figure 39. The tooth depicted was a maxillary left canine from a mature animal. Instead of the cervical loop structures being present, postcapillary-sized venules directly below the circular plexus enlarged rapidly to form venules 50 to 80 μm in diameter. Smaller postcapillary-sized venules were seen coursing along the wall of the larger diameter venules and eventually drained into these vessels. An arterio-venous anastomosis appeared to be present.

ii. Middle Third of the PDL

The vessels in the middle third of the PDL in the anterior sockets were mainly postcapillary-sized and collecting-sized venules. Venules larger than collecting-sized venules ranging from 50 to 80 μm were commonly seen. These ran occluso-apically with intercommunicating branches forming a network similar to a "fishing net". Arterioles could be seen running occlusally. Most were at a deeper level although occasionally arterioles could be seen closer to the tooth surface. Arterio-arterio, arterio-venous as well as venous-venous anastomoses were seen.

Loop structures as described for the cervical third of the PDL were not found, nor was the rapid change in descending vessel diameter seen in the middle third of the PDL. In the cervical/middle third of the lower anterior sockets on the mesial side, the venous vessel diameter increased from being postcapillary-sized venules to venules ranging in diameter up to 100 μm as they coursed apically (Figure 46). On the labial and palatal sides the vessels remained postcapillary-sized and collecting-sized venules.

iii. Apical Third of the PDL

The apical third of the PDL showed an increased vessel density compared with the cervical and middle thirds. Collecting-sized venules were the most common vessels found although postcapillary-sized venules were also common. A tight meshwork of vessels encircled the root apex. These collecting-sized venules were seen to bulge and then constrict with vessel diameter fluctuating in size and with numerous communications being present. Terminal arterioles were also more common in the apical portion and arterio-venous anastomoses were seen (Figure 41). The vessels showed a greater amount of curvature as the circumference around the socket was reduced considerably here.

In Figure 40, pulpal vessels formed a fan shape as they coursed below the level of the apical foramen. The apical foramen here appeared to be coronal to the root apex as the pulpal vessels below the apical foramen coursed apically for up to 1000 μm before reaching the apical PDL vessels. The majority of pulpal vessels were arterioles with diameters ranging from 10 to 15 μm. Communication of pulpal vessels with each other in the apical third of the pulp canal was not seen. The diameter of the apical foramen was 80 to 100 μm. In this particular example, the animal was mature and the socket was a mandibular right canine.

A close up view of these pulpal vessels showed venous drainage of a pulpal venule into an apical PDL venule (Figure 42). Here the pulpal vessel was a postcapillary-sized venule. The diameter increased to that of a collecting-sized venule before it anastomosed with a PDL venule. No direct communication was seen between pulpal arterioles and PDL arterioles. Pulpal arterioles appeared to originate from larger arterioles beneath the PDL.

Fanning of pulpal vessels below the apical foramen was not seen in all the sockets examined (Figure 43). In this micrograph pulpal venules beneath the apical foramen drained into a large collecting-sized venule. Pulpal arterioles ran up along this collecting-sized venule from beneath the apex. PDL venules from the labial side of the socket drained into this collecting-sized venule which ran lingually into the surrounding bone (Figure 44).

In the middle third of the pulp canal, branching of the pulpal vessels occurred (Figure 45). An outer capillary network was seen with an inner core of larger diameter venules and arterioles being present. The capillaries emerged from the inner core of arterioles and coursed outwards towards the dentine layer of the tooth, and upwards towards the pulp horn. They curved back and drained into the venules running along the central core of vessels.

In the coronal portion, the pulpal capillary network was extensive (Figure 23). Capillaries ran coronally in an outer layer near the dentine and towards the pulp horn. They joined larger venules which ran mainly in the central core region of the pulp canal and drained apically.

iv. Other Significant Findings

A significant finding was an arteriole, 40 to 50 μm in diameter, which was seen in a mandibular right canine socket. It originated from larger arterial vessels directly below the root apex (Figure 45). This vessel coursed along the mesial PDL

wall and branched on numerous occasions as it ran coronally. Branches of this arteriole could be followed into the cervical PDL. The branches ran deep to the circular plexus to supply the crevicular loops and ran labially and palatally to supply the gingival tissues.

In the lower anterior sockets, large venules ranging up to 100 μm in diameter appeared to course down the mesial PDL wall (Figures 35, 46). Figure 46 is a higher power view of the mesial PDL region of the lower right central incisor socket shown in Figure 35, and is at a level between the middle and apical PDL thirds of that socket. The venules on the mesial side of this socket increased in diameter as they ran from the cervical PDL region towards the apex. They appeared to be in the PDL although they may in fact be coursing in the bone very close to the PDL. These venules merged to form one large venule which passed through the mesiolabial plate of bone at a level between the middle and apical PDL thirds on the mesial side of the tooth socket and into the labial alveolar mucosa and towards the labial sulcus.

Groups of vessels in the apical third of the labial PDL wall could be seen passing through a thin labial plate of bone to the labial alveolar mucosa (Figures 47, 48). Included in these groups of vessels were venules, 15 to 25 μm in diameter, and arterioles, 25 to 30 μm in diameter (Figure 48). The arterioles appeared to originate from vessels in the labial gingival sulcus, and coursed through the labial plate of bone to supply the apical labial PDL wall. The venules passed out from the labial PDL and coursed towards the labial gingival sulcus.

Direct communication of PDL vessels between adjoining tooth sockets was also observed (Figure 49). Communication between the distal PDL wall of a mandibular first premolar socket and the mesial PDL wall of a mandibular second premolar socket is shown in this figure. Both arterial and venous communication were observed, although the venous vessels were more common.

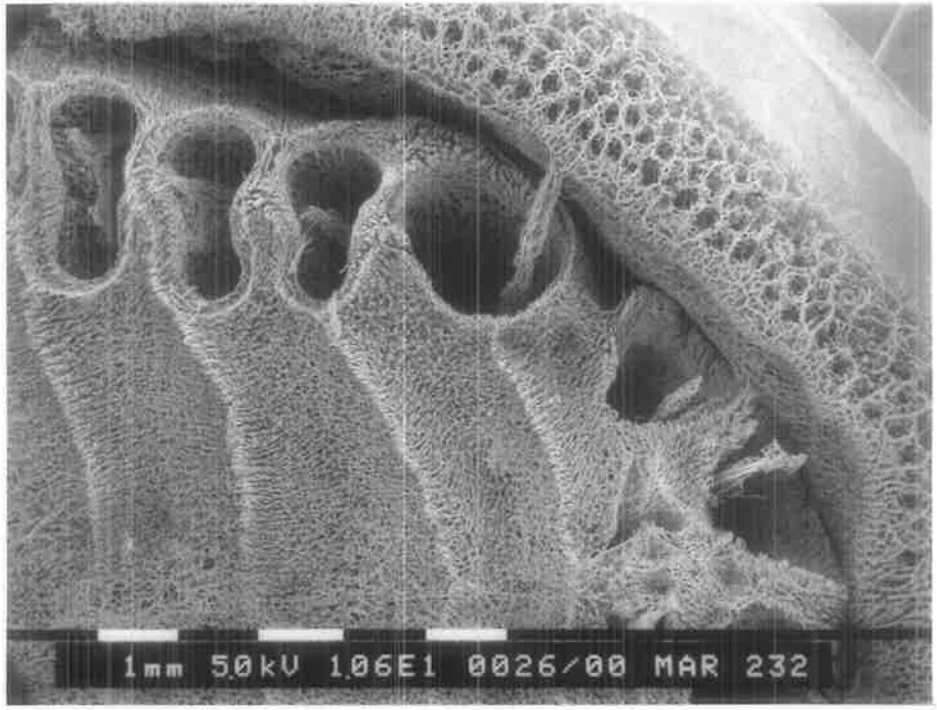
1mm 50kV 106E1 0026/00 MAR 232

ANTERIOR

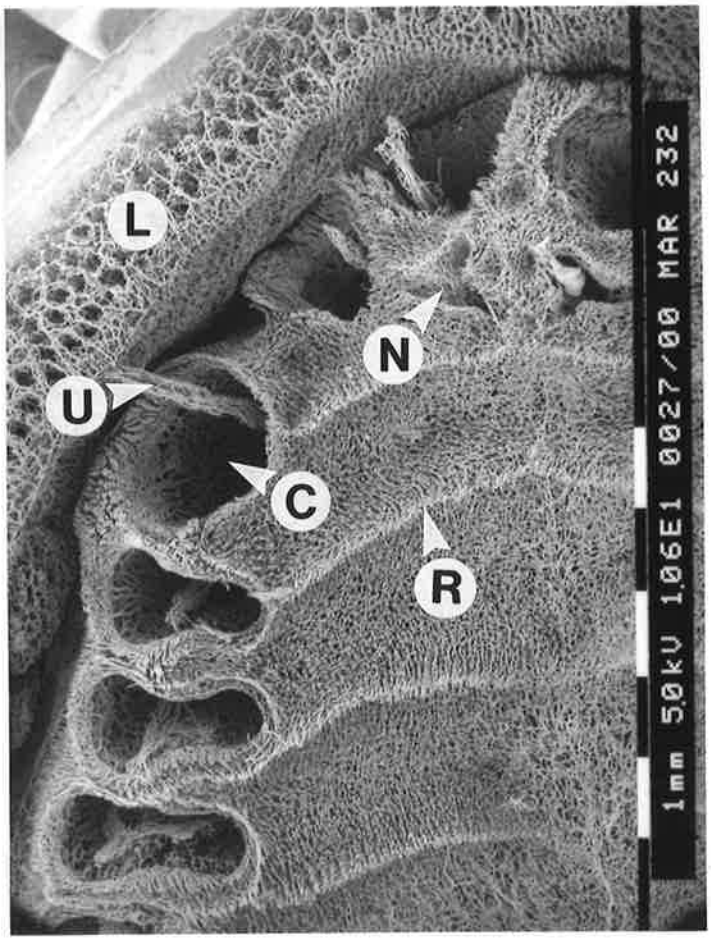

MIDDLE

C = Canine socket.
L = Lip vessels.
N = Nasopalatine foramen.
R = Rugal vessels.
U = Pulpal vessels.

FIGURE 12: VASCULATURE OF THE RIGHT MAXILLA. (YOUNG ANIMAL, MARMOSET 232)

The tooth sockets for the three upper right premolars, the canine (C) and incisors can be seen. Vessels of the upper lip (L) are labial to the tooth sockets.

Rugae (R) extend from the canine and premolar sockets. These were not present with the incisor sockets, however the two nasopalatine foramen (N) can be seen.

Pulpal vessels (U) can be found in the right canine, the right central and lateral incisors.

This micrograph taken by the current author is similar to one used by **LEE** (1988).

MIDDLE

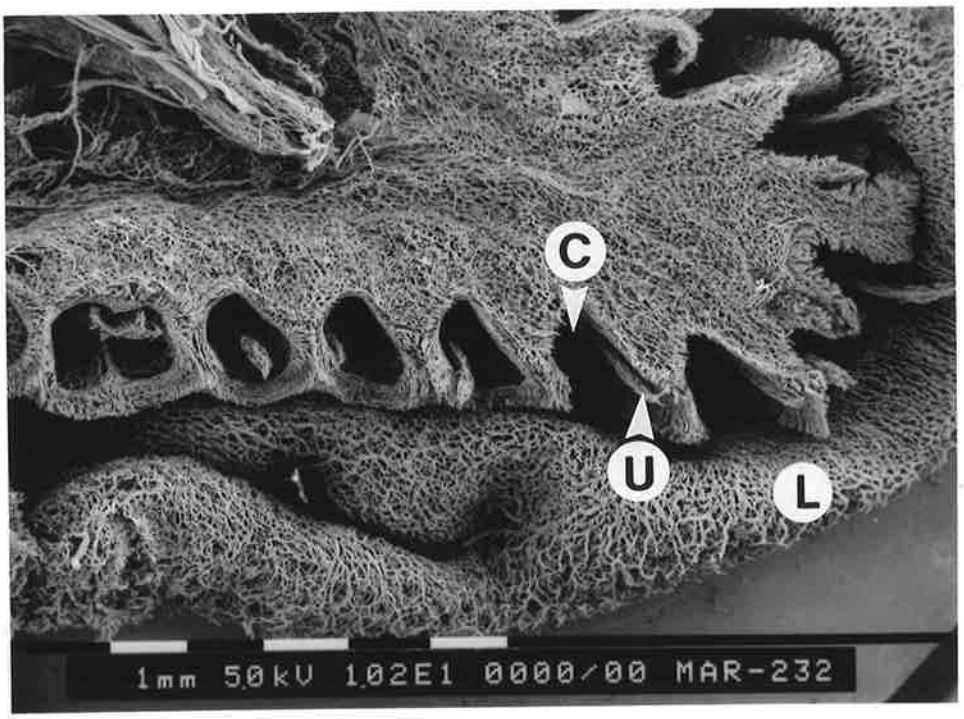

ANTERIOR

C = Canine socket.
L = Lip vessels.
U = Pulpal vessels.

FIGURE 13: VASCULATURE OF THE RIGHT MANDIBLE. (YOUNG ANIMAL, MARMOSET 232)

The tooth sockets for the lower right first molar, the three right premolars, the canine (C) and incisors can be seen. Lower lip vessels (L) are labial and buccal to the tooth sockets. Pulpal vessels (U) are present in most of the sockets.

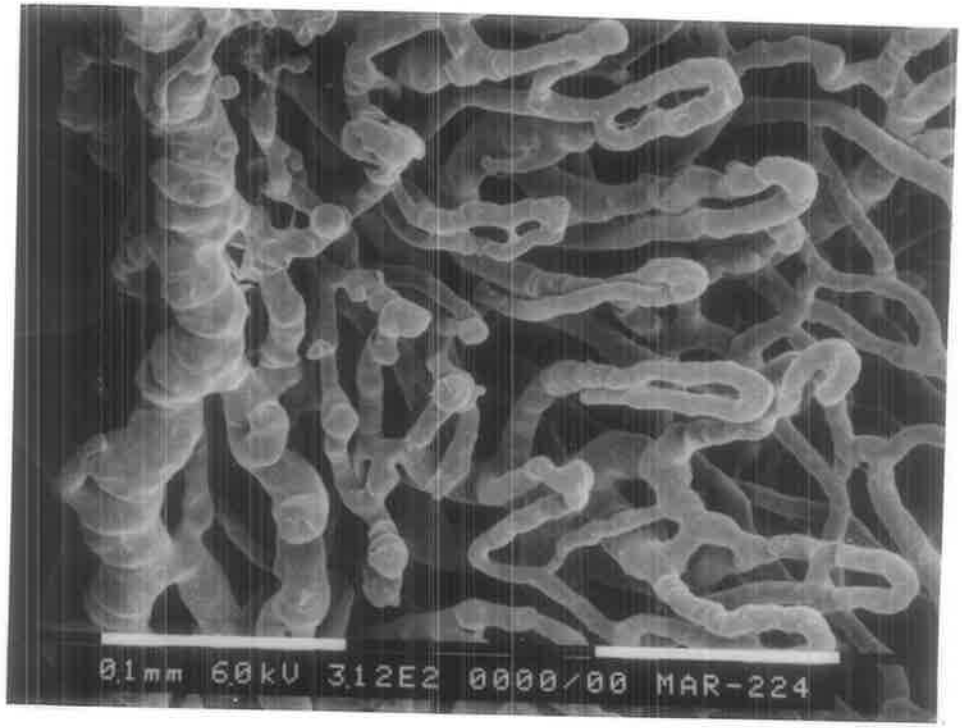
0.1mm 6.0kV 312E2 0000/00 MAR-224

OCCLUSAL

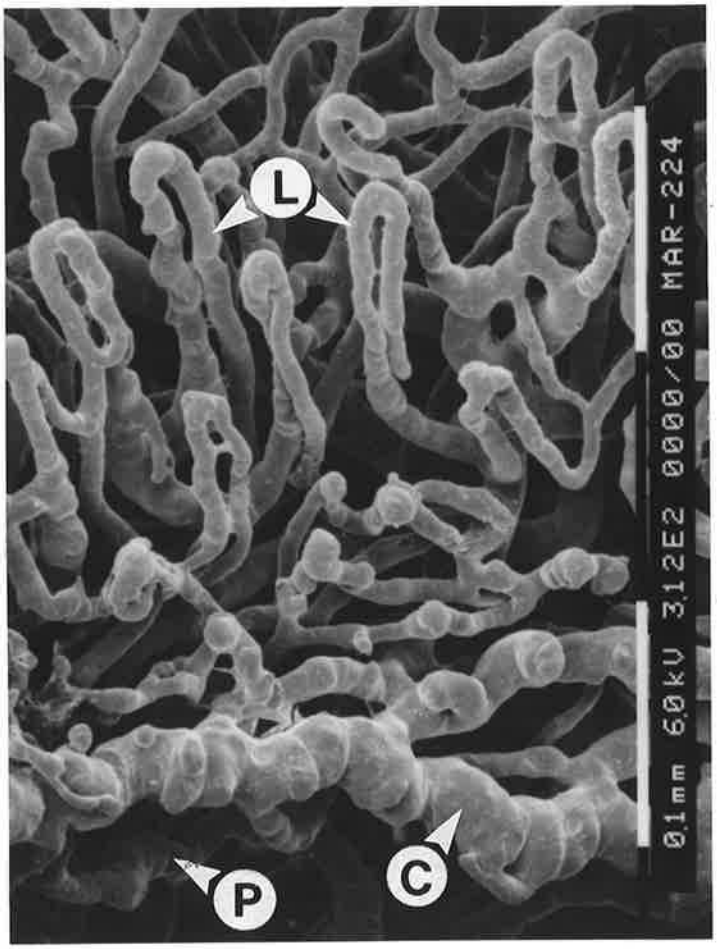

MESIAL

C = Circular plexus vessel.
L = Crevicular loops.
P = PDL vessels.

FIGURE 14: CIRCULAR PLEXUS AND HAIRPIN CREVICULAR LOOPS - MAXILLARY RIGHT CENTRAL INCISOR. (YOUNG ANIMAL, MARMOSET 224)

The diameter of the circular plexus vessel (C) is enlarged around the labial surface in this socket. Diameter here is approximately 30 μm. The crevicular loops (L) have an ascending and a descending limb of approximately equal diameters. Communication of the circular plexus vessel with the cervical PDL vessels (P) can also be seen.

The circular plexus vessel returns to its normal diameter around to the mesial and distal of the socket. Endothelial imprints indicate the circular plexus vessel is venous in nature in this area.

OCCLUSAL

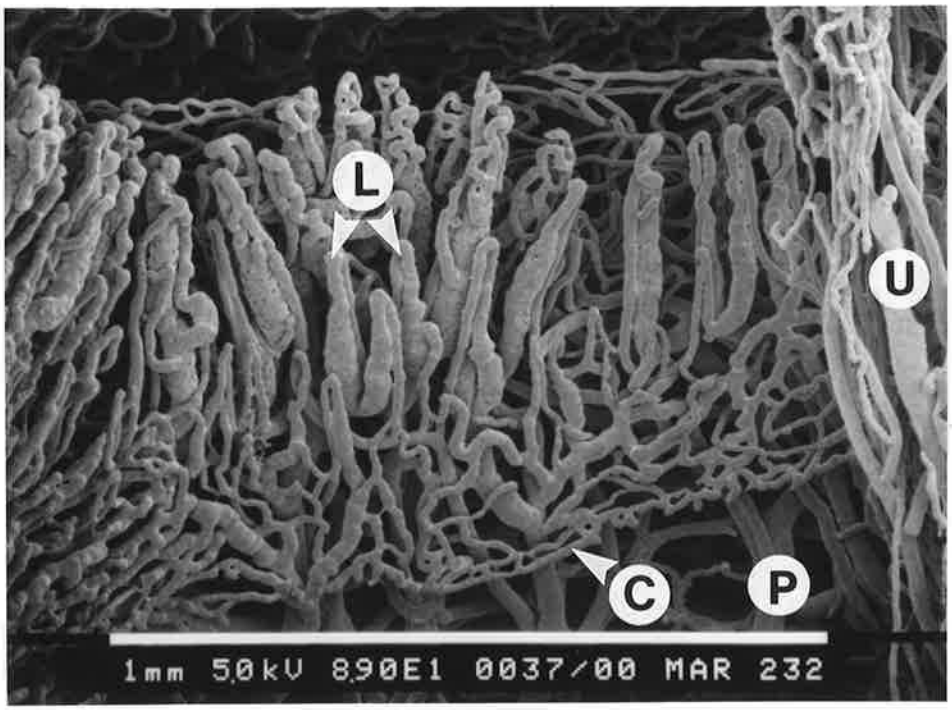

MESIAL

C = Circular plexus vessel.
L = Crevicular loops.
P = PDL vessels.
U = Pulpal vessels.

FIGURE 15: CREVICULAR VESSELS - MAXILLARY RIGHT CANINE. (YOUNG ANIMAL, MARMOSET 232)

In the middle of the labial surface of a maxillary right canine, the crevicular loops (L) are composed of a smaller diameter ascending limb and a larger diameter postcapillary-sized venule descending limb.

Communication between the postcapillary-sized venules of the cervical PDL (P) and the descending limbs of the crevicular loops and the circular plexus (C) can be seen.

OCCLUSAL

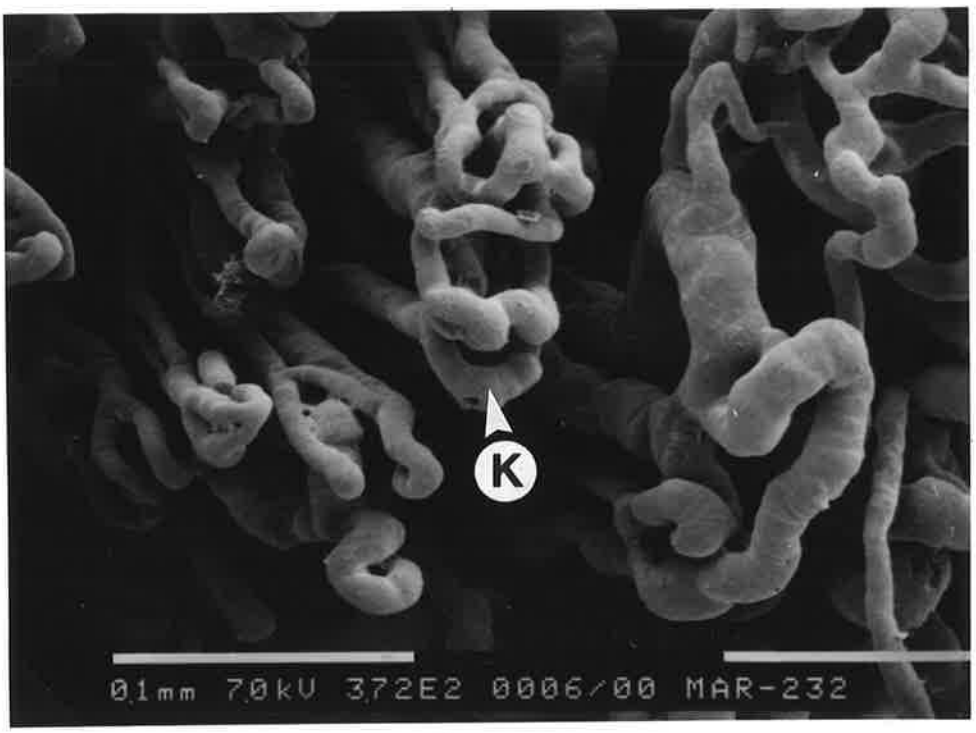

LABIAL

K = Knot-like crevicular loops.

FIGURE 16: KNOT-LIKE CREVICULAR LOOPS - MANDIBULAR RIGHT CENTRAL INCISOR. (YOUNG ANIMAL, MARMOSET 232)

Knot-like crevicular loops (K) of varying shapes and sizes, and with ascending and descending limbs were present on the mesial side of this socket. Communication can be seen between the loops.

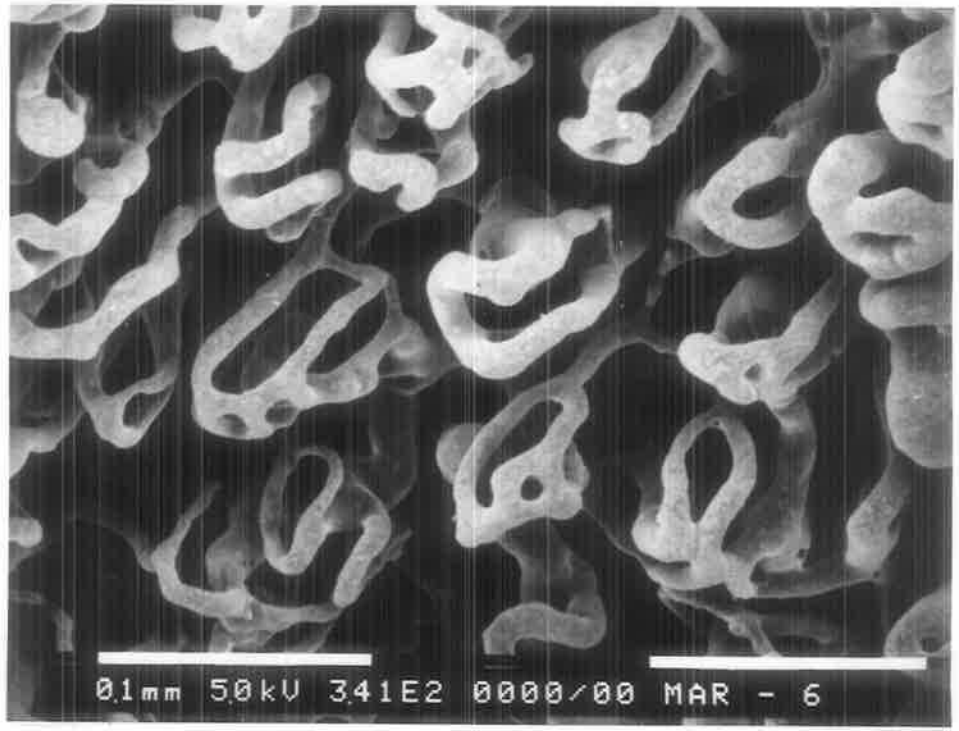
0.1mm 5.0kV 3.41E2 0000/00 MAR - 6

LABIAL

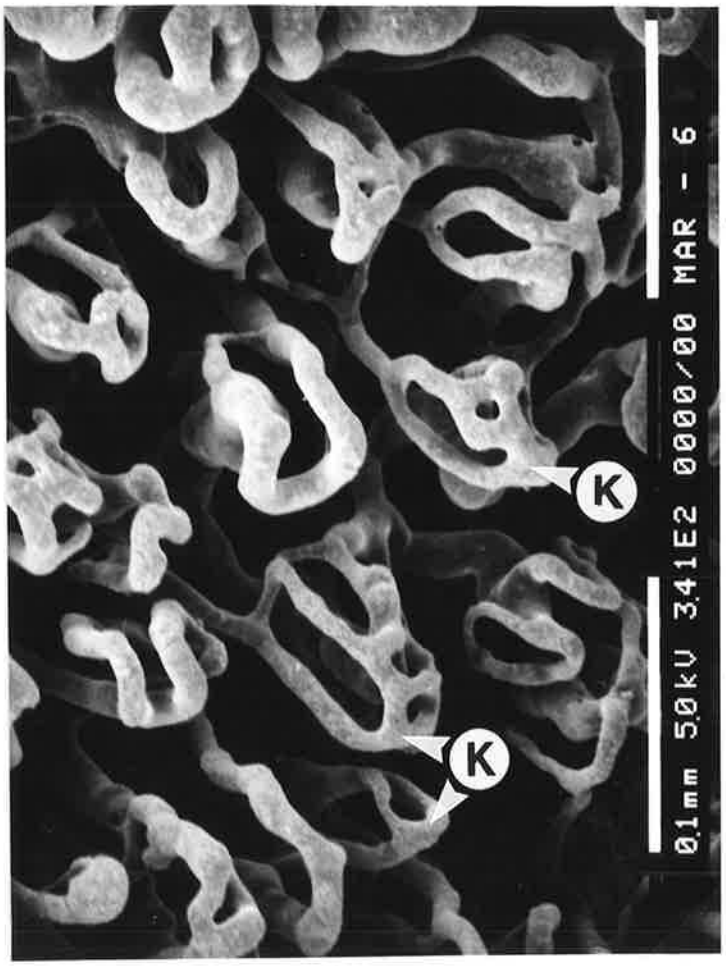

APICAL

K = Knot-like crevicular loops.

FIGURE 17: KNOT-LIKE CREVICULAR LOOPS - MAXILLARY RIGHT CENTRAL INCISOR. (MATURE ANIMAL, MARMOSET 6)

Small knot-like (ring shaped) loops (K) were present in the distolabial crevicular region of this socket. They appeared to have an ascending and descending limb. Communication between adjacent loop structures can also be seen. These loops could be the precursors to the more complex glomerular-like crevicular loops.

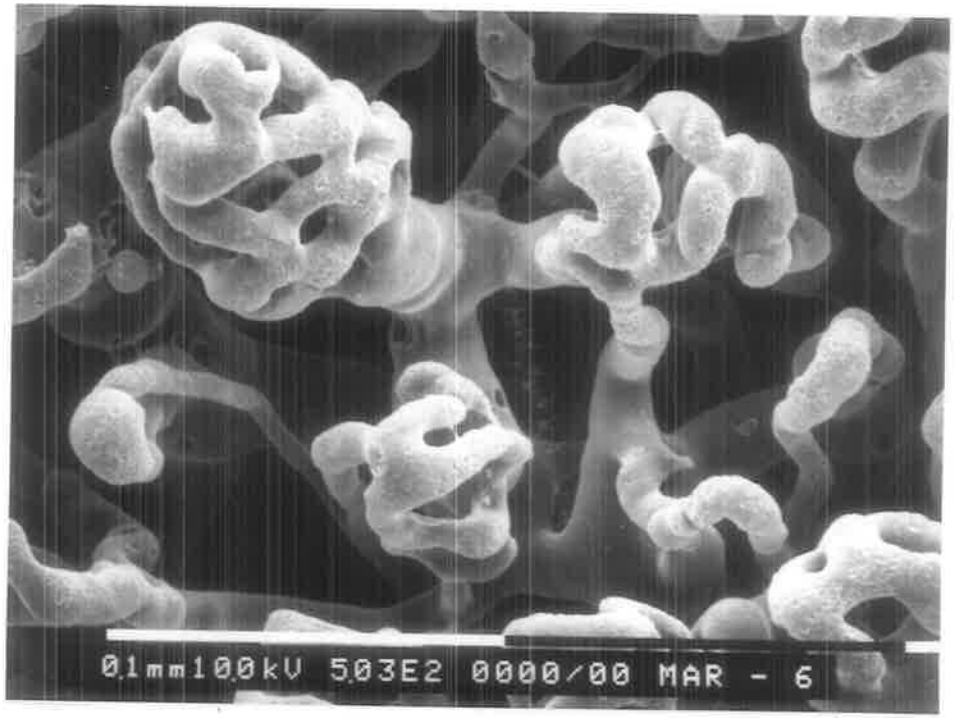
0.1mm10.0kV 5.03E2 0000/00 MAR - 6

DISTAL

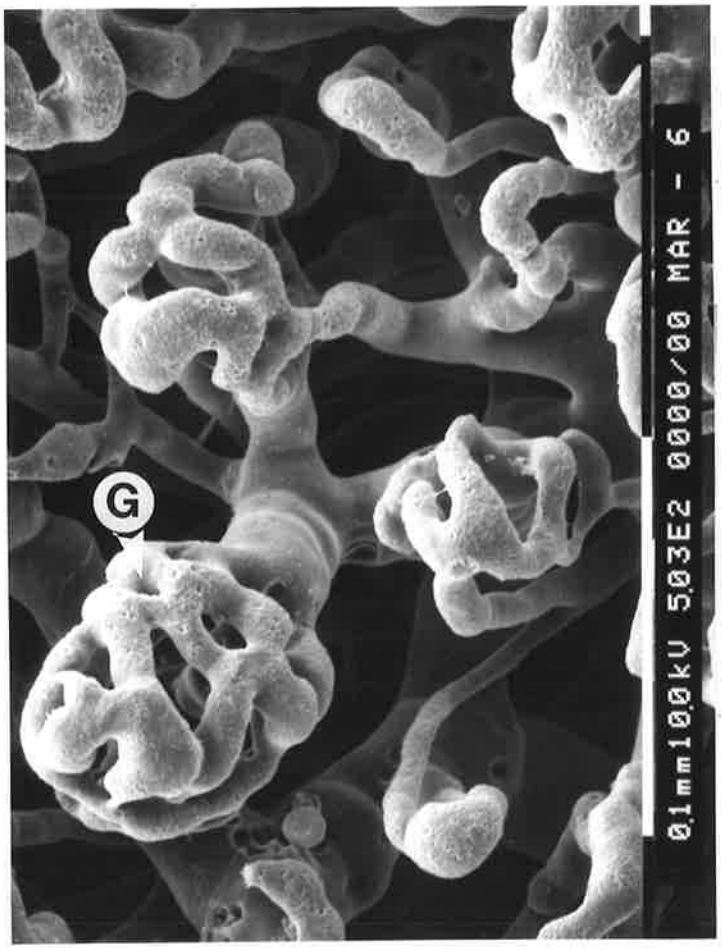

APICAL

G = Glomerular-like crevicular loops.

FIGURE 18: KNOT-LIKE AND GLOMERULAR-LIKE CREVICULAR LOOPS - MAXILLARY LEFT CENTRAL INCISOR. (MATURE ANIMAL, MARMOSET 6).

The glomerular-like crevicular loops (G) on the labial surface are reduced in size and complexity compared with the crevicular loops found associated with the canine sockets of the same animal. These may be earlier (less developed) forms of the more complex glomerular-like loops.

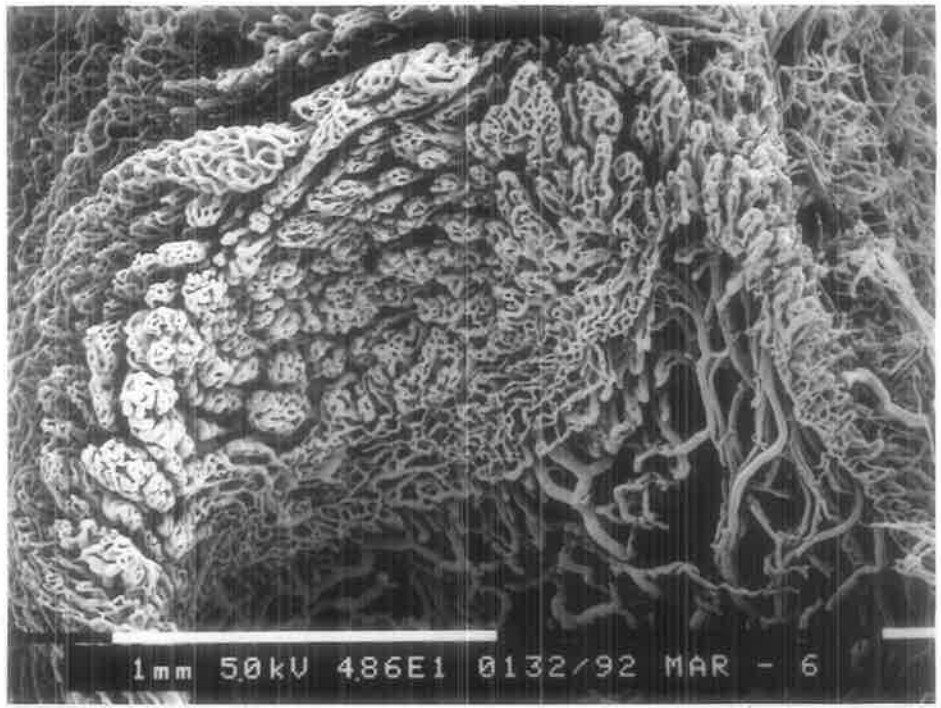
1mm 5.0kV 486E1 0132/92 MAR - 6

LINGUAL

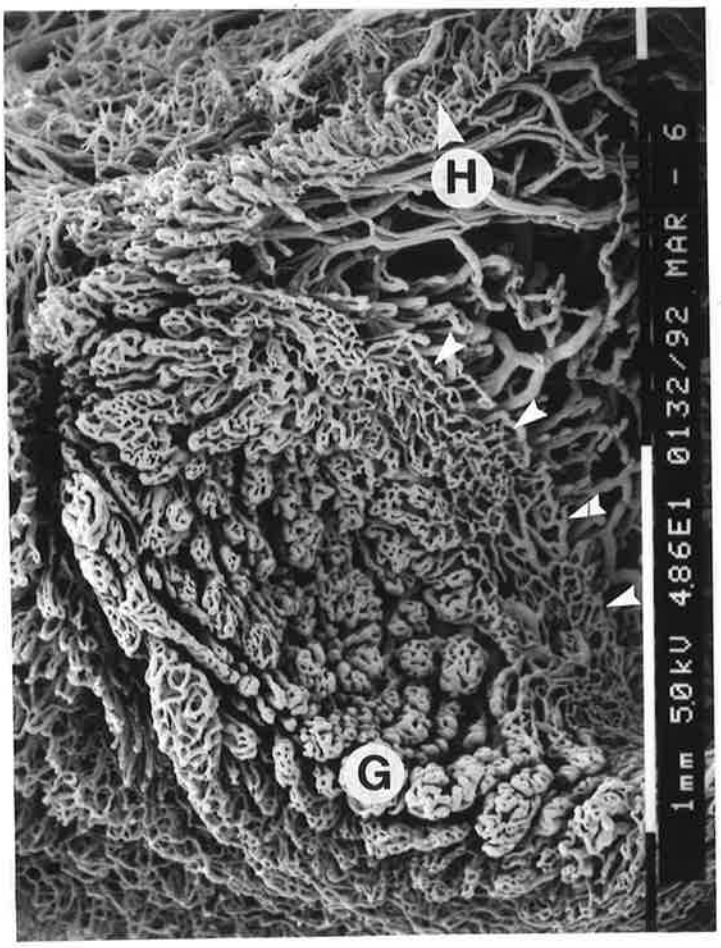

DISTAL

G = Glomerular-like crevicular loops.
H = Hairpin crevicular loops.

FIGURE 19: MESIAL AND PALATAL CREVICULAR REGION - MANDIBULAR LEFT CANINE. (MATURE ANIMAL, MARMOSET 6)

Glomerular-like crevicular loops (G) have extended along the mesial side of the socket towards the lingual. The loop structures change abruptly to simple hairpin loops (H) on the lingual side of the socket.

Note the extension of the crevicular loop structures apically (arrows), which may be an indication of periodontal pocket formation.

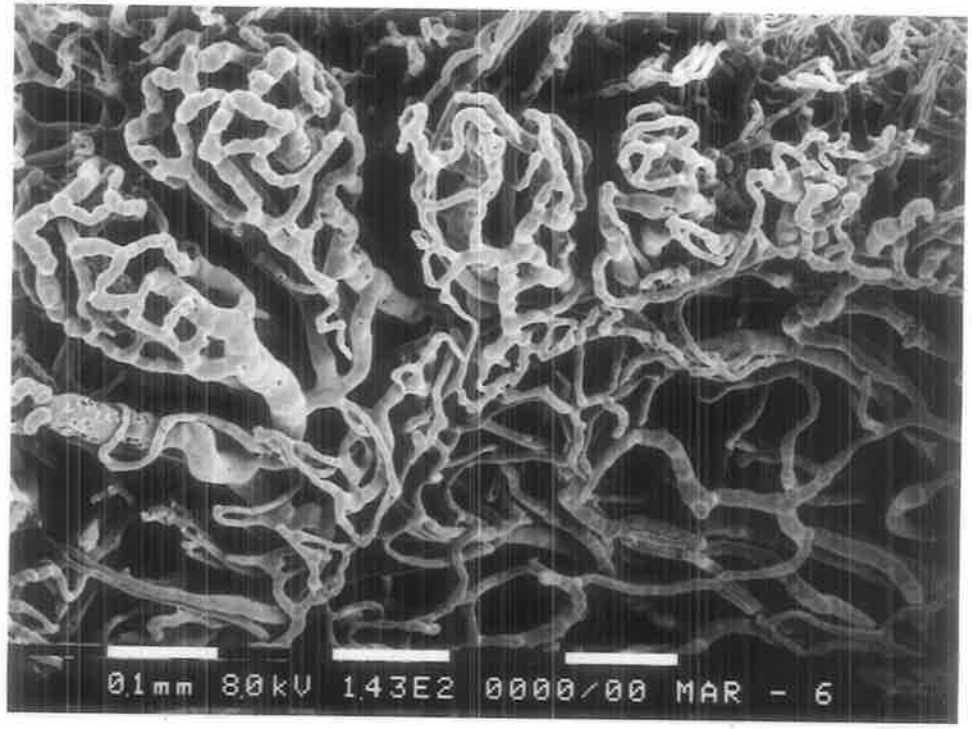
0,1mm 8,0kV 1,43E2 0000/00 MAR - 6

PALATAL

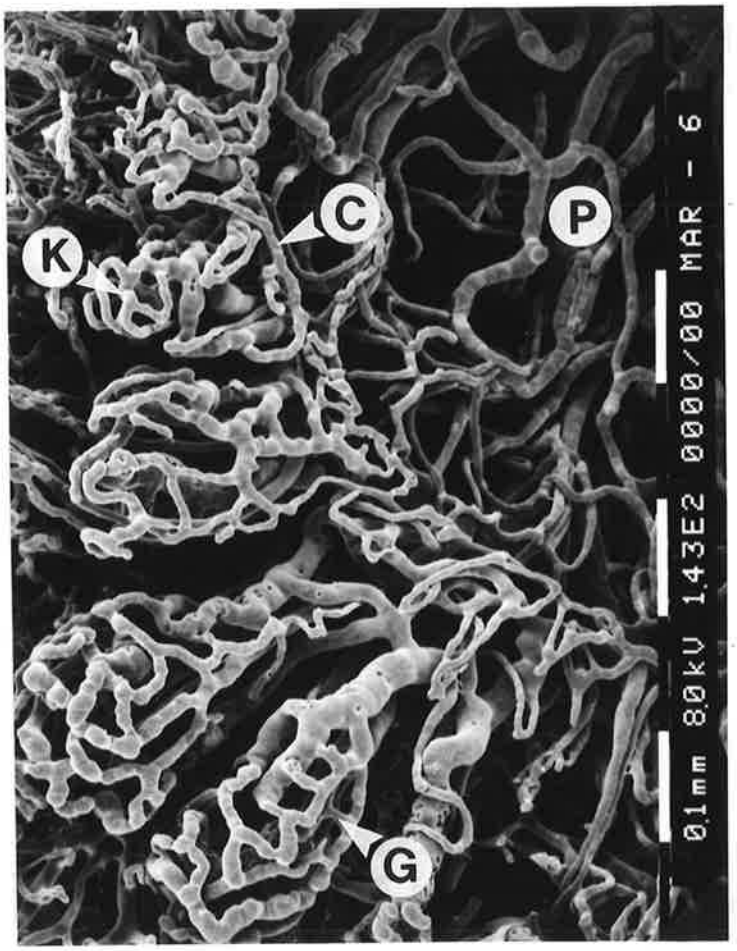

DISTAL

C = Circular plexus vessel.
G = Glomerular-like crevicular loops.
K = Knot-like crevicular loops.
P = PDL vessels.

FIGURE 20: GLOMERULAR-LIKE CREVICULAR LOOPS - MAXILLARY RIGHT CENTRAL INCISOR. (MATURE ANIMAL, MARMOSET 6)

The glomerular-like crevicular loops (G) have reduced in height going from the mesial, 350 to 400 μm, around to the palatal, 50 μm. Their complexity has also reduced towards the palatal where they have a knot-like (K) appearance.

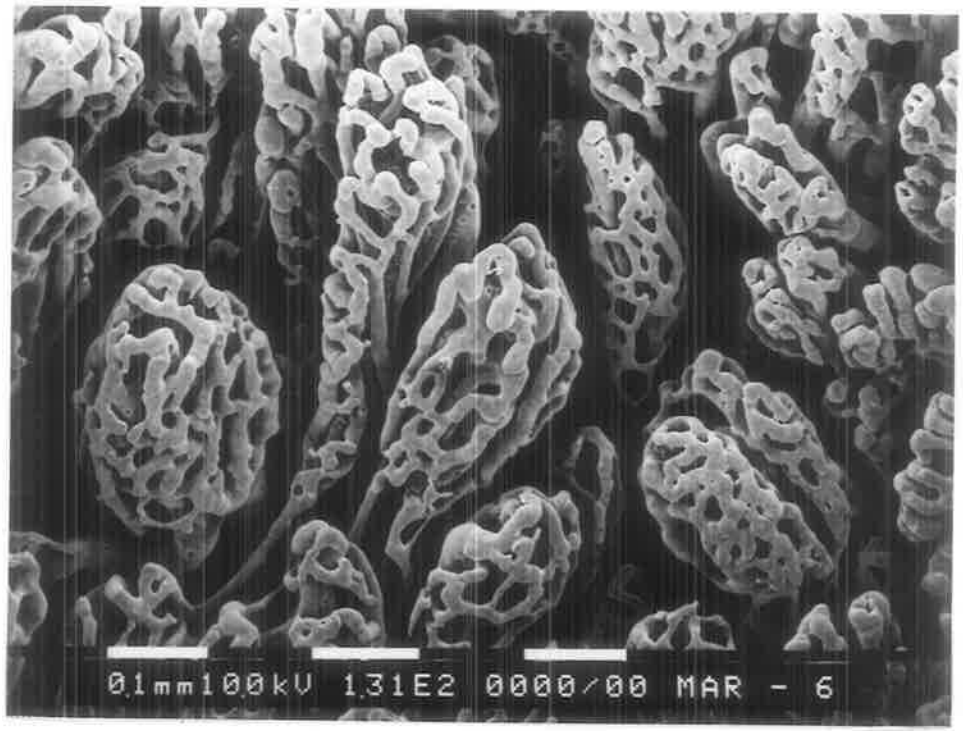
0.1mm 10.0kV 1.31E2 0000/00 MAR - 6

DISTAL

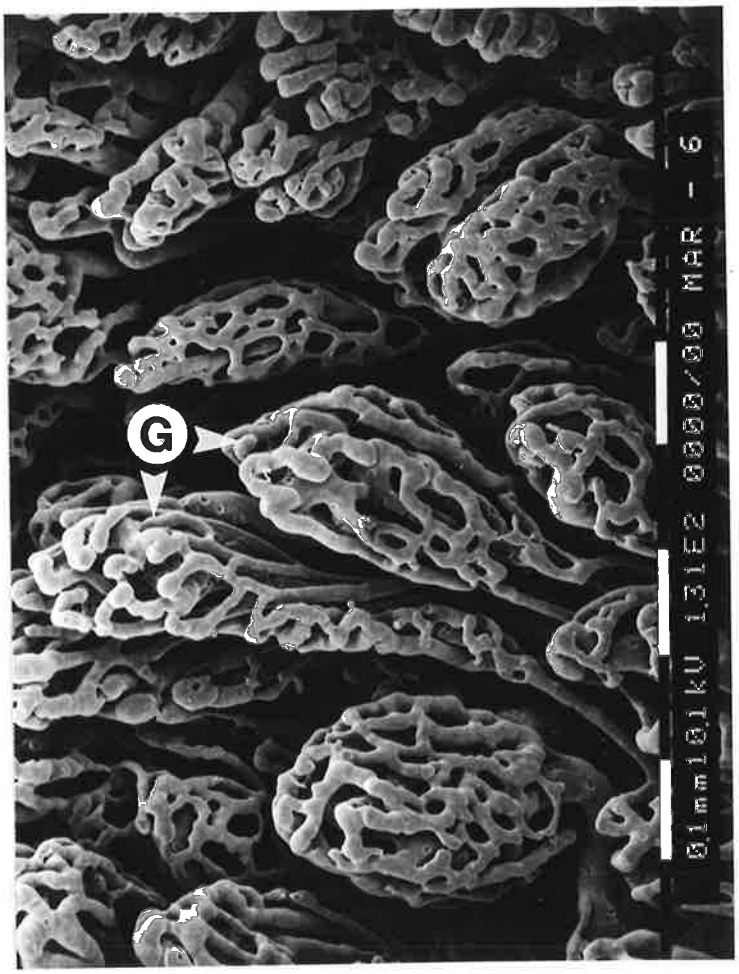

APICAL

G = Glomerular-like crevicular loops.

FIGURE 21: GLOMERULAR-LIKE CREVICULAR LOOPS - MAXILLARY LEFT CANINE. (MATURE ANIMAL, MARMOSET 6)

Various shapes and sizes of glomerular-like crevicular loops (G) were present on the labial side of this tooth socket. The complexity of these structures is generally greater in the canine sockets compared to the incisors in the same animal.

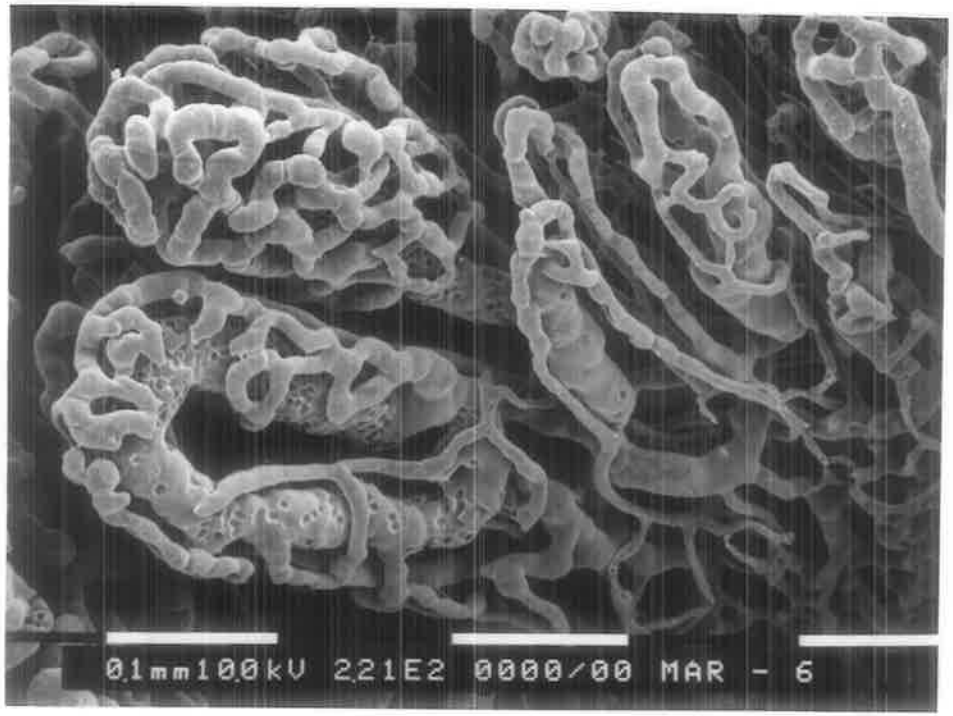
01mm10.0kV 221E2 0000/00 MAR - 6

OCCLUSAL

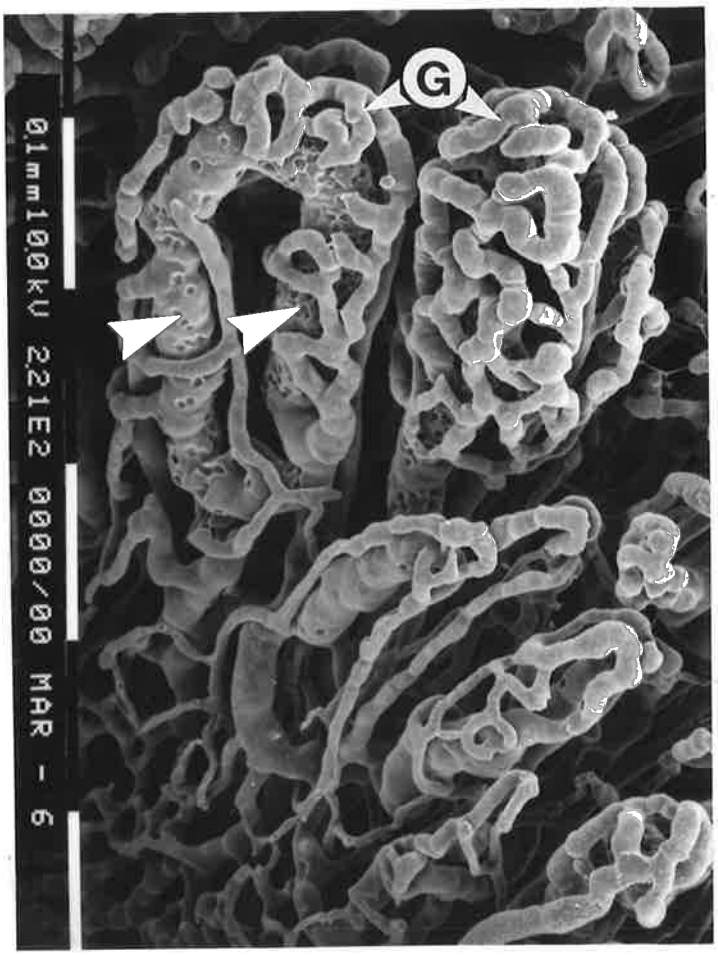

DISTAL

G = Glomerular-like crevicular loops.

FIGURE 22: GLOMERULAR-LIKE CREVICULAR LOOPS - MAXILLARY LEFT LATERAL INCISOR. (MATURE ANIMAL, MARMOSET 6)

These were the only glomerular-like crevicular loops (G) found around the maxillary left lateral incisor socket in this animal. They were found on the distolabial side. The other loops were either knot-like or hairpin loops.

There appeared to be incomplete casting which has allowed the central larger diameter ascending and descending vessels (arrows) to be viewed. They form a "horse shoe" shape. A capillary network surrounds these central vessels.

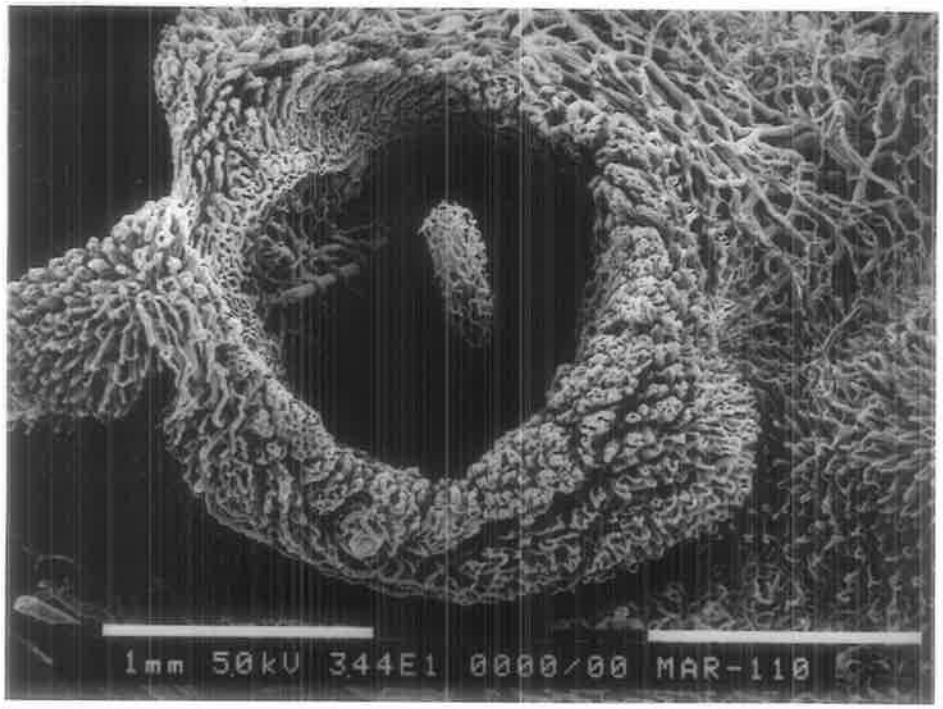
1mm 5.0kV 344E1 0000/00 MAR-110

MESIAL

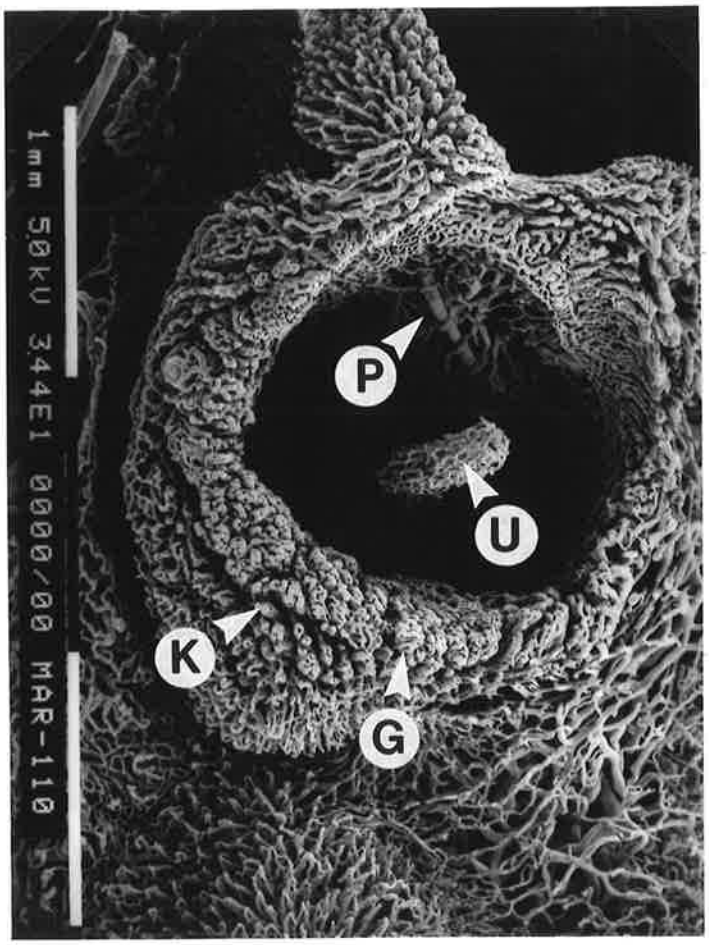

PALATAL

G = Glomerular-like loops.
K = Knot-like loops.
P = PDL vessels.
U = Pulpal vessels.

FIGURE 23: OCCLUSAL VIEW - MAXILLARY RIGHT LATERAL INCISOR. (MATURE ANIMAL, MARMOSET 110)

Occlusal view showing glomerular-like (G) and knot-like (K) loops extending onto the labial gingival surface. The pulpal vessels (U) form a network of capillaries in the region of the pulp horn.

PALATAL

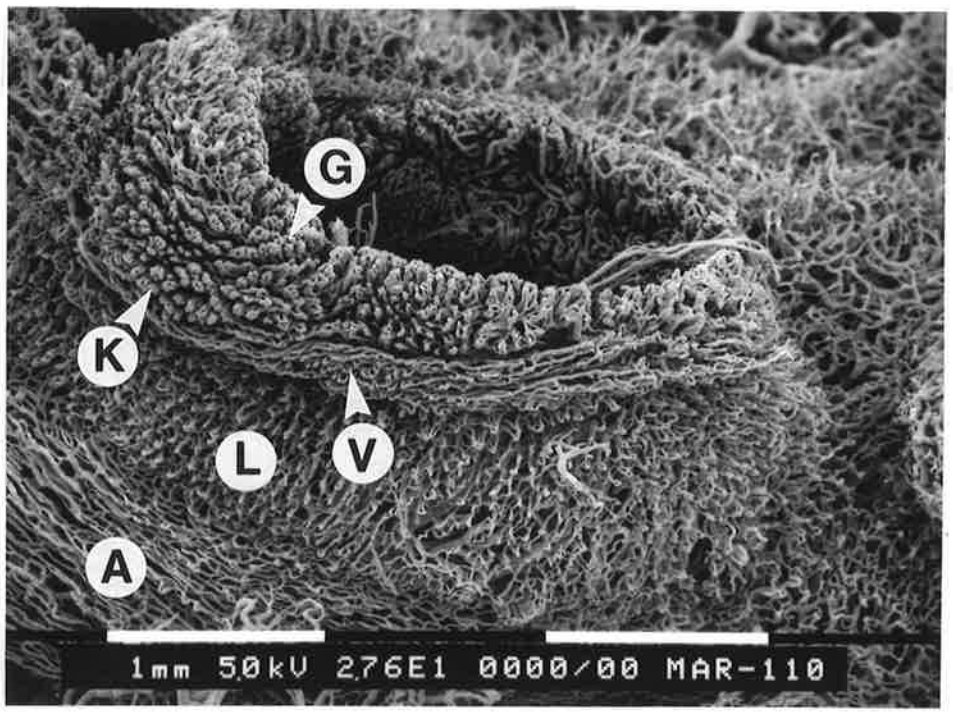

MESIAL

A = Alveolar mucosal vessels.
G = Glomerular-like loops.
K = Knot-like loops.
L = Labial gingival loops.
V = Vestibular gingival vessels.

FIGURE 24: LABIAL GINGIVAL VESSELS - MAXILLARY LEFT CANINE. (MATURE ANIMAL, MARMOSET 110)

Glomerular-like (G) and knot-like (K) loops extend down the labial gingival surface. Below this layer, bands of vestibular gingival vessels (V) run horizontally.

Below the vestibular gingival vessels the loops have an occluso-apical orientation. This is the area where the labial gingival loops (attached gingival tissue) (L) are found. The orientation of the capillary network changes suddenly again as the sulcus is approached at the presumptive mucogingival junction so that the capillary vessels are running horizontally again and form an open meshwork. This is the area where the alveolar mucosal vessels (A) are found.

OCCLUSAL

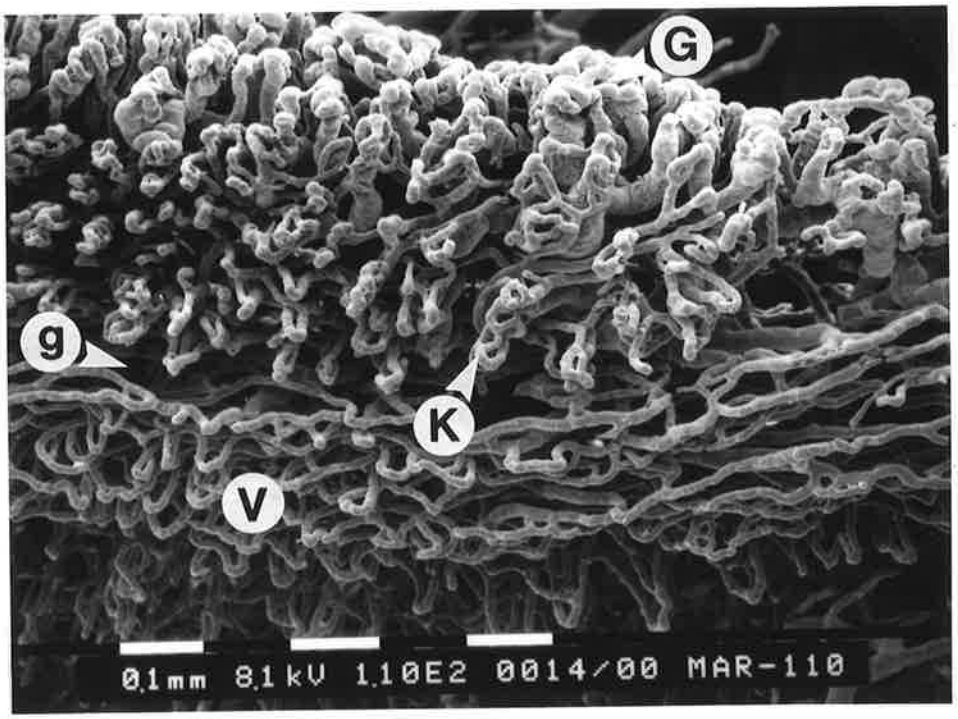

MESIAL

G = Glomerular-like loops.
g = Gap.
K = Knot-like loops
V = Vestibular gingival vessels.

FIGURE 25: GLOMERULAR-LIKE AND KNOT-LIKE LOOPS EXTEND OVER ONTO THE LABIAL GINGIVAL SURFACE - MAXILLARY LEFT CANINE. (MATURE ANIMAL, MARMOSET 110)

This is a higher power view to that shown in Figure 24. Glomerular-like (G) and knot-like (K) loop structures extend onto the labial gingival surface. These are not as complex as some of the loop structures seen in the crevicular region of the older animals.

A distinct gap (g) below these loops is present which separates them from the vestibular gingival vessels (V) below.

OCCLUSAL

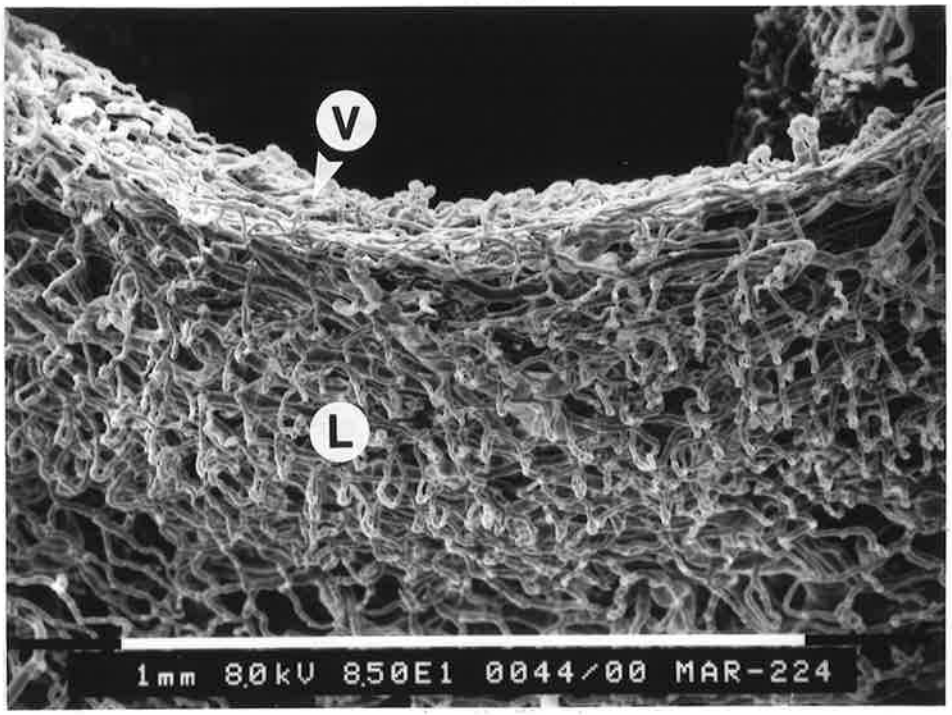

DISTAL

L = Labial gingival loops.
V = Vestibular gingival vessels.

FIGURE 26: LABIAL GINGIVAL VESSELS - MAXILLARY RIGHT CANINE. (YOUNG ANIMAL, MARMOSET 224)

The vestibular gingival vessels (V) were at the crest of the tooth socket. The labial gingival loops (L) have an occluso-apical orientation and project labially. This is the area where attached gingiva would be found.

This micrograph should be compared with Figure 25. Note the absence of glomerular-like loops extending onto the labial surface.

OCCLUSAL

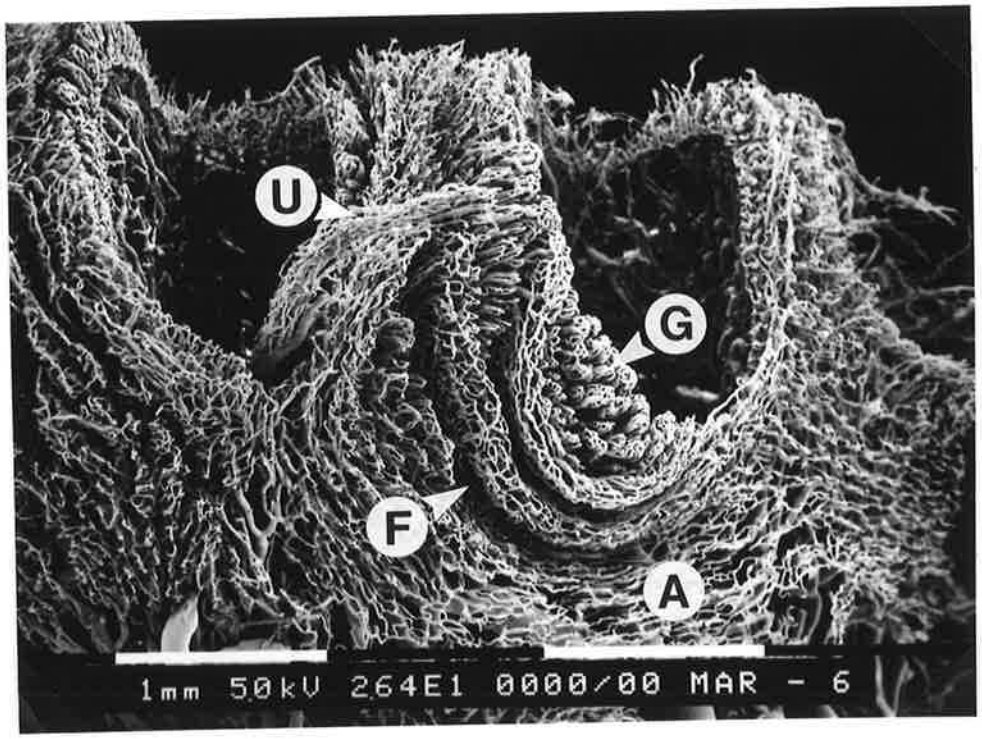

DISTAL

A = Alveolar mucosal vessels.
F = Clefts.
G = Glomerular-like loops.
U = Pulpal vessels.

FIGURE 27: LABIAL GINGIVAL VESSELS - MANDIBULAR LEFT LATERAL INCISOR AND CANINE. (MATURE ANIMAL, MARMOSET 6)

Clefts (F) were present on the labial gingival surface in the region of a mandibular left canine. They extend up into the col region between the left canine and lateral incisor. The open capillary meshwork of the alveolar mucosa (A) was directly below these clefts.

Glomerular-like loops (G) extend onto the labial gingival surface of the canine. Pulpal vessels (U) emerge from the lateral incisor socket.

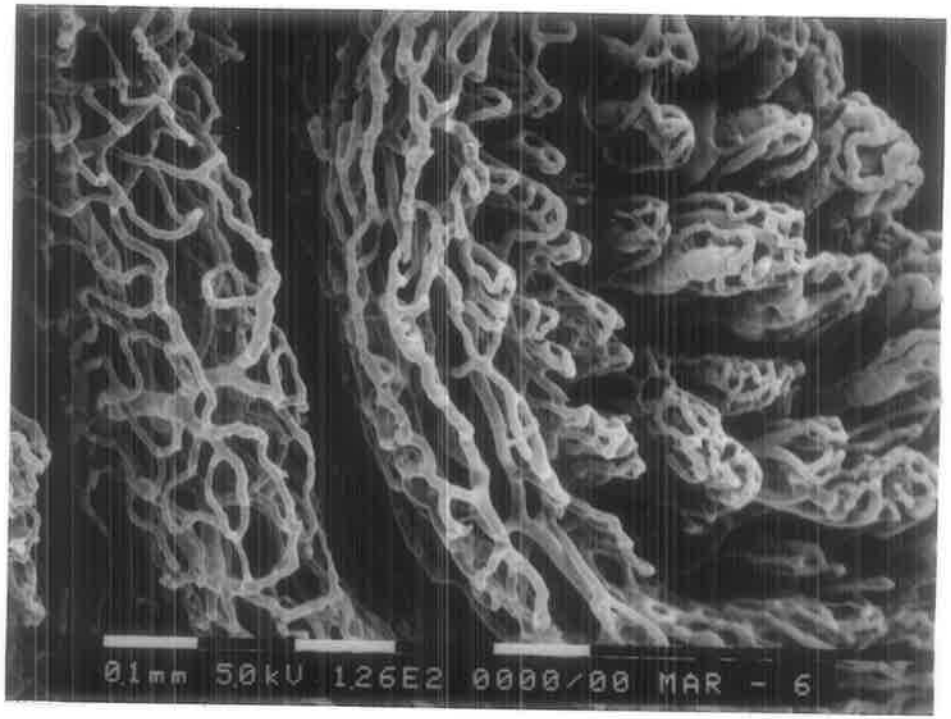
0.1mm 5.0kV 1.26E2 0000/00 MAR - 6

DISTAL

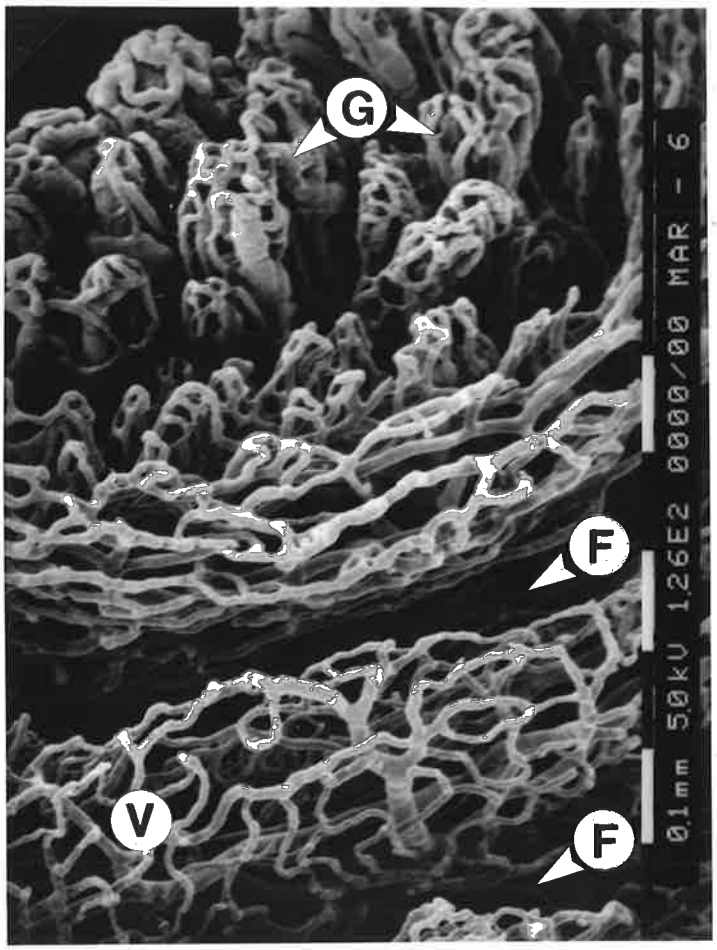

APICAL

F = Clefts.
G = Glomerular-like loops.
V = Vestibular gingival vessels.

FIGURE 28: LABIAL GINGIVAL VESSELS - INTERPROXIMAL REGION BETWEEN THE MANDIBULAR LEFT CANINE AND LATERAL INCISOR. (MATURE ANIMAL, MARMOSET 6)

This is a higher power view of Figure 27. A band of vestibular gingival vessels (V) was present with a cleft (F) either side. Glomerular-like loops (G) extend onto the labial gingival surface.

OCCLUSAL

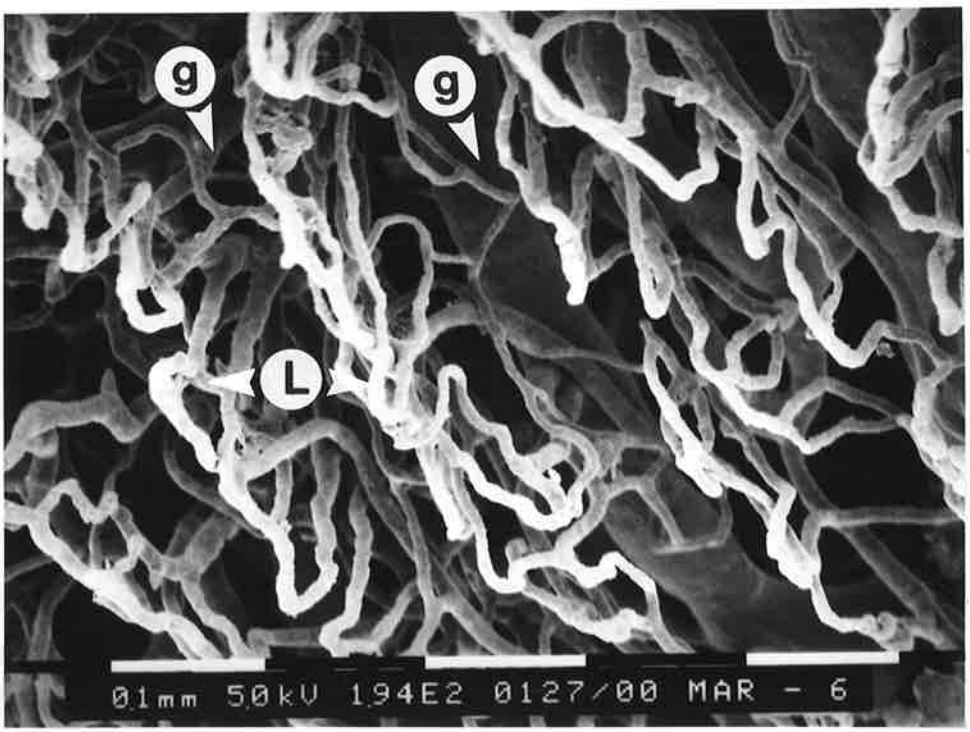

g = Gap.
L = Labial gingival loops.

FIGURE 29: LABIAL GINGIVAL LOOPS - MANDIBULAR CENTRAL INCISORS. (MATURE ANIMAL, MARMOSET 6)

Long cords of labial gingival loops (L) run occluso-apically in the attached gingival region between the mandibular central incisors. Larger diameter venules deep to this capillary layer also run occluso-apically. Distinct gaps (g) are present between these labial gingival cords with communication being found at a deeper level.

OCCLUSAL

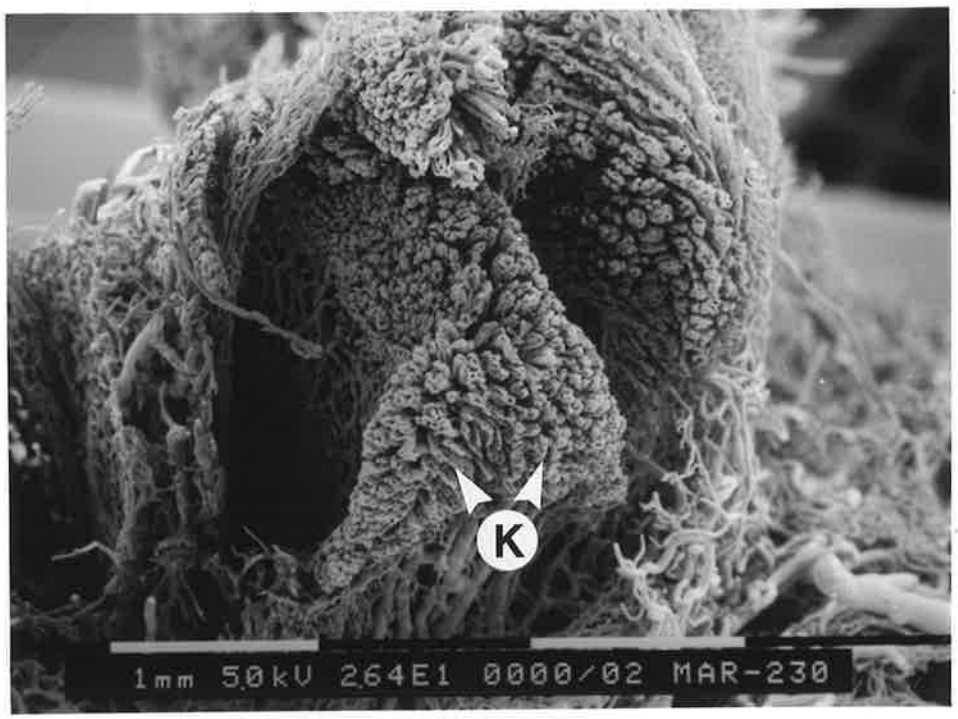

K = Knot-like loops.

FIGURE 30: LABIAL VIEW - MANDIBULAR CENTRAL INCISORS. (YOUNG ANIMAL, MARMOSET 230)

Knot-like (K) loops are not confined to the crevicular region but extend down the labial surface and interproximally. These knot-like loops are more prolific in this young animal than with any of the mature animals. The more complex glomerular-like crevicular loops are found only in the older animals.

OCCLUSAL

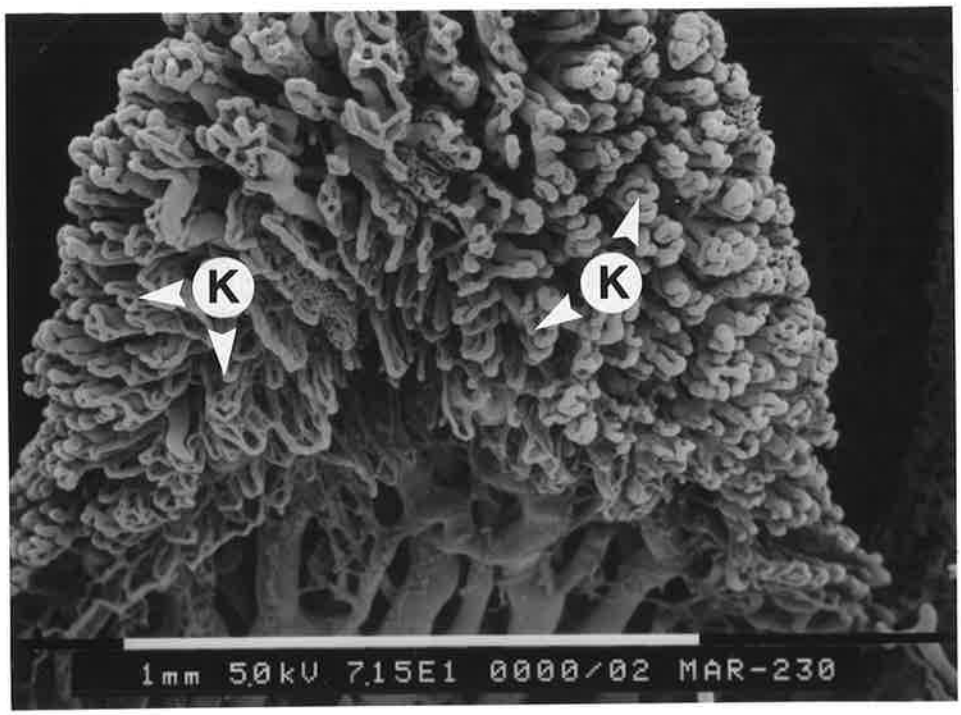

K = Knot-like loops.

FIGURE 31: LABIAL GINGIVAL VESSELS - BETWEEN THE MANDIBULAR CENTRAL INCISORS. (YOUNG ANIMAL, MARMOSET 230)

This is a higher power view of Figure 30 and represents the area marked with the arrow in that illustration. Extensive proliferation of knot-like loops (K) onto the labial gingival surface between the lower central incisors can be seen. Some of these loops are tending towards being small, glomerular-like loops. The more complex glomerular-like loops however were only found in the mature animals, suggesting that these structures increase in complexity with time.

OCCLUSAL

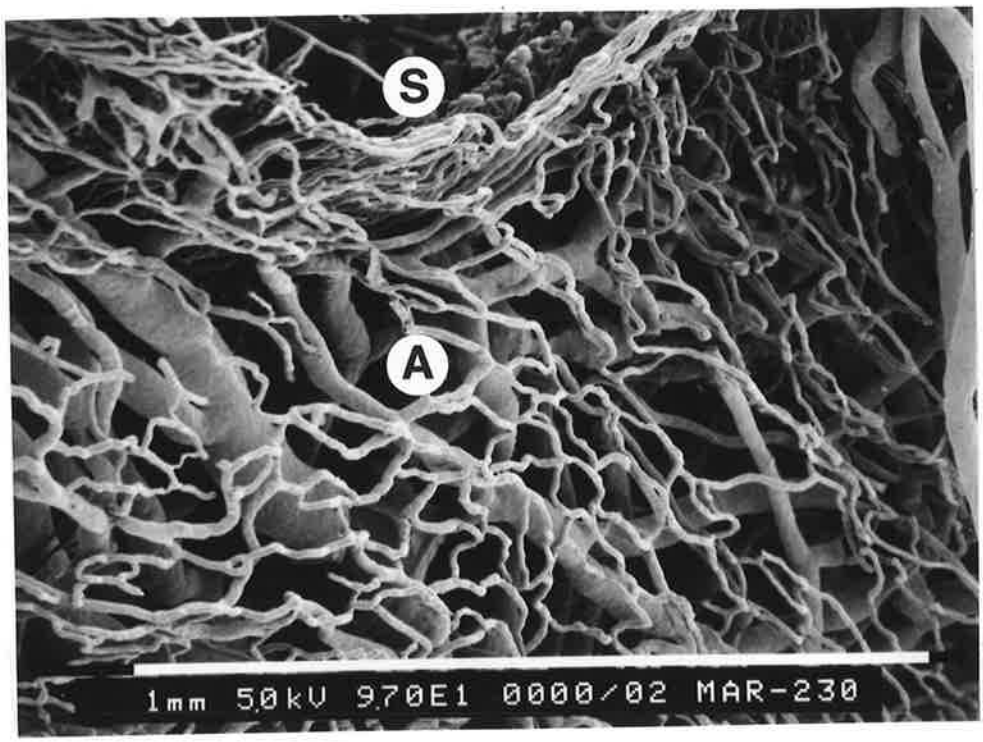

DISTAL

A = Alveolar mucosal vessels.
S = Tooth socket.

FIGURE 32: LABIAL GINGIVAL VESSELS - MANDIBULAR LEFT CANINE. (YOUNG ANIMAL, MARMOSET 230)

Wide arcades of capillaries are present on the labial gingival side of the tooth socket. This arrangement of vessels is consistent with that found in the region of the alveolar mucosa (A). These arcades of capillaries are present up to the tooth socket (S) which suggests that there is no attached labial gingiva with this animal's lower anterior teeth. Larger venules can be seen running at a deeper level to the capillary canopy.

This animal shows extensive knot-like loop structures extending onto the labial gingival surface and interproximal papilla around many of the lower anterior teeth - see Figures 30 and 31.

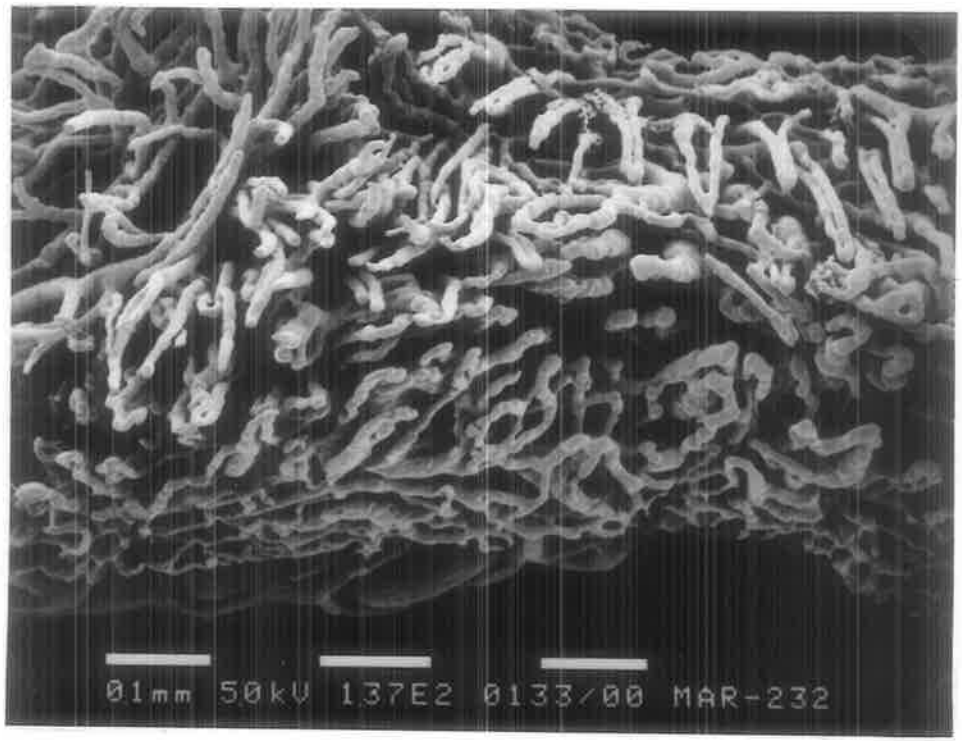
01mm 50kV 137E2 0133/00 MAR-232

LABIAL

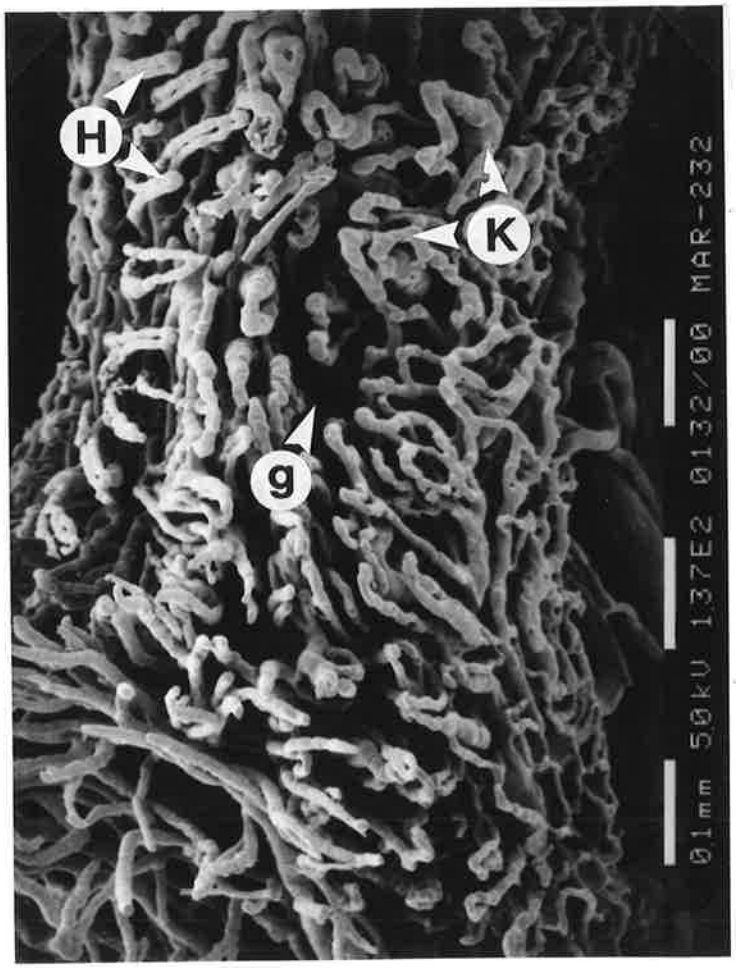

DISTAL

H = Hairpin crevicular loops.
K = Knot-like crevicular loops.
g = Gap.

FIGURE 33: COL AREA - BETWEEN THE MANDIBULAR RIGHT CANINE AND FIRST PREMOLAR. (YOUNG ANIMAL, MARMOSET 232)

This is an occlusal view. Simple hairpin (H) and knot-like (K) crevicular loops extend into the col region. A gap (g) is present, however this is not continuous and may have been caused due to shrinkage of the cast.

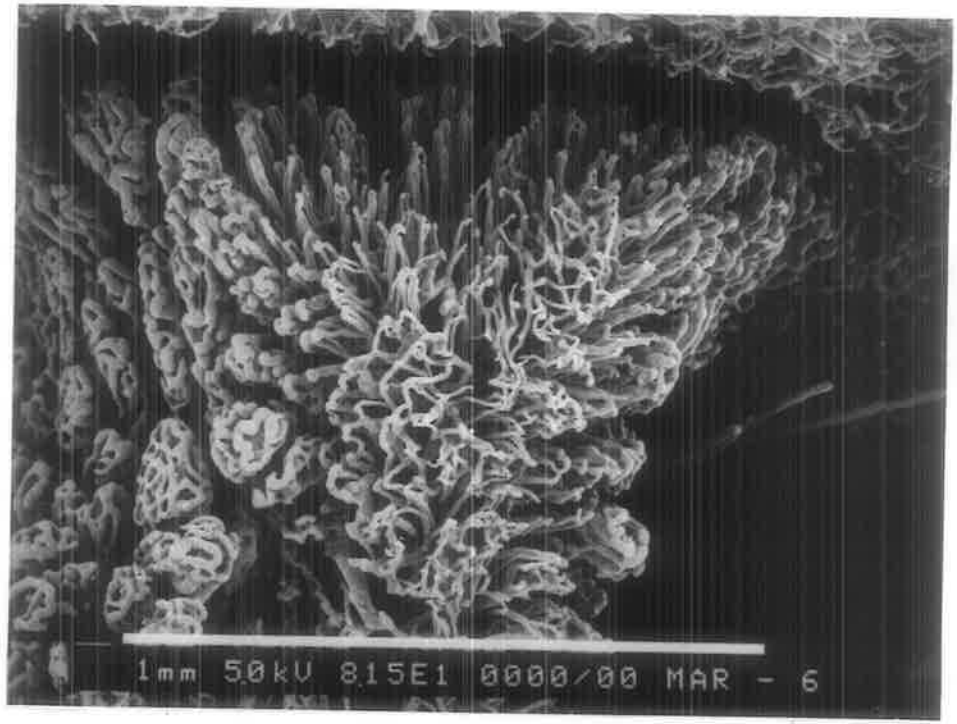
1mm 50kV 815E1 0000/00 MAR - 6

DISTAL

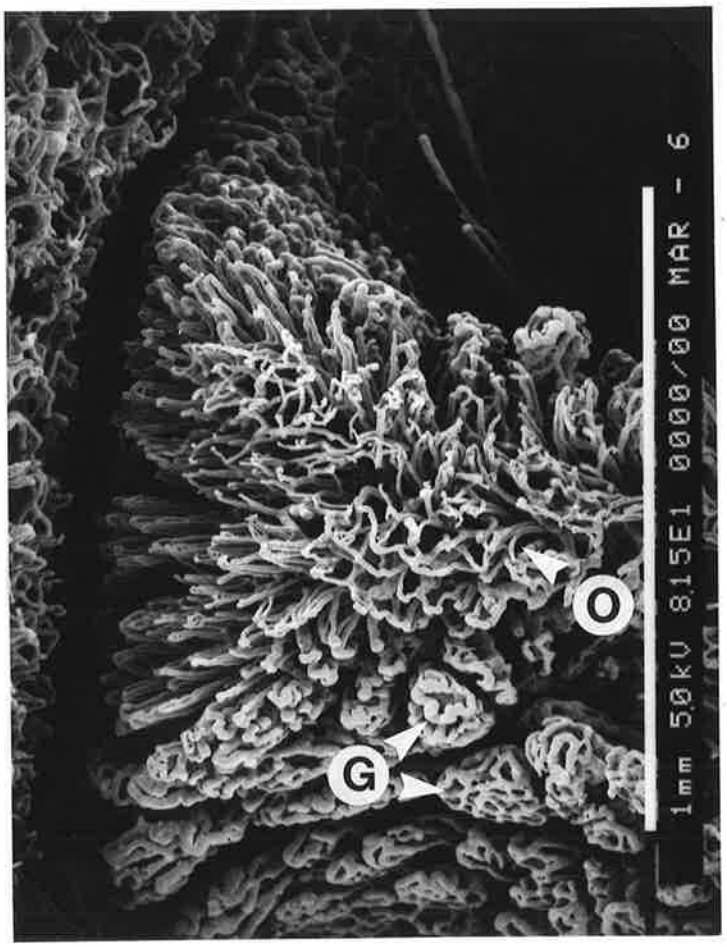

PALATAL

G = Glomerular-like crevicular loops.
O = Col loops.

FIGURE 34: COL AREA - BETWEEN THE MAXILLARY RIGHT CENTRAL AND LATERAL INCISORS. (MATURE ANIMAL, MARMOSET 6)

Glomerular-like crevicular loops (G) on the distal side of the maxillary right lateral incisor socket appear to extend into the interproximal col region. The col loops (O) have a hairpin arrangement and are orientated labio-palatally. A distinct gap separating the crevicular and col loops cannot be seen.

OCCLUSAL

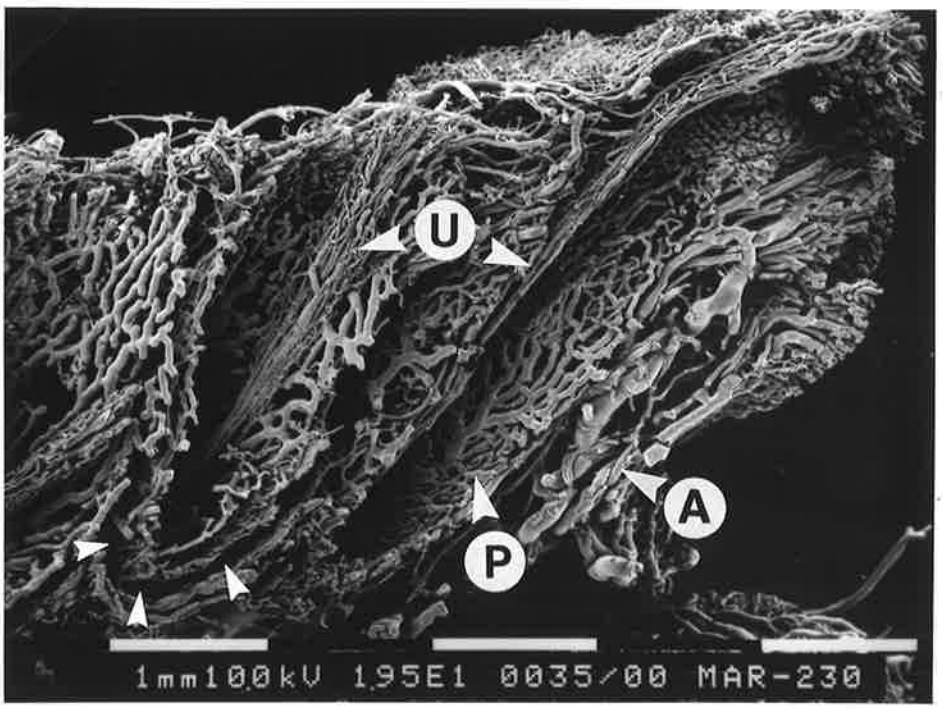

LABIAL

A = Alveolar mucosal vessels.
P = PDL vessels.
U = Pulpal vessels.

FIGURE 35: MESIAL SOCKET WALL - MANDIBULAR RIGHT CENTRAL INCISOR. MESIOLINGUAL SOCKET WALLS - MANDIBULAR RIGHT LATERAL INCISOR AND CANINE. (YOUNG ANIMAL, MARMOSET 230)

The sockets have been sectioned to reveal both the pulpal (U) and PDL vessels (P). The mandibular right central incisor socket is to the right of the micrograph. Alveolar mucosal vessels (A) can be seen coursing towards the labial sulcus. Note the gap (arrows) around the apical portion of the lateral incisor which suggests an area of increased bone density and reduced vascularity.

MESIAL

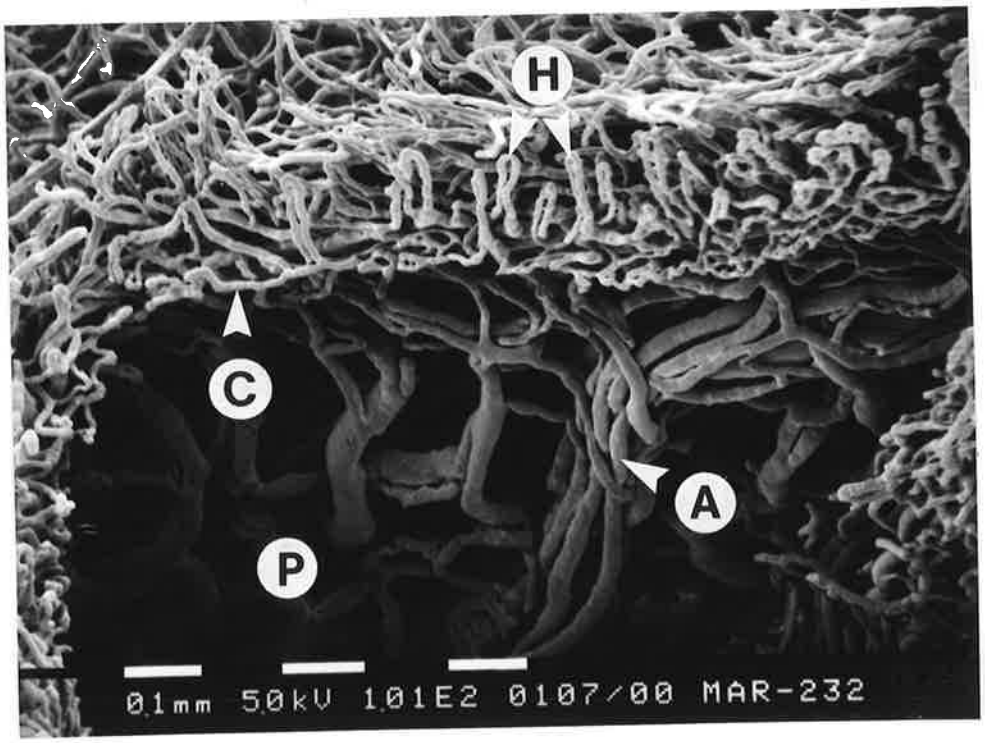

LINGUAL

A = Arterioles.
C = Circular plexus vessel.
H = Hairpin crevicular loops.
P = PDL vessels.

FIGURE 36: CERVICAL PDL - MANDIBULAR RIGHT LATERAL INCISOR. (YOUNG ANIMAL, MARMOSET 232)

Simple hairpin crevicular loops (H) are present on the mesial side of the tooth socket. Some appear to originate at the level of the circular plexus vessel (C). Directly below in the cervical PDL (P), a large group of arterioles (A) can be seen. They deviate both labially and lingually to supply the gingival and crevicular vessels. Groups of arterioles were also seen in the cervical PDL on the distal sides of the mandibular sockets.

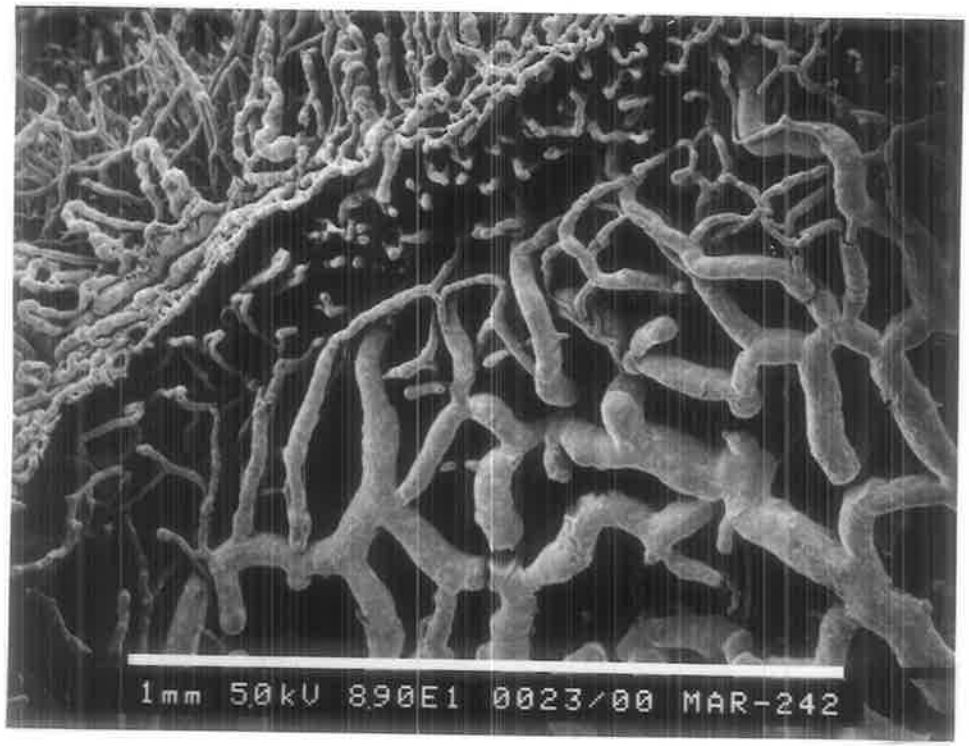
1mm 5.0kV 8.90E1 0023/00 MAR-242

MESIAL

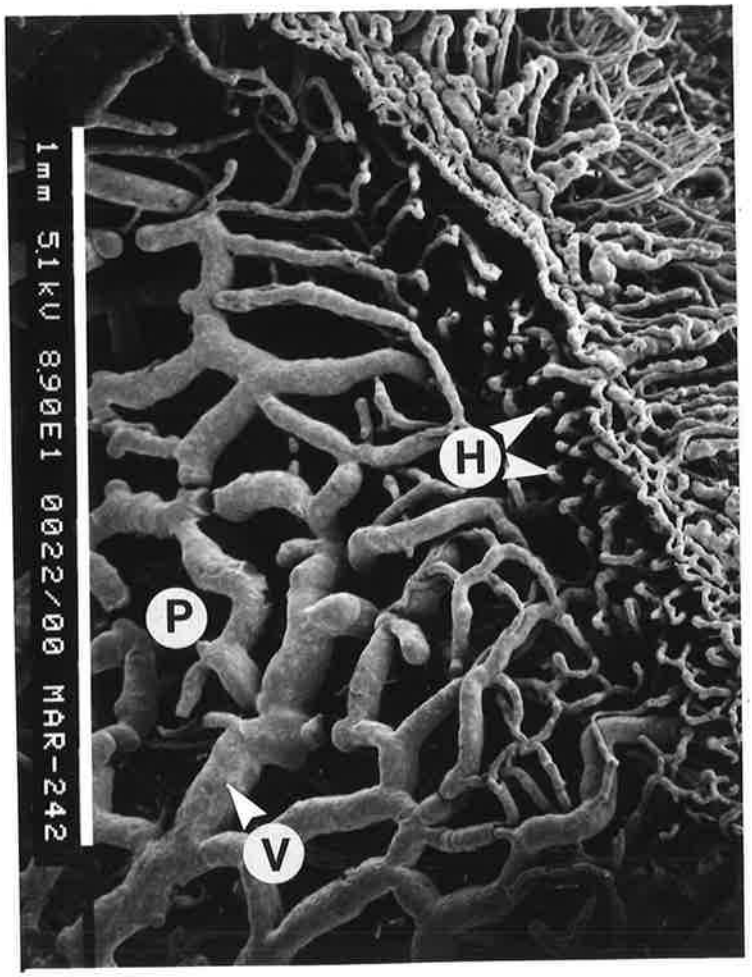

PALATAL

H = Hairpin loops.
P = PDL vessels.
V = Collecting-sized venule.

FIGURE 37: CERVICAL PDL - MAXILLARY LEFT LATERAL INCISOR. (YOUNG ANIMAL, MARMOSET 242)

The view is of the mesio-palatal socket wall. The cervical PDL vessels (P) enlarge rapidly to form collecting-sized venules (V) as they descend apically. Hairpin loops (H) are present in the cervical PDL just below the level of the circular plexus vessel. These have an ascending and a descending limb and project out towards the tooth root.


0.1mm15.2kV 3.72E2 0000/00 MAR - 6

DISTAL

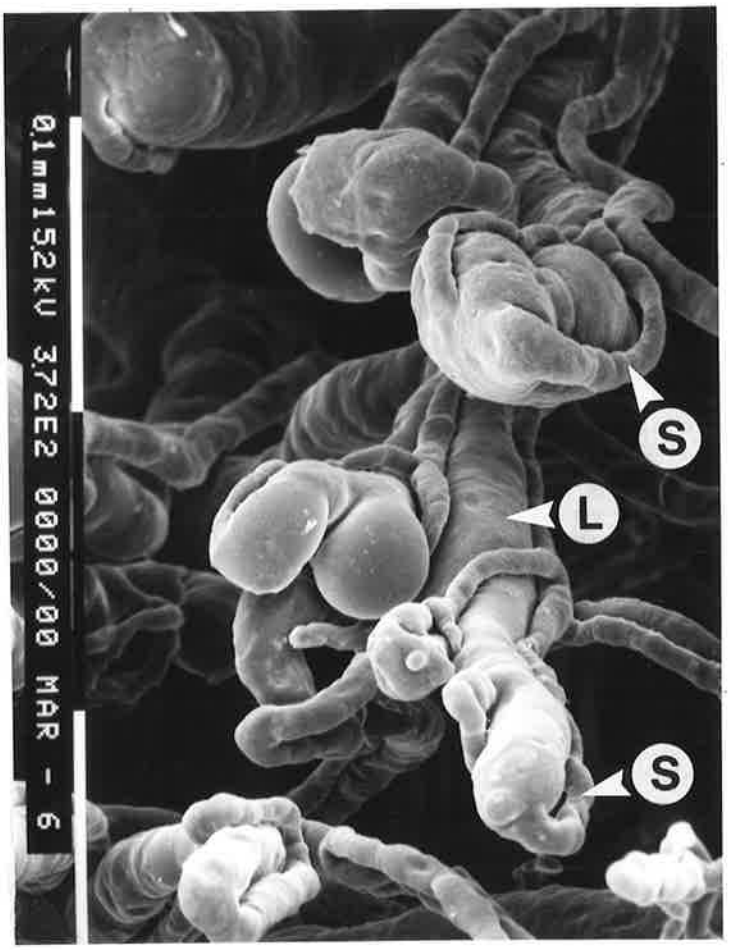

OCCLUSAL

L = Larger diameter limb.
S = Smaller diameter limb.

FIGURE 38: PALATAL CERVICAL PDL - MAXILLARY LEFT LATERAL INCISOR. (MATURE ANIMAL, MARMOSET 6)

In the palatal cervical PDL region of this socket, loop structures having a large diameter limb (L), 20 to 60 μm in diameter, and smaller diameter limbs (S), 10 to 15 μm in diameter were present. Rapid expansion in vessel diameter occured with the vessels taking a hairpin bend to drain back into the cervical PDL.

The larger diameter vessels were venules, however it was difficult to tell whether the smaller diameter vessels were also venous in nature or whether they were arterioles.

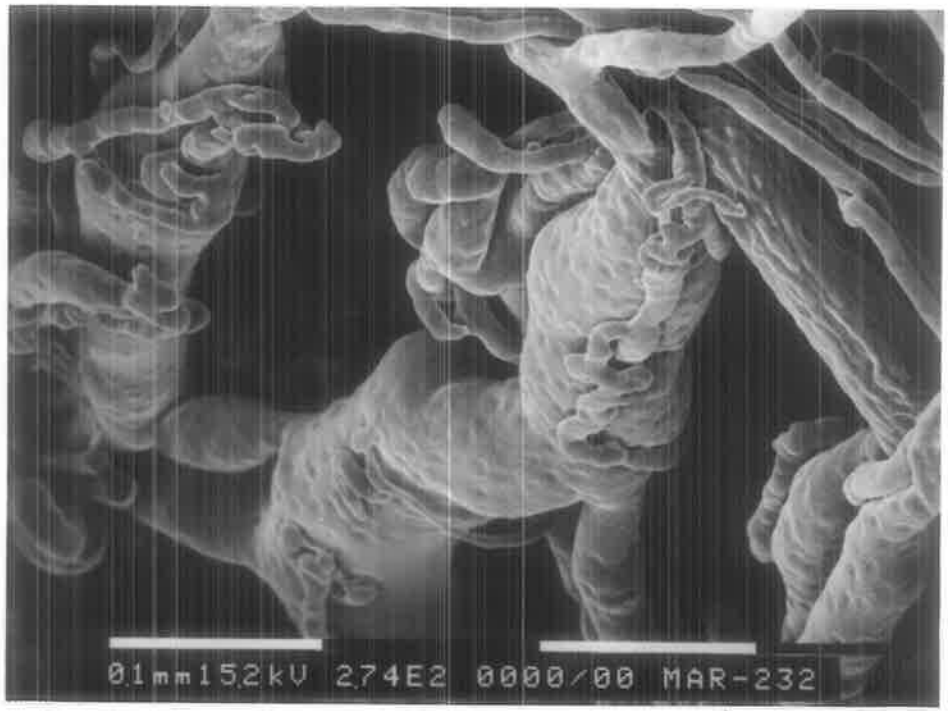
01mm15.2kV 274E2 0000/00 MAR-232

LABIAL

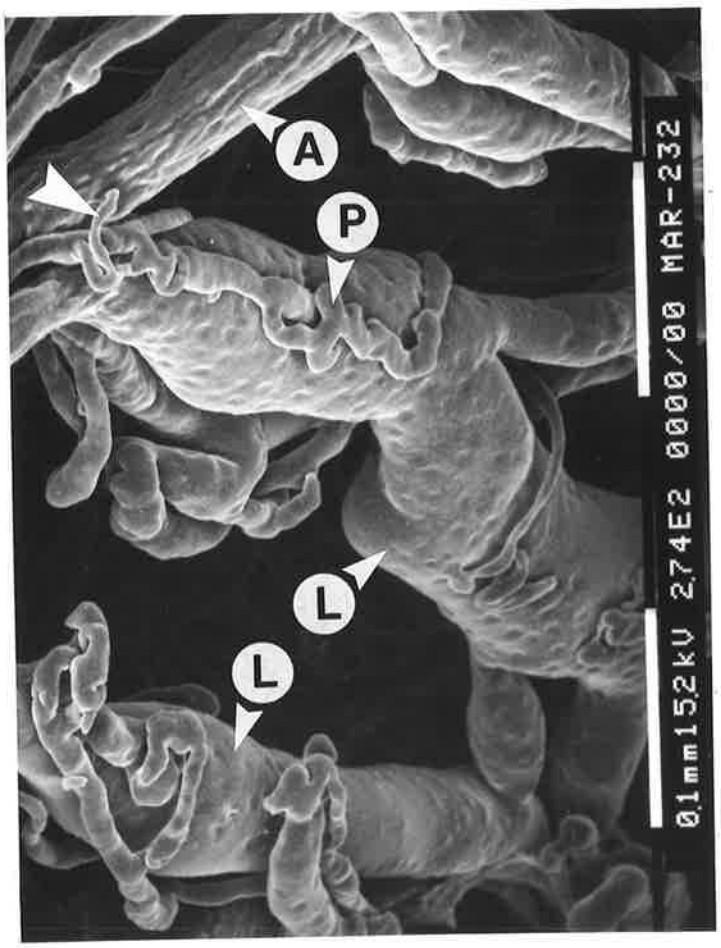

APICAL

A = Arteriole.
L = Large diameter venules.
P = Postcapillary-sized venule.

FIGURE 39: PALATAL CERVICAL PDL - MAXILLARY LEFT CANINE. (YOUNG ANIMAL, MARMOSET 232)

Large venules (L), 50 to 80 μm in diameter drain down the palatal cervical PDL. Accompaning these were smaller postcapillary-sized venules (P) which appeared to drain into these larger vessels. To the top left of the micrograph, communication between an arteriole and a venule can be seen (arrow).

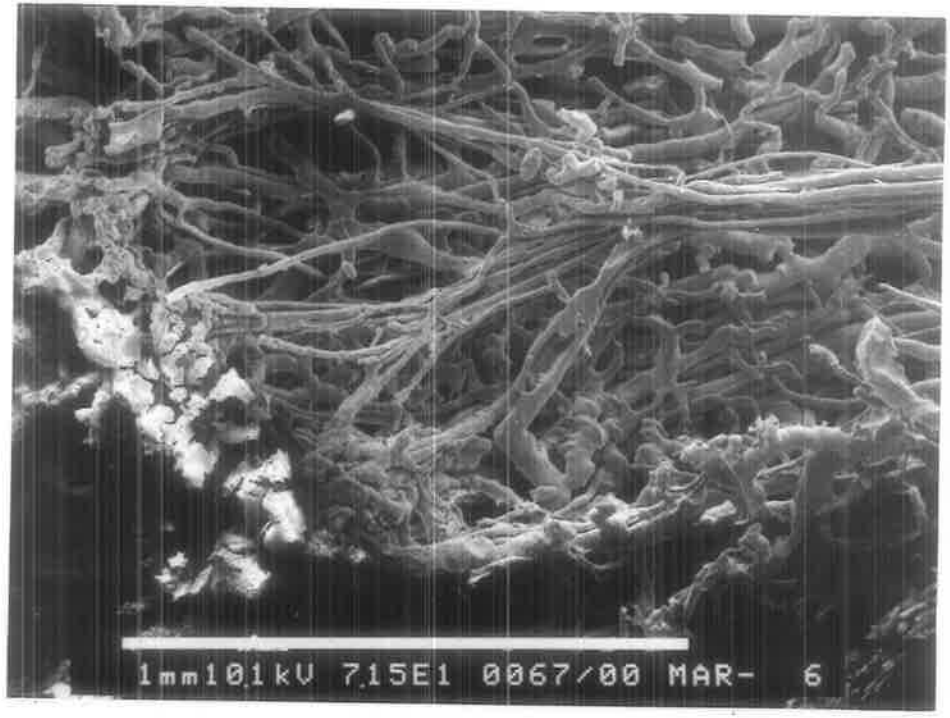
1mm10.1kV 7.15E1 0067/00 MAR- 6

OCCLUSAL

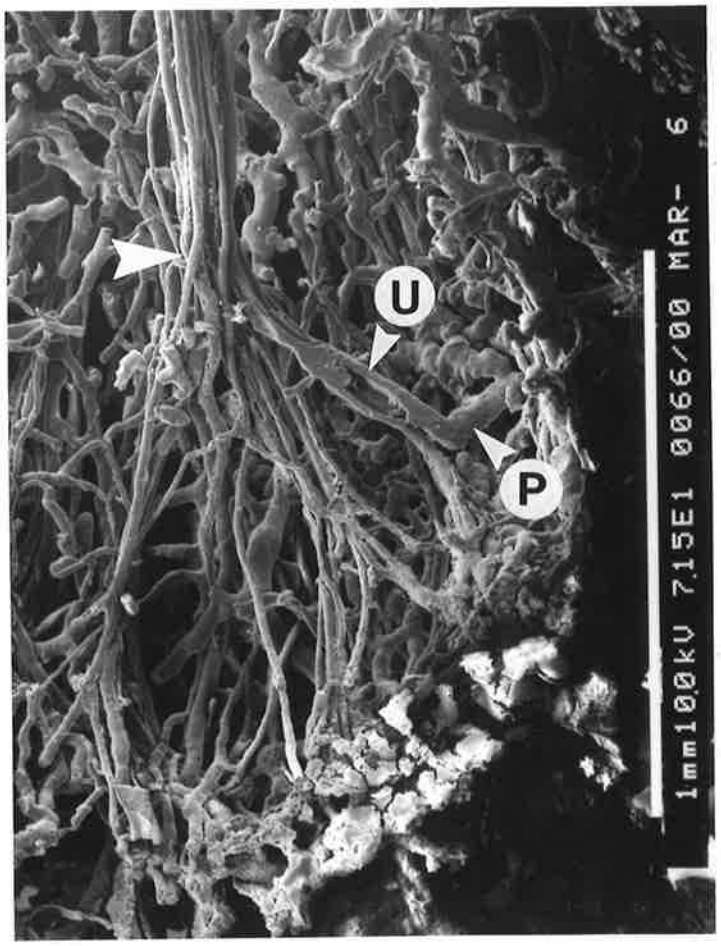

LABIAL

P = PDL venule.
U = Pulpal venule.

FIGURE 40: APICAL PDL AND PULPAL VESSELS - MANDIBULAR RIGHT CANINE. (MATURE ANIMAL, MARMOSET 6)

This view was towards the apical PDL and pulpal vessels on the mesial side of the tooth socket. Pulpal vessels fan out below the apical foramen (large arrow). See Figure 42 for a higher power view. These pulpal vessels course apically for up to 1000 μm before reaching the apical PDL vessels. This finding suggests that the apical foramen for this tooth was coronal to the root apex. The pulpal vessels fan out below the apical foramen and course apically between the mesial root surface, which has been removed, and the mesial PDL. The three-dimensional stereopair image supports this suggestion.

Communication between a pulpal venule (U) and a PDL venule (P) can be seen. Pulpal arterioles converge at the apical foramen to enter the root canal. Their origin is presumed to be from the mental branch of the inferior alveolar artery.

OCCLUSAL

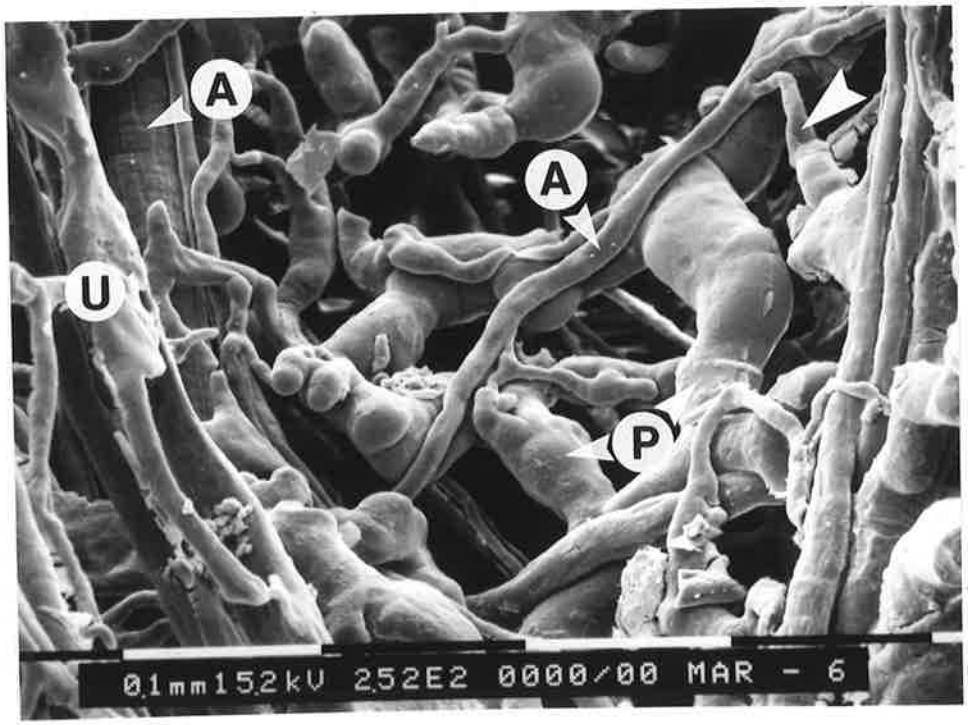

LABIAL

A = Arterioles.
P = PDL venules.
U = Pulpal vessels.

FIGURE 41: APICAL PDL REGION - MANDIBULAR RIGHT CANINE. (MATURE ANIMAL, MARMOSET 6)

This view was towards the apical PDL on the mesial side of the tooth socket. The apical PDL was highly vascular. A small arteriole (A) was seen anastomosing with a larger venule (arrow). Change in the diameter of the PDL venous vessels (P) occurred frequently. Pulpal vessels (U) are to the left of the micrograph.

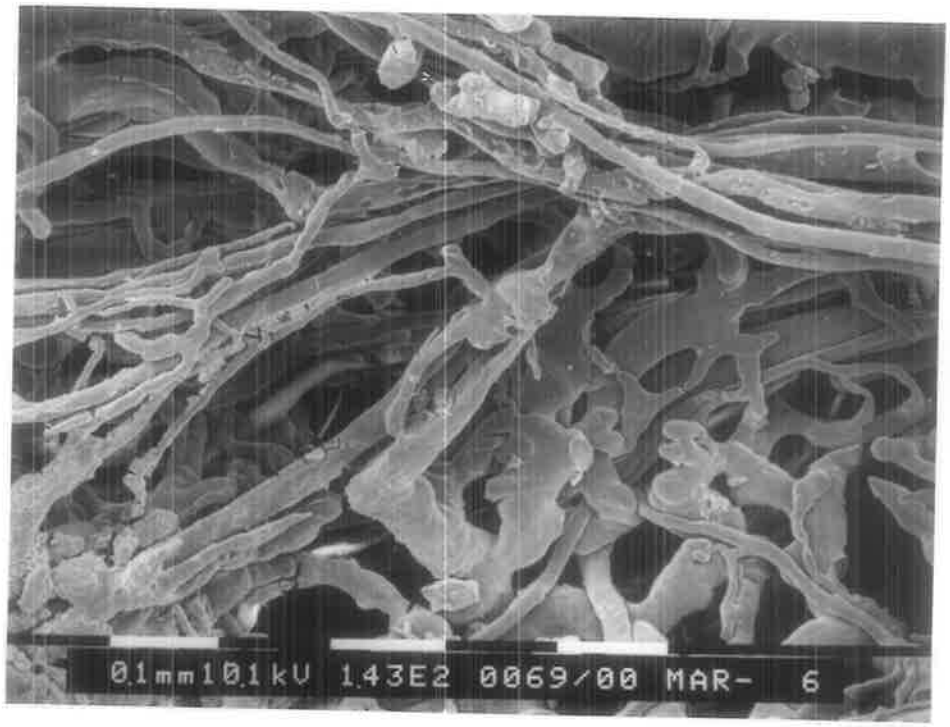
0.1mm 10.1kV 1.43E2 0069/00 MAR- 6

OCCLUSAL

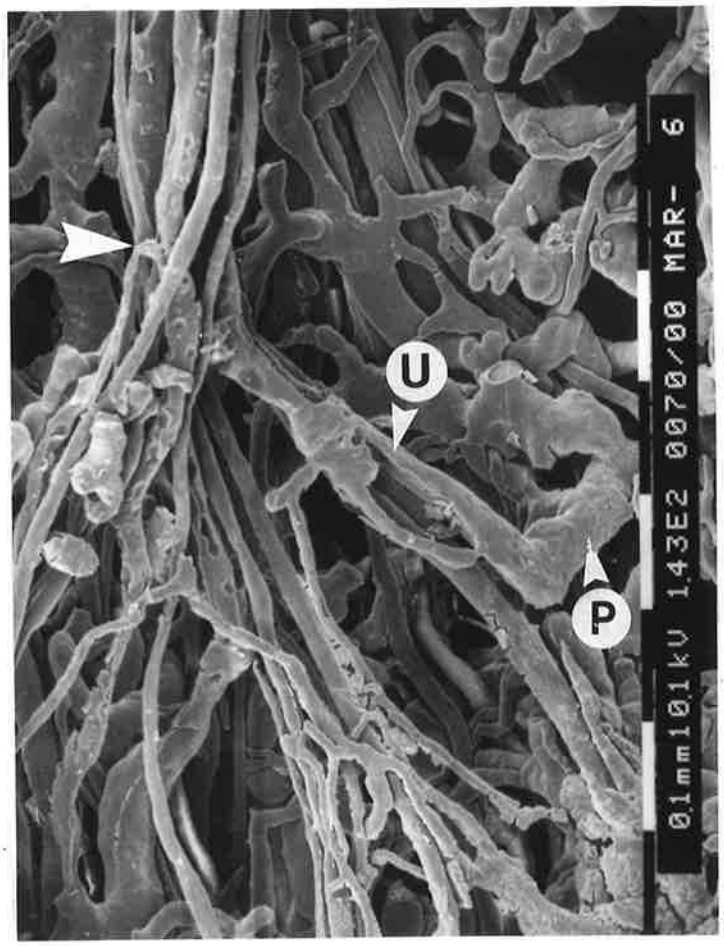

LABIAL

P = PDL venule.
U = Pulpal venule.

FIGURE 42: APICAL PDL AND PULPAL VESSELS - MANDIBULAR RIGHT CANINE. (MATURE ANIMAL, MARMOSET 6)

This is a higher power view of Figure 40. The pulpal vessels fan out as they pass through the apical foramen (arrow). Communication between a pulpal venule (U) and PDL venule (P) can be seen.


0.1mm15.2kV 600E2 0048/00 MAR-230

OCCLUSAL

MESIAL

A = Pulpal arteriole.
U = Pulpal venule.
V = Collecting-sized venule.

FIGURE 43: COMMUNICATION OF PULPAL VENULES WITH A LARGER COLLECTING-SIZED VENULE BELOW THE APICAL FORAMEN - MANDIBULAR RIGHT CENTRAL INCISOR. (YOUNG ANIMAL, MARMOSET 230)

This view was towards the lingual. Pulpal venules (U) drain into a larger diameter collecting-sized venule (V) below the tooth apex. Pulpal arterioles (A) pass up along this vessel to enter the pulp canal.

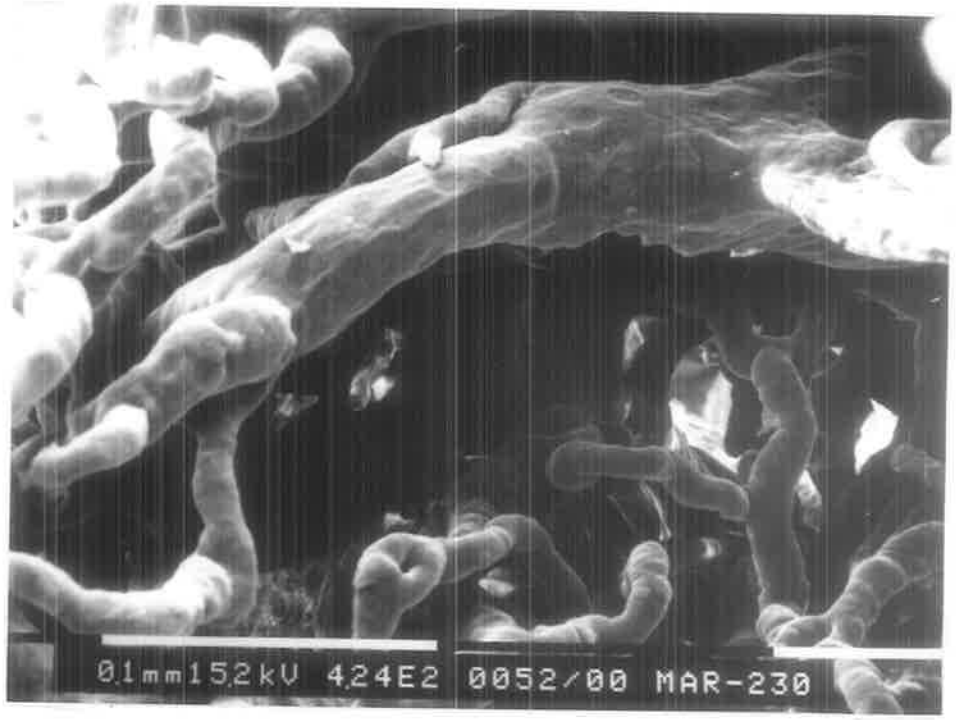
0.1mm 15.2kV 4.24E2 0052/00 MAR-230

OCCLUSAL

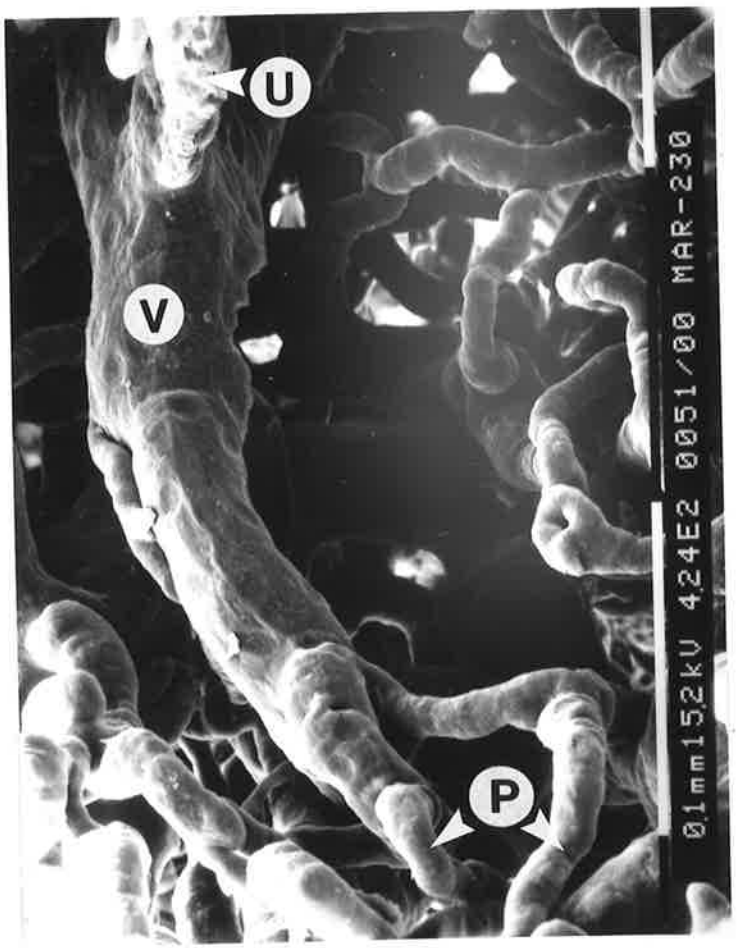

MESIAL

P = PDL venules.
U = Pulpal venules.
V = Collecting-sized venule.

FIGURE 44: COMMUNICATION OF PULPAL AND PDL VENULES WITH A LARGER COLLECTING-SIZED VENULE BELOW THE APICAL FORAMEN - MANDIBULAR RIGHT CENTRAL INCISOR. (YOUNG ANIMAL, MARMOSET 230)

This is a different view of the same socket as shown in Figure 43. The pulpal venules (U) described in the previous micrograph drain into a larger diameter collecting-sized venule (V) below the tooth apex. To the bottom of the micrograph, PDL venules (P) also drain into this collecting-size venule which then runs apically and lingually.

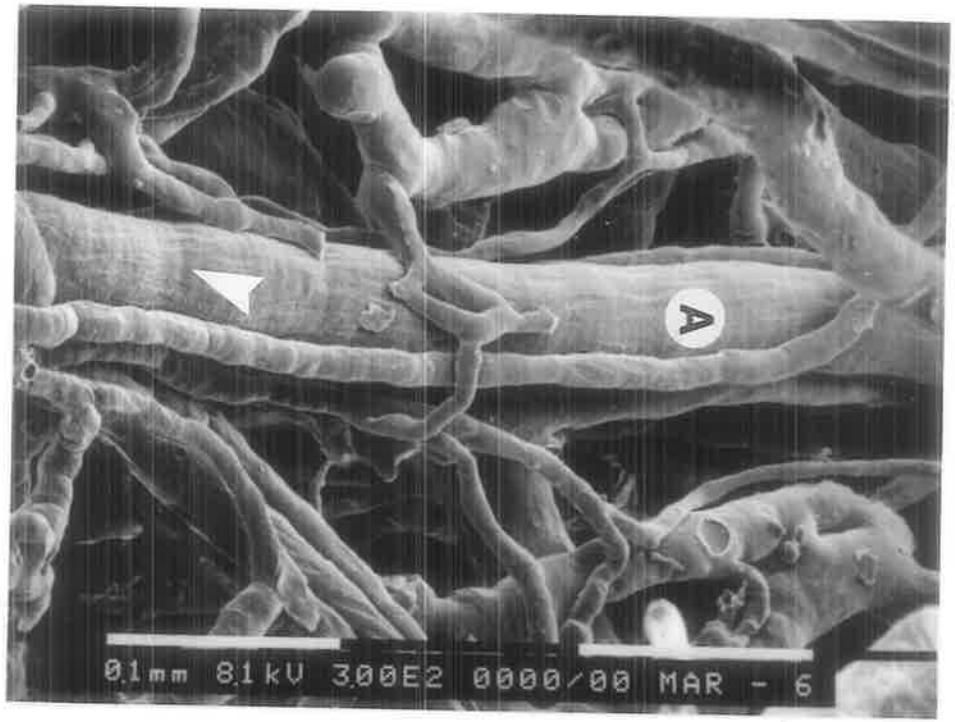
A
0.1mm 8.1kV 3.00E2 0000/00 MAR - 6

OCCLUSAL

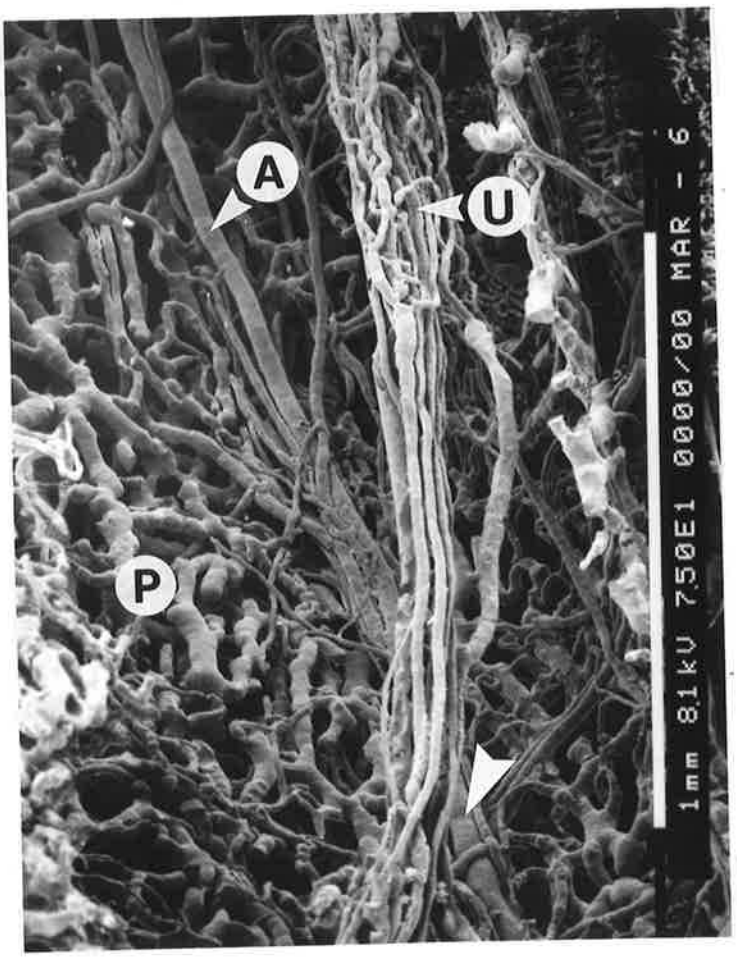

LABIAL

A = Arteriole.
U = Pulpal vessels.
P = PDL vessels.

FIGURE 45: APICAL PDL AND PULPAL VESSELS - MANDIBULAR RIGHT CANINE. (MATURE ANIMAL, MARMOSET 6)

This view was towards the apical PDL and pulpal vessels on the mesial side of the tooth socket. An arteriole (A), 40 to 50 μm in diameter runs along the mesial PDL wall (P). The vessel branches numerous times as it passes occlusally. It can be followed up to the cervical PDL region where it enters into the gingival tissues.

Pulpal vessels (U) can also be seen. In the apical third no branching of these vessels was present. In the middle third of the socket a pulpal capillary network has formed with a central core of larger diameter vessels being present (arrow).

The opposite page shows a higher power view of the arteriole (A) described above. The arteriole here is close to the apical foramen. The large arrow in both photomicrographs is at the same location. Note the oval shaped endothelial imprint pattern.

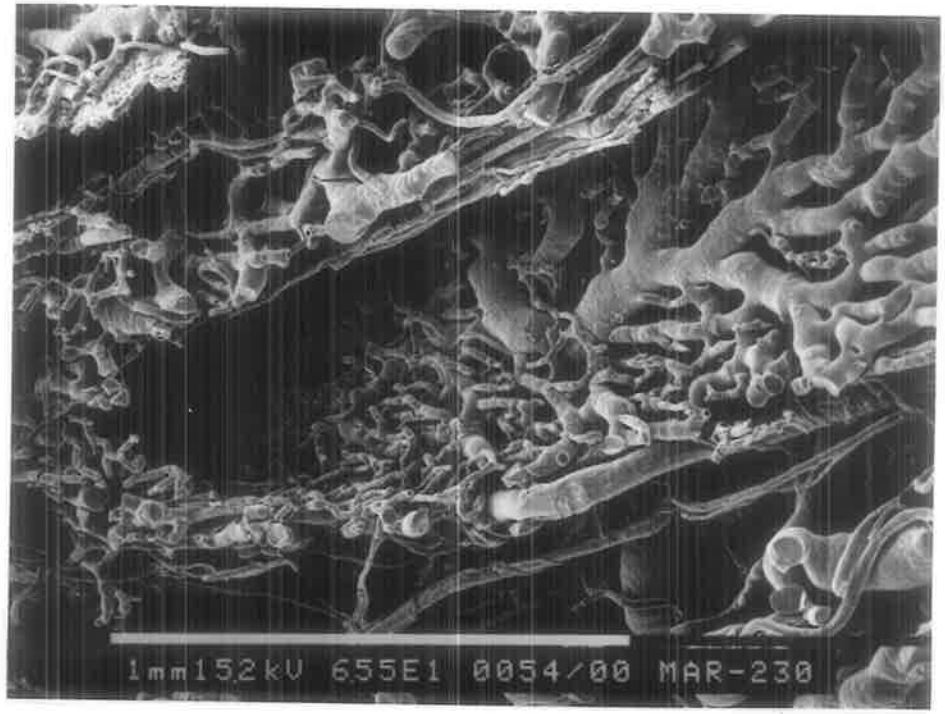
1mm15.2kV 655E1 0054/00 MAR-230

OCCLUSAL

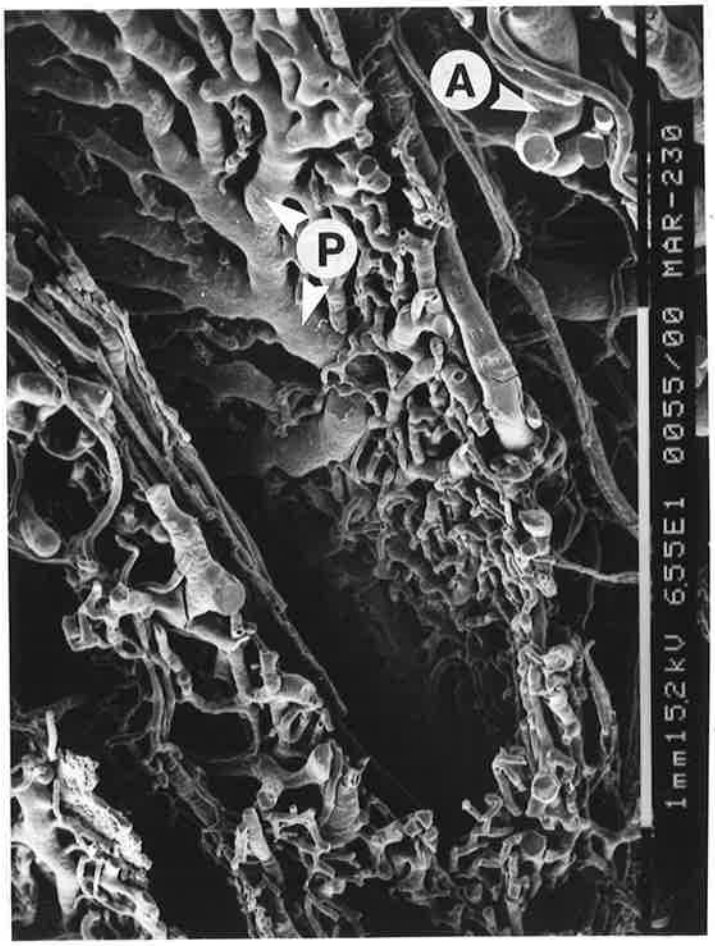

LABIAL

A = Alveolar mucosal vessels.
P = PDL venules.

FIGURE 46: APICAL PDL REGION - MANDIBULAR RIGHT CENTRAL INCISOR. (YOUNG ANIMAL, MARMOSET 230)

This is a higher power view of Figure 35 and shows the area indicated by the (P) in that figure. Large venules which appear to be from the PDL (P) and ranging up to 100 μm in diameter drain down in the region of the mesial PDL. They converge and seem to pass from the PDL at the level between the middle and apical PDL thirds. They pass through the labial bony plate to communicate with the labial alveolar mucosal vessels (A).

Large venules similar to the vessels described above were observed coursing down the mesial PDL in other mandibular anterior sockets and for both young and mature animals. These observations support the above findings.

OCCLUSAL

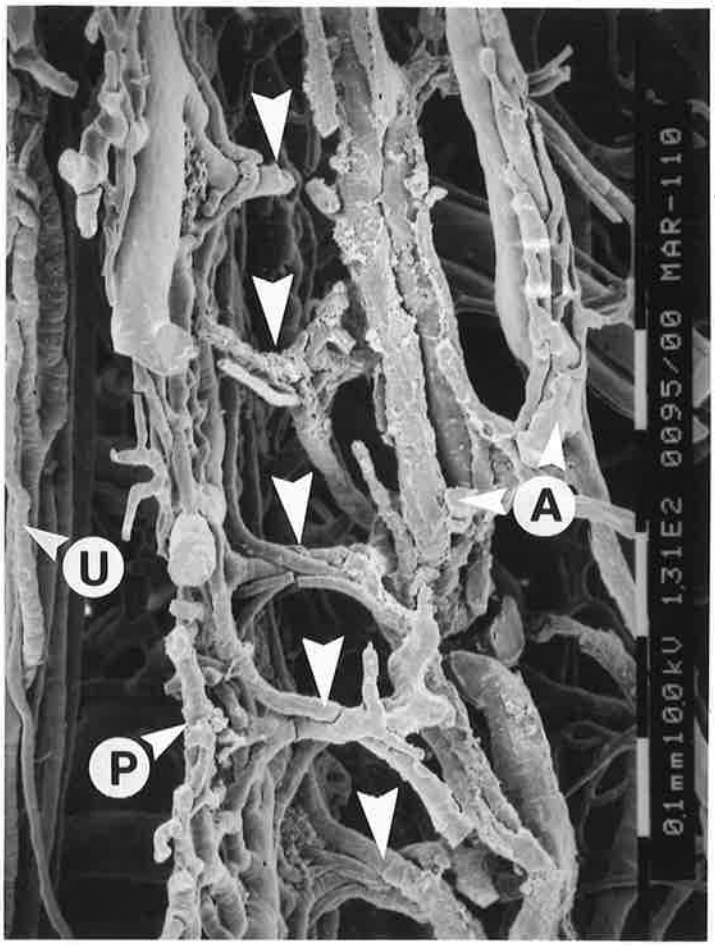

LABIAL

A = Alveolar mucosal vessels.
P = PDL vessels
U = Pulpal vessels.

FIGURE 47: LABIAL APICAL PDL AND ALVEOLAR MUCOSA - MANDIBULAR RIGHT LATERAL INCISOR. (MATURE ANIMAL, MARMOSET 110)

In the apical third of the PDL, groups of vessels (arrows - both arterioles and venules) pass through the labial plate of bone to communicate with alveolar mucosal vessels (A). Arterioles appeared to enter the apical PDL (P) via this route while venules appeared to exit the apical PDL to run into the labial sulcus.

OCCLUSAL

LABIAL

A = Arterioles.
V = Venules.

FIGURE 48: LABIAL APICAL PDL AND ALVEOLAR MUCOSA - MANDIBULAR RIGHT LATERAL INCISOR. (MATURE ANIMAL, MARMOSET 110)

This is a high power view of Figure 47 and shows the group of vessels indicated by the large arrow at the bottom of that figure. The endothelial imprint patterns of the vessels passing from the apical PDL through the labial plate of bone to communicate with alveolar mucosal vessels can be seen. Both arterioles (A) and venules (V) are present. Following the direction of these vessels it appeared that arterioles (A) entered the apical PDL via this route, while venules (V) exited the apical PDL to run into the labial sulcus.

OCCLUSAL

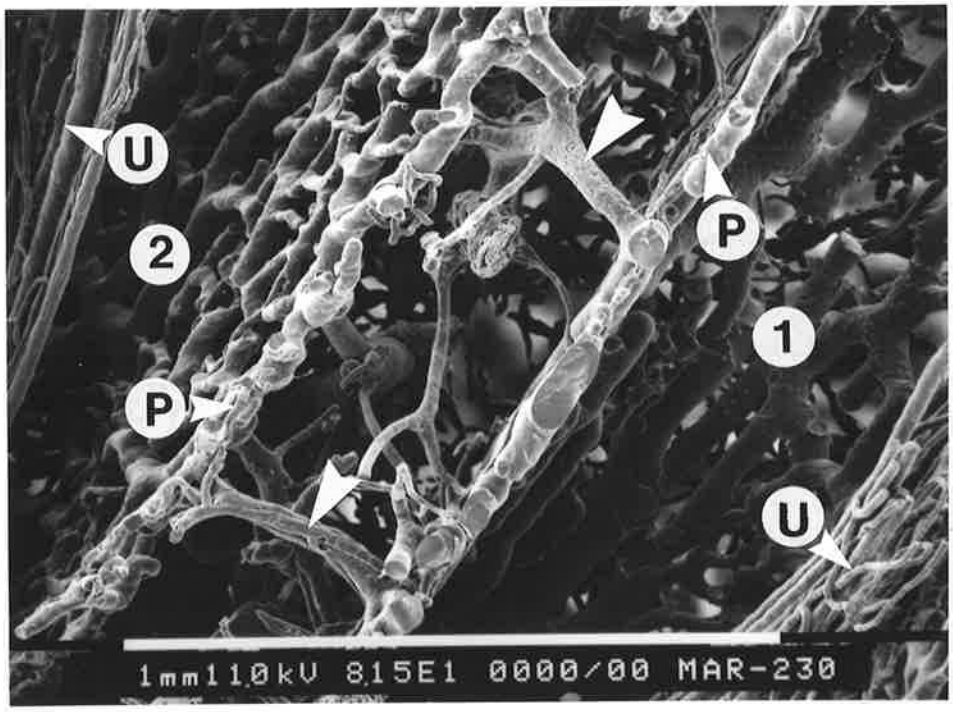

LABIAL

1 = First premolar socket.
2 = Second premolar socket.
P = PDL vessels.
U = Pulpal vessels.

FIGURE 49: DIRECT COMMUNICATION BETWEEN THE PDL OF ADJOINING TOOTH SOCKETS - MANDIBULAR RIGHT FIRST AND SECOND PREMOLARS. (YOUNG ANIMAL, MARMOSET 230)

Direct communication, both arterial and venous (arrows) between the mesial PDL (P) vessels of a mandibular right first premolar (1) and the distal PDL (P) vessels of a mandibular right second premolar (2) can be seen. The sockets have been sectioned mesio-distally. These communications were present in the middle and cervical thirds of the sockets and were more common in the posterior segments.

The communicating vessel to the top of the micrograph was a collecting-sized venule with a luminal diameter of 40 μm. An arteriole and two venules were communicating between the sockets towards the bottom of the micrograph.

POSTERIOR

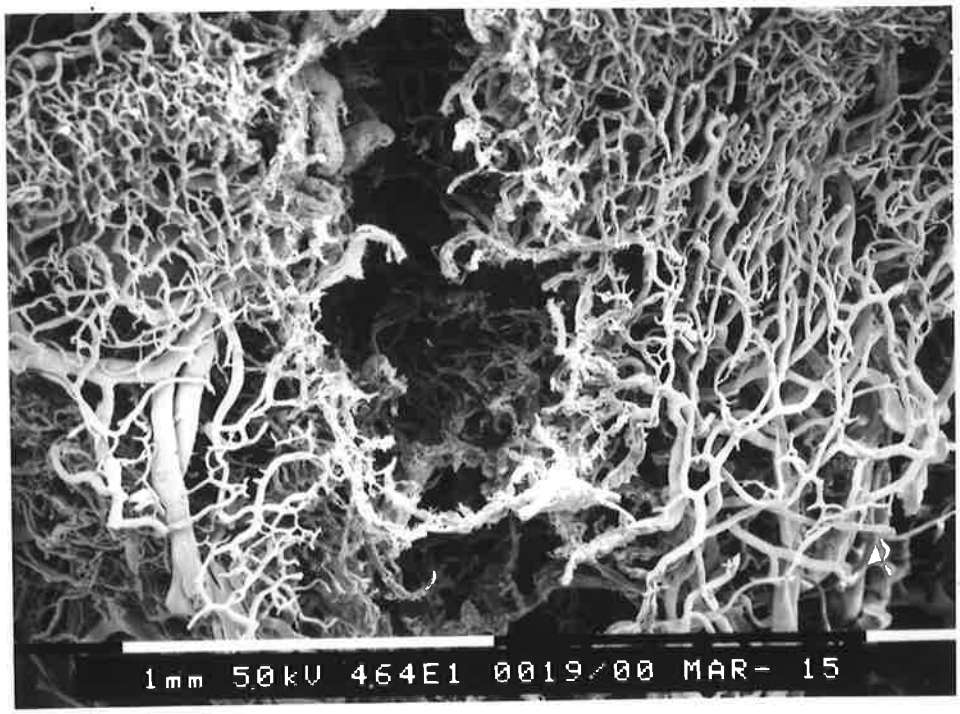

FIGURE 50: EFFECT OF USING THE DENTAL LASER TO SECTION THROUGH THE CORROSION CASTS.

The dental laser has melted through the outer layers of the corrosion cast in the palate region. The beam left a hole in the cast ranging from 300 μm up to 700 μm in width. This area was made up of fine capillary loops and the laser beam melted through the cast quite rapidly here. In other areas the beam had to be passed over several times for the resin to be cut through.

CHAPTER 6

DISCUSSION

6.1 TECHNICAL CONSIDERATIONS

The concept of using the corrosion casting technique is several hundred years old (**HODDE**, 1981). Technical advances have been rapid over the past 15 to 20 years so that high quality corrosion casts can be produced from a variety of tissues and organs. Improved perfusion techniques, the modification of the casting resins used, the introduction of the SEM and the viewing in three-dimensions using stereopairs has enabled the morphology of various tissues to be examined with far greater clarity. The technique is still extremely difficult and very sensitive to a large number of variables with the results being often unpredictable.

LEE (1988) noted that incomplete casting could be due to:

1. Vascular spasm.
2. Blockage of the fine vessels.
3. Insufficient perfusion pressure.
4. The use of a high viscosity resin.
5. The use of too small a cannula size.
6. Inadequate mixing of the resin leading to incomplete polymerization.
7. Breakage of the delicate casts during handling.
8. External pressure could cause vascular occlusion.
9. Rupture of vessels.
10. Cannulation too far from the target organ.
11. Insufficient perfusion time.

The corrosion casts used by the current author had been stored in air tight containers and were in very good condition seeing they were more than 3 years old now. The containers were dust free and this had stopped moisture contamination. The corrosion casts in most areas appeared to have been adequately cast. The casts of the older animals showed incomplete casting of the palatal plexus.

A. TRIMMING THE CORROSION CASTS

LEE (1988) sectioned many of his casts before the tissue corrosion phase using sharp saftey razor blades. This meant that the casts were not disturbed after the tissues had been removed.

The technique of using the mini-motor and diamond cutting wheel as well as a safety razor blade to do the final sectioning of the ice embedded corrosion casts enabled the apical portion to be viewed in the dissecting microscope while the socket was being sectioned. This was in contrast to the sectioning technique used by **WEEKES** (1983), **WONG** (1983) and **LEE** (1988) whereby the ice embedded sockets were sectioned from the occlusal towards the apex using a razor blade only and where visibility was considerably reduced. Sectioning through the apex to include the pulpal vessels using a razor blade was only achieved with great difficulty.

If the technique of just using a razor blade had been used in the current study, then one portion of the corrosion cast would have needed to be removed from the SEM stub so that the other portion could be viewed. Damage to the portion of the cast being removed would have ocurred with possible damage to the other portion also.

HODDE and **NOWELL** (1980) were the first to descibe a technique whereby corrosion cast vessels could be sectioned using a laser beam. Unlike the current author, they magnified and precisely focussed the laser beam into a slit

approximately 50 μm across using various shaped lenses. These lenses were not available to the current author. It appears **HODDE** and **NOWELL** (1980) were also the only researchers to have successfully attempted this technique. **LAMETSCHWANDTNER et al.** (1990) in a comprehensive review of the literature mentioned no other authors that had used lasers successfully and suggested that improvements were necessary in beam focussing to reduce the tendency of the beam to melt the cast. They also felt that the high costs required made it prohibitive to most users.

The use of the American Dental Laser and larger CO_2 Sharp Plan Laser to cut through the casts proved unsatisfactory for several reasons. Firstly, the width of the cutting beam especially in the case of the American Dental Laser was too wide. The cut in the cast ranged from 300 to 700 μm. Secondly, the surrounding cast tended to be affected by the laser's heat so that vessels that were to be viewed could not be close to the direct laser beam. Thirdly, the laser beam only penetrated to a very shallow level. Deeper vessels could only be reached if the peripheral vessels were first removed. This meant that some of the cast would need to be destroyed to get to the area of interest.

The technique whereby some of the specimen was removed using fine tweezers and small spring scissors under the dissecting microscope showed the greatest potential initially. The SEM stub was mounted into a small resin block so that both of the operators' hands were free to carry out the procedure. The cast was then broken away in stages. The dissecting microscope allowed for accurate viewing. The risk of breaking away excess cast while using the tweezers and scissors was reduced by removing small portions of the cast at a time. The advantages of a clear field of vision made this technique attractive initially, however some damage to the surrounding vessels was observed when the specimen was viewed in the SEM.

B. LIMITATIONS OF THE CORRROSION CASTING TECHNIQUE

The advantages of using the corrosion casting technique appear to far outweigh its limitations. Viewing the corrosion casts in the SEM in combination with stereopair recording provides a useful way of assessing the vasculature in three-dimensions. The readers of this project, however, need to be aware of the possible limitations of the technique.

The limitations of the corrosion casting technique are as follows:

1. The accuracy of the luminal diameter is of question. **RHODIN** (1973) suggested that an increased injection pressure used for perfusion of substances into the vessels may cause expansion of the vessel wall. Thinner walled vessels tended to dilate to a greater degree than thicker walled vessels (**IRINO et al.**, 1982).

2. The direction of blood flow can only be inferred by following the path of a vessel and by observing its branching with other vessels.

3. The physiological state of the vessels during perfusion is unknown. Perfusion may change the state of the vascular bed.

4. The precise relationship of the blood vessels to surrounding structures cannot be determined.

5. To gain a three-dimensional appreciation of the cast the use of stereopairs is essential. Without this the interpretation of lateral distances on a micrograph can show major errors (**CHATFIELD**, 1978).

6. The effects of the casting resin on the vessel wall is unknown.

7. The physical and chemical properties of the casting resin materials are still incompletely known. According to **LAMETSCHWANDTNER et al.**, (1990), volume shrinkage ranged from 1% up to 20%. The data, however are not comparable since shrinkage values were obtained under different conditions. In general, the less viscous the injected resin is the more the final shrinkage will be. The size of the vessel, the thickness of the vessel wall, the curing of the resin under pressure as well as the temperature the resin is cured at will all have an influence on the degree of shinkage.

8. Fenestrations do not appear to be recorded in the corrosion casts (**HODDE**, 1981).

C. CORROSION CASTING ARTIFACTS

The recognition of corrosion casting artifacts is an important consideration. Artifacts are common and can range from incomplete filling of the vessels which produce blunted rounded endings, voids, craters and a lack of an endothelial imprint pattern to charging of the specimen due to a build up of electrons on the surface of the cast.

Artifacts can include fractures of the cast during handling; constrictions in the cast due to incomplete filling or due to the presence of sphincters (**DUVERNOY et al.**, 1981; **MOTTI et al.**, 1987); dust, fragments of non-corroded tissue or foreign bodies due to contamination of the specimen.

Surface charging due to the build up of electrons from the SEM produced white spots on the micrographs. These could be reduced and even eliminated by reducing the accelerating voltages used and by evenly and completely coating the corrosion casts to increase electrical and thermal conductivity. The current author noted charging from some of the corrosion casts even when using moderately low kilovoltages around 8 kV. These corrosion casts had been initially coated when they were examined by **LEE** (1988). They were recoated with the problem being eliminated. This suggested that corrosion casts which had been stored for any length of time should be recoated routinely to ensure that an adequate coating was still present. **MURAKAMI et al.** (1973) exposed the corrosion casts to vapourized osmium to help reduce charging and to assist in producing good contrasted images by giving off a beam of secondary electrons in the SEM.

Extravasated resin was common in the specimens observed and was often seen in association with the crevicular loops and in the area of the gingival margin. It was characterized by masses of resin material with indistinct shapes and various sizes. It was demonstrated by **CASLEY-SMITH** and **VINCENT**, (1978) that high perfusion pressures could allow semi-polymerized methyl methacrylate to pass

through pores and junctions in the vessel wall and into the interstitial channels. They were looking at interstitial channels in rat and rabbit tissues however. Perhaps the same mechanism allowed leakage of resin through the crevicular loops.

D. S.E.M. VIEWING

The use of the SEM to view and to record on micrographs both the gingival vascular structures and the cervical PDL structures at the same time without first sectioning the casts proved to be difficult. The Philips SEM 505 needed to be adjusted for contrast manually every time a micrograph was taken and this proved difficult when trying to balance the contrast when viewing inside the tooth socket as well as when looking at the gingival vasculature and recording both at the same time. A compromise method was used whereby the contrast was reduced to allow all the structures to be included in the one view.

6.2 MORPHOLOGICAL FINDINGS

A. DIRECTION OF BLOOD FLOW

Diagramatic representation of the direction of blood flow for the pulpal, labial PDL and gingival vessels in the mandibular anterior region can be seen in Figure 51 on the next page. The direction of blood flow is similar to that suggested by **LEE** (1988), for the vasculature of the palatal gingiva in the posterior region of the marmoset although minor variations have been suggested. The diagram covers a larger area of the tooth socket with the direction of flow of the pulpal vessels (including capillary loops in the middle and coronal thirds) and vessels below the tooth apex being included.

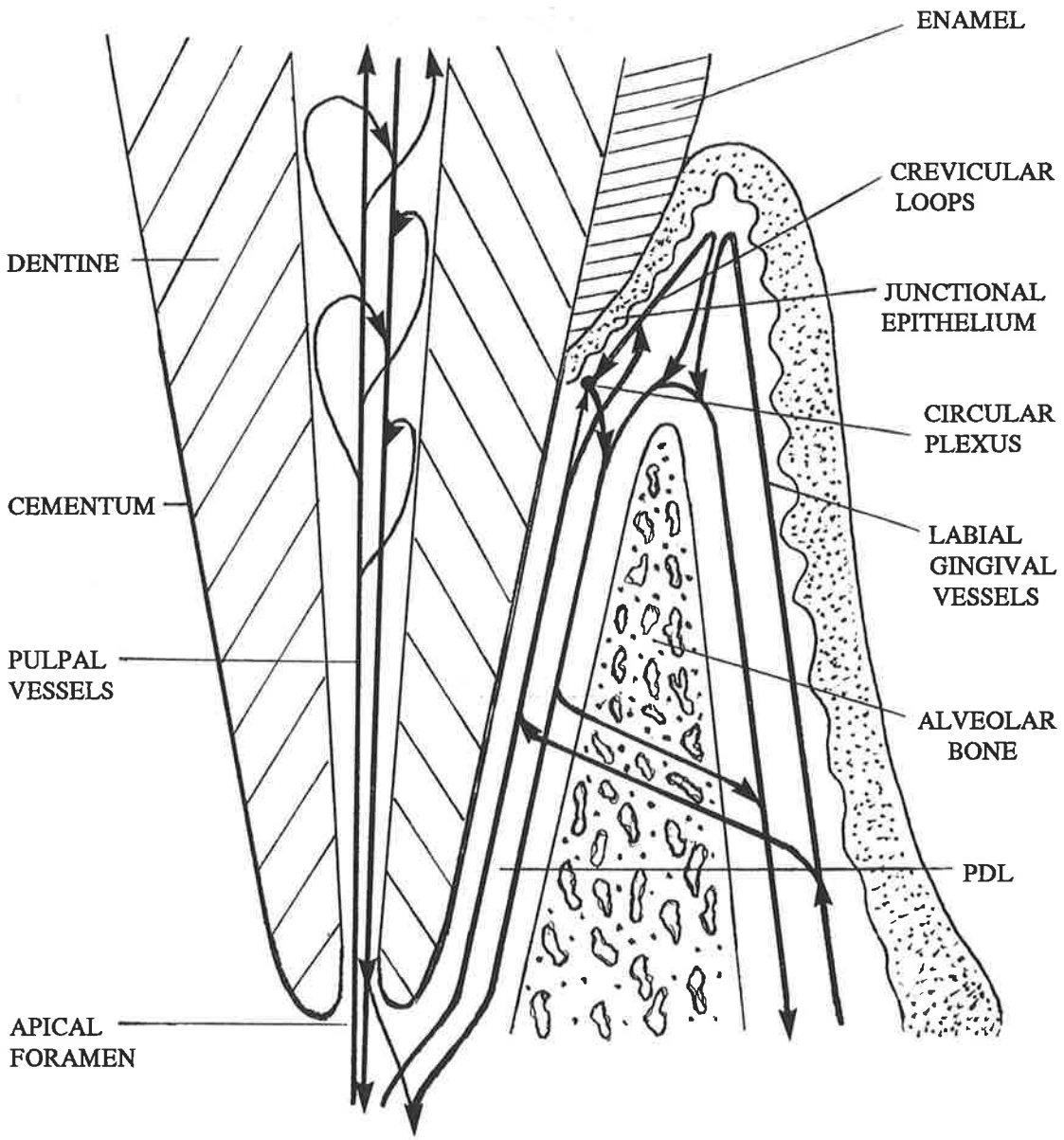

FIGURE 51: PRESUMPTIVE DIRECTION OF BLOOD FLOW IN THE LABIAL GINGIVA AND PDL OF THE MANDIBULAR ANTERIOR REGION.

The direction of blood flow to and around the circular plexus is confusing. The possibility that the direction of flow may change both at rest and during function must be considered. Both arterioles and venules were seen communicating with the circular plexus from the cervical PDL although venules were the more common finding. This suggests that blood entered the circular plexus either from the crevicular loops or the cervical PDL at various sites around the socket and

exited the circular plexus to the cervical PDL at other sites. Blood once it has entered the circular plexus may be redistributed either around the circular plexus and back into the cervical PDL or it may pass coronally into the crevicular loops to supply blood to the area of need during function.

With a greater number of venules exiting the circular plexus versus arterioles entering via the cervical PDL, the presumptive direction of blood flow would be mainly from the circular plexus to the cervical PDL. The circular plexus may be arterial in nature in certain regions and may be venous in nature at other sites. **LEE** (1988) in his diagram has indicated blood flow from the circular plexus to the crevicular loops but did not indicate the reverse.

In the apical PDL third on the labial side of the anterior mandibular tooth sockets, groups of vessels were seen communicating between the labial PDL and the alveolar mucosa (Figure 47). Endothelial imprint identification, as well as following these vessels along the labial PDL and alveolar mucosa, suggested an arterial supply from the alveolar mucosa through the labial plate of bone to the labial PDL. Venous drainage appeared to be from the labial PDL through the labial plate of bone to the alveolar mucosa and labial sulcus. The reverse could be true however. This collateral route may ensure an adequate blood supply to the PDL of the anterior teeth during function as well as an alternate route for venous drainage.

The concept of a collateral blood supply is not new. **KENNEDY** (1969) showed that initial revascularization of occluded gingival tissues was via vessels from the PDL. The results indicated that the PDL was a source of blood supply not only to the crevicular gingiva but also for the oral gingival tissues. **KENNEDY** (1969, 1974) suggested that a compensatory blood supply to the oral gingiva could be provided via the PDL.

CUTRIGHT and **HUNSUCK** (1970a, 1970b) in examining the oral microvasculature of the *Macaca* rhesus monkey noted that the gingival tissue

received its blood supply mainly from the alveolar mucosa and to a lesser extent from the gingival vessels anastomosing with the PDL plexus and a minor contribution from the alveolar bone.

NOBUTO et al. (1987) looked at the healing of gingival wounds and found that healing was more rapid from the gingival margin. This suggested that a collateral blood supply from the PDL was involved in the initial revascularization although an arterial supply from the palatal tissues via the interproximal col region cannot be ruled out.

The concept of a collateral blood supply to the gingival tissues from the PDL was supported in the current study. Arterioles were seen running deep to the circular plexus to supply the crevicular loops and gingival tissues. Also a large arteriole was followed from below the apical PDL up the mesial PDL wall with branches supplying the crevicular loops, and the labial and lingual gingiva (Figure 45).

LEE (1988) in looking at the posterior regions of the same corrosion casts as the current author did not find collateral vessels coursing between the alveolar mucosa and the labial PDL. This suggests they may be a feature of the anterior region in the primate where different types and amounts of stress loading on the PDL are present compared to the posterior region.

WEEKES (1983) in examining the rat molar vasculature did not find these collateral routes. **WONG** (1983) also did not find these collateral routes between the alveolar mucosa and the PDL when looking at the mouse molar although he did find communication of PDL vessels between adjacent tooth sockets. The current author found vessels joining the PDL of adjacent sockets. Both arterial and venous communication between the mesial PDL of one socket and the distal PDL of the adjacent socket were seen (Figure 49).

B. VESSEL CLASSIFICATION

The classification of blood vessels using the endothelial imprint pattern as described by **HODDE et al.** (1977); **HODDE** (1981); **MIODONSKI et al.** (1981); using the vessel diameters as described by **RHODIN** (1967, 1968); and using the description of arterioles and venules provided by **LEE** (1988) enabled the current author to make a sound estimate regarding the types of blood vessels present. The identification cannot be definitive, however, without an ultrastructural survey being carried out.

The vessel luminal types noted included the following:

1. Arterioles.
2. Terminal Arterioles.
3. True Capillaries.
4. Postcapillary-sized Venules.
5. Collecting-sized Venules.
6. Muscular-sized Venules.
7. Small Collecting-sized Veins.

C. GINGIVAL VASCULATURE

The microvascular morphology of the marmoset's gingiva and PDL in the anterior region have been examined in the current study. The microvascular morphology of the pulpal vessels was also noted in this region, although a detailed description has not been included in this report. Corrosion casts from both the mature and young animals were examined with morphological variations being noted in relation to the circular plexus, the crevicular loops, the vestibular loops, the gingival loops and alveolar mucosal vessels.

i. Circular Plexus Vasculature

The circular plexus encircled the marmoset's anterior tooth sockets as a single vessel at the level of the gingival attachment in both the young and mature animals. **LEE** (1988) noted that for the posterior tooth sockets of the marmoset the circular plexus consisted of one to four rings of capillary vessels that anastomosed frequently with each other throughout the circular ring. He did not differentiate which teeth had which number of vessels and if there was a difference between the young and the mature animals or between the maxilla and mandible.

WONG (1983) in the mouse and **WEEKES** (1983) in the rat noted a similar structure to the circular plexus in the marmoset at the level of the epithelial attachment. Morphological variation occurred between the different species with the rat's circular plexus being composed of a single continuous vessel (**WEEKES** and **SIMS**, 1986b).

Similar structures to the circular plexus were also described by early investigators of the oral vasculature including **KINDLOVA** and **MATENA** (1962) while looking at the rat, **KINDLOVA** (1965) while looking at the *Macacus* rhesus monkey and **CARRANZA et al.** (1966) while looking at a number of animal species including dogs, cats, rats, mice, hampsters and guinea pigs.

The function of the circular plexus is still unclear. **LEE** (1988) suggested that because it had multiple anastomoses with the crevicular loops above and the cervical portion of the PDL below, it could possibly provide a means for rapid redistribution of blood when the tooth was being loaded during mastication. The larger vessels found at a deeper level would also be likely to provide a means for rapid redistribution of blood under loading.

ii. Crevicular Gingival Vasculature

The morphology of the crevicular gingival network around the anterior teeth varied considerably. The crevicular loop structure varied from simple hairpin loops (Figure 14) to loops having a small diameter ascending limb and a thicker postcapillary-sized descending limb (Figure 15). More complex loop arrangements showed what the current author described as a knot-like appearance (Figures 16, 17), to finally the most complex structures which had a bulb-like appearance and resembled renal glomeruli (Figures 19 to 22). An illustration of a complex glomerular-like crevicular loop structure is shown in Figure 52.

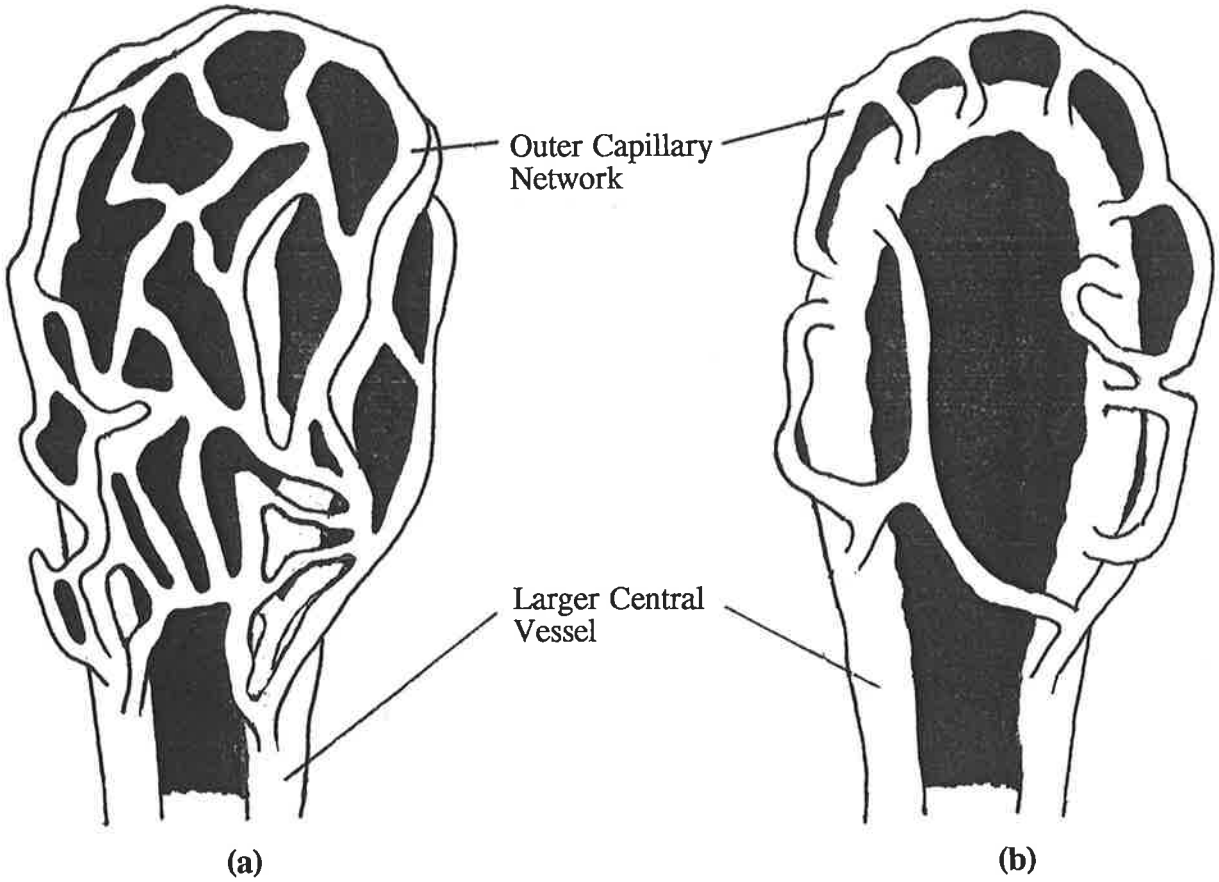

FIGURE 52: SCHEMATIC REPRESENTATION OF A GLOMERULAR-LIKE CREVICULAR LOOP STRUCTURE.

Diagram (a) is an illustration of a glomerular-like crevicular loop structure. The outer capillary network and the start of the larger central vessel have been shown. In diagram (b), the outer capillary network has been removed. The larger central vessel forms a U-shape. Some of the outer capillary network as well as capillaries communicating between the limbs of the larger central vessel have be shown.

The glomerular-like structures have been found in a number of animal species including monkeys (**KINDLOVA**, 1965; **FOLKE** and **STALLARD**, 1967; **WEEKES** and **SIMS**, 1986c; and **LEE**, 1988), rat (**KINDLOVA**, 1967b; **WEEKES**, 1983), mouse (**WONG**, 1983) and dog (**EGELBERG**, 1966; **ICHIKAWA et al.**, 1977). **SIMS et al.** (1988) felt that there was sufficient evidence to suggest that there was both inter-species and intra-species differences in the glomerular-like crevicular loop structures.

Very early descriptions of glomerular-like structures were reported by investigators studying the oral vasculature in man. These included **WEDL** (1881); **SCHWEITZER** (1909); **HAYASHI**, (1932); **PROVENZA et al.** (1960) and **PROVENZA** (1964).

KINDLOVA (1965) looked at the *Macacus* rhesus monkey oral vasculature. She differed from the other researchers by suggesting that these glomerular-like loop structures were apical to the epithelial attachment. She may in fact have been describing the cervical PDL loop structures directly below the circular plexus. These often had a bulb-like appearance (Figure 38).

LEE (1988) suggested that the blood supply to the crevicular gingival vasculature appeared to be mainly from the PDL and surrounding alveolar bone although a route from the labial and lingual gingiva is also suggested by the current author.

The findings from the current study suggested that the complexity of the crevicular loops generally increased over time. The posterior segments appeared to be more resistant to the formation of the more complex loop structures. Variation occurred in the proliferation of the knot-like loop stuctures in the young animals and in the proliferation of knot-like and glomerular-like loop structures in the mature animals. For example, the youngest of the mature animals showed greater

proliferation than the other mature animals. This suggested that other factors (probably environmental) may have had an influence with time.

The formation and proliferation of the glomerular-like crevicular loops may be due to the following reasons:

1. The formation and proliferation of the glomerular-like crevicular loops is thought to be related to the degree of inflammation of the oral gingival tissues (**PROVENZA**, 1960; **KINDLOVA**, 1967b; **HOCK** and **NUKI** 1971 and 1975, **KINDLOVA** and **TRNKOVA**, 1972).

2. SIMS et al. (1988) however noted the presence of these structures in germ free rats that lacked leukocyte infiltration. They suggested the glomerular-like crevicular loops structures are components of normal healthy gingiva.

3. KINDLOVA (1968, 1970) claimed that such vessels develop from the enamel organ.

The function of the glomerular-like crevicular loops is still not clear. The suggested functions include the following:

1. They may act like coil springs absorbing the forces produced during mastication (**WEDL** 1881).

2. They may be capable of regulating blood flow through the PDL as there are numerous arterio-venous anastomoses present in these glomerular-like structures (**GASPARINI**, 1949; **ISHIMITSU**, 1960).

3. In the presence of periodontal disease, they may act as an alternative blood supply to the PDL. The larger glomerular-like vessels may resist being compressed and having the blood flow reduced due to an infiltration of connective tissue (**PROVENZA et al.**, 1960).

4. It has also been suggested by a number of investigators that the crevicular loops consist mainly of exchange vessels (**KINDLOVA** and **MATENA**, 1962; **NUKI** and **HOCK**, 1974; **DE ALMEIDA** and **BOHM**, 1979). They may play a role in the formation of crevicular exudate (**EGELBERG**, 1966; **CIMASONI** 1983).

The current author is unable to confirm or refute any of the suggested functions for these structures. In fact it is more than likely they may have more than one of the above functions. Their formation and increase in complexity is thought

to be a response to inflammation of the gingival tissues. It would be expected that the younger animals would show less gingival inflammation and that the tissues would have been exposed to the inflammatory response for a shorter period of time. The young animal with extensive proliferation of knot-like loop structures may have been more susceptable than the other animals. This animal appeared to have an absence of attached labial gingiva which may have contributed to its susceptability. The other animals in contrast showed varying degrees of the occlusoapically orientated capillary loops which are associated with attached gingiva.

The formation of the more complex glomerular-like crevicular loops may be a response to a chronic inflammatory condition. The location of these glomerular-like crevicular loops in the marmoset would seem to suggest that they form not only because of the presence of an inflamatory response which would also be expected to be present in the posterior segments, but due to other yet to be explained reasons. The canine sockets may be more prone than the incisors to this inflammatory assault and this may be why the more complex glomerular-like crevicular loops are more commonly found associated with these teeth. These canine teeth may be subject to more occlusal stress than the incisors and posterior teeth as the animal chews and tears at its food and other objects (wooden posts) resulting in increased gingival loading and trauma.

LEE (1988) unfortunately did not record the condition of the gingiva around the teeth of the marmosets photographically prior to the animals being sacrificed. This makes the interpretation of the findings more difficult as an association could have been made between the extent of the glomerular-like formations and the gingival condition.

iii. Labial Gingival Vasculature

Distinct differences were seen with the labial gingival microvascular morphology between the young and mature animals and between animals in the same age range. The vestibular gingival network varied from having a network of capillaries at the crest of the socket in a young animal (Figure 26), to having a capillary network orientated in a horizontal direction and in rows in one of the mature animals. The widened horizontal band of loops in this mature animal was displaced down onto the labial gingival surface by the proliferation of knot-like and glomerular-like loops (Figures 24, 25).

LEE (1988) described the vestibular gingival network as being positioned below the gingival margin and having a horizontal orientation. He did not describe the knot-like and glomerular-like loops which extended onto the labial gingival surface in the mature animal. The proliferation of these loops thereby displacing the vestibular gingival network towards the labial gingival sulcus may be a feature of the anterior region.

A distinct gap was seen between the vestibular gingival network and the crevicular gingival network for both the young and mature animals. The clefts seen in the labial gingival mandibular region in Figures 27 and 28 may be an area of fibrous scar tissue which had reduced vascularity. This may have been caused from previous gingival trauma perhaps while chewing or tearing at food or other objects such as the wooden posts in the cages. **WEIR**, 1990 showed a photograph of wooden posts that had been chewed almost through by a marmoset. The clefts may also have been caused by a build up of supragingival calculus or from an infection which has resulted in fibrous scar tissue formation.

Due to the lip vasculature being present in a number of the corrosion casts it was not possible to ascertain whether there was a distinct gap between the vestibular gingival network and the labial gingival capillary network in all of the animals

examined. To dissect these vessels from the corrosion casts may have resulted in damage to the underlying vessels. In the mature animal where the lip vasculature had been dissected away prior to the tissue corrosion phase (Figures 24, 25), a distict gap could be seen between the vestibular gingival network and the labial gingival capillary network which was suggestive of the changing of the gingiva from being free to being attached. No such gap was seen between the vestibular gingival network and the labial gingival capillary network in the younger animal that had the lip vasculature dissected away prior to tissue corrosion (Figure 26).

Both the young and mature animals, where the lip vasculature had been dissected away prior to the tissue corrosion phase, had a labial gingival capillary network with loops having an occluso-apical orientation. These loops were found in the region of the attached gingival tissues. Considerable variation in the quantity of these loops occurred between the different animals and between different sockets in the same animal (Figure 27). One of the younger animals appeared to have a complete absence of these loops which suggested an absence of the attached gingiva (Figure 32).

The occluso-apical orientation of the labial gingival capillary network was also reported for several other animal species, including dog (**KISHI et al.**, 1987b and **NOBUTO et al.**, 1987), and *Macaca* rhesus monkey (**CUTRIGHT** and **HUNSUCK**, 1970a, 1970b). A similar arrangement was seen in man (**MORMANN et al.**, 1979) while carrying out *in vivo* fluorescein angiography studies. **WONG** (1983) and **WEEKES** (1983) did not report on the labial gingival vasculature for the mouse and rat molars respectively.

The presumptive muco-gingival junction and the wide arcades of capillaries of the alveolar mucosa could be seen as the sulcus was approached in both the young and mature animals. The deeper labial vascular network of venules,

capillaries and arterioles ran an occluso-apical course in both the young and the mature animals.

The vascular morphology of the gingival capillary network and that of the alveolar mucosa were similar to that described by **LEE** (1988) in the posterior segments. The vascular morphology at a deeper level was also similar.

D. PERIODONTAL LIGAMENT VASCULATURE

AHARINEJAD et al., 1991 have described the techniques used to examine the PDL vasculature. Out of the techniques described, only the corrosion casting technique in combination with stereopairs provides the opportunity for three-dimensional interpretation of these structures.

Recent developments in using computer-aided three-dimensional reconstruction programmes in combination with serial TEM sections are providing an opportunity to reconstruct objects such as cells, blood vessels and nerves in three-dimensions using computer imaging systems (**HUIJSMANS et al.**, 1986). Technical improvements have made it possible to go from the embedded tissue stage to sectioning, staining, microscopy or electron microscopy to having in hand a complete reconstruction of cells, organelles and microtubules etc. in less than a week.

PARLANGE (1991) in carrying out a TEM stereological analysis of the blood vessels in the PDL of the upper central incisors of the cotton ear marmoset has shown that the venous luminal vascular bed comprised approximately 90% of the total vascular pool. This finding was supported by **CROWE** (1989) who reported a similar finding in the subapical region of the same animals.

PARLANGE (1991) also noted that the total mean luminal blood vessel volume within the mesial PDL was approximately 11%. The larger venous vessels

constituted about 88% of the vascular bed, with postcapillary-sized venules being 47%, and collecting venules 41%. It was noted that postcapillary-sized venules had an internal luminal diameter ranging from 10 to 26 μm, while collecting venules had diameters ranging from 32 to 80 μm. The diameter of these venules was consistent with the diameter of venules observed by the current author for the maxillary anterior teeth. Because the vessel wall was dissolved away using the corrosion casting technique, the current author is unable to confirm whether venules above 50 μm are collecting venules and not muscular venules.

Vessels in the PDL being predominantly venous in nature were also observed by the current author as well as by numerous other researchers including **WONG** (1983) and **FREEZER** (1984) - mouse, **WEEKES** (1983) - rat, **DOUVARTZIDIS** (1984), **LEE** (1988) and **WEIR** (1990) - marmoset.

LEE (1988) in contrast to the findings of **PARLANGE** (1991) and the current author found vessels in the PDL of the posterior segments of the cotton ear marmoset to be composed mainly of occluso-apically orientated postcapillary-sized venules, 20 to 35 μm in diameter. He states that there appeared to be a higher proportion of larger-sized venules in the apical third, compared to the cervical and middle thirds and that these vessels seemed more closely packed there. He did not describe the size of these larger sized venules and it is unclear as to whether venules ranging up to 80 μm in diameter were seen.

The predominantly occluso-apical orientation of the PDL vessels described by **LEE** (1988) for the posterior segments was also seen in the anterior segments by the current author. The increased vascularity, the tighter packing of vessels, as well as the increased communication between vessels in the apical third of the PDL were consistent with both authors. In contrast to this, **AHARINEJAD et al.** (1991) described the PDL vessels in adult rats as having a "ladder-like" pattern and in guinea pig molars as having a "honey-comb" pattern. No mention was made by

these authors as to whether they were describing the PDL of the continuously erupting incisor teeth in the rat or the non-continuously erupting molars (**MOXHAM** and **BERKOVITZ**, 1982). **AHARINEJAD et al.** (1991) also suggested that the vascular architecture in human teeth was similar to that of rabbits. However they did not state whether this was in relation to PDL vessels or pulpal vessels. No references were provided to confirm these claims and again they did not differentiate between the continuously erupting incisor teeth in the rabbit and the non-continuously erupting molars (**MOXHAM**, 1979; **MOXHAM** and **BERKOVITZ**, 1982).

The cervical PDL hairpin loops found just below the level of the circular plexus showed both site and animal variability in the current study (Figures 37, 38). They ranged from being simple hairpin loops with an equal diameter ascending and descending limb (Figure 37) to loops having more than one ascending limb and a thickened descending limb (Figure 38). **LEE** (1988) described cervical PDL loop structures in the posterior segments of the marmoset. He reported that the loops were mainly hairpin shaped and orientated towards the root surface. They had only one ascending and one descending limb which were approximately equal in diameter.

Loop structures in the PDL were also seen in the middle third of the mouse molar PDL (**WONG**, 1983, **WONG** and **SIMS**, 1987) and in the cervical and apical regions of the rat molar PDL (**WEEKES** and **SIMS**, 1986a). **AHARINEJAD et al.** (1990) did not report these loop structures in the PDL of the mandibular molars in the albino guinea pig.

In the anterior region of the marmoset these cervical PDL loop structures were commonly found on the palatal (lingual) side. It is thought by the current author that the orientation of these vessels may resist being occluded during function when the root of the tooth was compressed against the surrounding bone.

They can also stretch when the tooth was displaced labially and may develop as a response to increased occlusal loading. The fact that they were not found in all of the anterior teeth although the castings appeared to be complete, cannot be explained.

Large venules ranging up to 100 μm in diameter, were observed to course down the mesial PDL wall, or in the bone close to the mesial PDL in the mandibular anterior tooth sockets (Figures 35, 46). Only the apical area for the canine sockets of the maxillary anterior teeth were observed in the current study and these large venules were not present with these sockets. As mentioned previously by **GANNON** (1985), the corrosion casting technique often needs to be used in combination with other techniques to accurately locate vessels in relation to the surrounding tissues.

The large venules described in the previous paragraph appeared to converge into a larger venule which then passed through the labial plate of bone to drain into the alveolar mucosa and labial gingival sulcus. **LEE** (1988) did not report these venules in the posterior PDL of the marmoset and they may be peculiar to the anterior region only. Their functional role is unknown although they may provide venous drainage from the surrounding gingival tissues including the interdental papilla. Being located on the mesial side may protect them from being occluded and possibly damaged from labial-lingual tooth movement of the anterior teeth during function. Further study is required to determine whether they were present on the distal PDL wall and whether they were present in the maxillary incisor sockets. Their exact location needs to be determined using other techniques.

The finding of these larger diameter venules coursing down the mesial PDL wall in the mandibular anterior teeth and not on the labial and palatal sides, suggests that PDL vessel size and type may vary around the tooth sockets. Studies which have looked at PDL vessel type and vascular volume from one side of the

tooth only may not necessarily represent the vasculature around the other sides. In fact, many of the studies that have looked at vascular type and volume have looked at the PDL from one side of the sockets only. These have included **FREEZER** (1984), **CROWE** (1989), **WEIR** (1990) and **PARLANGE** (1991).

The pulpal vascular morphology was not recorded by **LEE** (1988) for the posterior region of the marmoset, nor by **WEEKES** (1983) for the rat molar. **WONG** (1983) did provide a diagram which showed pulpal vessels in the apical portion of the mouse molar, although no mention was made regarding a pulpal capillary loop system.

In the current study variation in the arrangement of pulpal vessels both in the pulp canal and below the apical foramen was seen. The vessels in the apical third of the pulp canal appeared to be mainly terminal arterioles although larger diameter postcapillary-sized venules were also seen. Determination was made using endothelial imprints and looking at the branching patterns and morphology of the vessels. Pulpal arterial input however, must equal pulpal venous output. It was interesting to note that the blood vessels were mainly arterial in the pulp and were mainly venous in the PDL. Perhaps the PDL in not being a closed vascular system like that of the pulp, may provide a significant route for venous drainage from the gingival tissues as well as for the PDL itself.

In the middle third of the pulp canal, capillary loops emerged from these arterioles and formed a network in the peripheral part of the pulp canal closest to the dentine layer (Figure 45). These capillaries coursed coronally with many branchings. They appeared to circle back towards the inner core of arterioles and postcapillary-sized venules and drained into these larger venules. There appeared to be an outer network of capillaries and an inner core of larger arterioles and venules. This type of arrangement was followed all the way to the pulp horn.

YOSHIDA et al. (1988) also described this peripheral pulpal capillary layer, while examining the vascular supply of the dental pulp in rat molars using corrosion casts. They found that the terminal capillaries invaded the odontoblast layer and were finally located close to the predentine. The diameter of the capillaries reduced with advancing dentine formation and the capillary network density increased gradually with the invasion of the odontoblast layer. They concluded that the capillaries played a role in dentine formation but they did not indicate how.

KISHI et al. (1989) examined the dental pulp of cats using corrosion casts. They described the vessel morphology in the pulp horn and root canal regions as having circular hairpin capillary loops during the maturation stage. Together with the narrowing of the pulp cavity, these vascular networks changed their structure with only a coarse capillary network remaining. They suggested that the vascular network remodelled during maturation of the tooth.

Another interesting feature in relation to pulpal vessels was their arrangement beneath the apical foramen. Fanning of pulpal vessels was a common finding with intercommunication between pulpal and PDL venules being seen (Figures 40, 42). Drainage of pulpal venules into a collecting-sized venule beneath the apical foramen showed that variation in the arrangement of vessels in this area also occurred (Figures 43, 44). What significance this variation in vessel morphology has can only be speculated upon. Perhaps the vascular response to injury of a tooth will be different depending on what type of vessel arangement is seen in this region. Perhaps the fanning of pulpal vessels beneath the apical foramen provides greater protection when a tooth is intruded during function.

E. THE ULTRACIRCULATION OF THE PDL

The study of the ultracirculation of the PDL and of other tissues is an area of research that has received increased attention recently. A knowledge of this circulatory system is essential in understanding the role of the microvascular system. The ultracirculation of the PDL consists of tissue channels which are found within the ground substance of the ligament.

Tissue channels are composed of a fine, loosely connected and randomly orientated network throughout the water rich sol phase of the ground substance. They form the "ultracirculation of the connective tissues and act as the final distributing vessels. (**CASLEY-SMITH**, 1983).

Tissue channels found in the ground substance of the PDL are believed to form an ultracirculatory extension to the PDL microvascular system. They are thought to form a radial, interweaving lattice-like network extending from the blood vessel wall out into the interstitial tissues (**TANG** and **SIMS**, 1992).

The tissue channels form such an extensive network throughout the PDL that they may in fact return the extravascular fluid back to the blood vessels of the PDL instead of to a lymphatic system (**TANG** and **SIMS**, 1992). This was in agreement with the findings of **BARKER** and **SIMS** (1981) who noted a lack of morphological evidence for the presence of lymphatics in the PDL.

TANG and **SIMS** (1992) while looking at rat molar PDL demonstrated that tissue channels increased markedly with orthodontic tension. They postulated that the mean number of tissue channels in the PDL were not directly related to the blood vessel number and distribution, but reflected the physiological function of the blood vessel segment, and their interactive surface and length densities. Their results suggested that a substantial fluid circulation existed between the microvascular system and the connective tissues via the tissue channel

ultracirculation and that these tissue channels extended from the cervical to apical PDL limits.

6.3 AGE CHANGES

Differences were seen in relation to the vascular morphology of the crevicular loops and vestibular gingival network in both the young and mature animals. The current author was unable to establish if these morphological differences were due to ageing alone or whether environmental influences played a part. Probably a combination of the two factors contributed to these changes.

The current author was unable to determine any differences in the vasculature of the PDL between the young and mature animals. It should be noted that the age difference was not great between the two groups of animals and that differences in vessel morphology may have been more noticeable if old animals were compared with the young animals. Differences may have occurred in the percentages of the various types of vessels present however this was not closely assessed in the current study.

LEE (1988) suggested that the marmoset palatal subepithelial network failed to cast completely in the mature animals because of age changes. He noted no other differences in the oral microvasculature which he thought were due to ageing.

SIMS et al. (1992) in a recent report looked at age changes in the mesial PDL microvascular bed of the mouse. It was reported that with ageing, the total vascular volume increased from 8.5% $\pm$ 1.37 to 19.5% $\pm$ 2.14 *SEM*. The collecting venule volume increased fourfold ($p < 0.001$). Ageing resulted in significant regional shifts in microvascular bed architecture, and a 2.3 times luminal volume increase in the mouse molar PDL. The article is significant because the current view is that the blood supply reduces with ageing (**BRADLEY**, 1972). Arteriosclerotic changes were thought to occur in the vessel wall resulting in

thickening of the vessel wall and a reduction in the lumen diameter (**GRANT** and **BERNICK**, 1970; **LEVY et al.**, 1972b).

6.4 FUTURE RESEARCH

The areas for future research using the corrosion casting technique are large. Corrosion casts can be processed after the teeth have been intruded, extruded, rotated, moved bodily or tipped. Casts can be processed after different force levels have been applied to the teeth. They can also be processed at particular intervals after the teeth have been moved so that changes in the vasculature can be assessed.

Future work needs to be carried out to determine whether the morphological variation described in the current project in relation to the gingival vasculature was due to an ageing process or whether environmental factors such as inflammation or trauma had an influence. The PDL vasculature around all the sides of the tooth socket needs to be evaluated.

A clinical assessment of the gingival condition before the animals are sacrificied as well as photographic recording of the gingival condition may be helpful when the results are analysed. Experimental procedures which cause the gingiva of one or several teeth to become inflammed in various ages of animals may enable more conclusions to be made about the influence of environmental factors.

Modern image systems which have been developed to quantify all types of cast structures may have an application in the assessment of the PDL vasculature. Grey level image analysis, point counting methods, stereophotogrammetry and planimetry all may have an application in the study of the oral vasculature including the PDL (**LAMETSCHWANDTNER et al.**, 1990).

The corrosion casting technique although often giving unpredictable results, is nevertheless invaluable when combined with the use of stereopairs to study the vascular morphology in three-dimensions.

CHAPTER 7

CONCLUSIONS

---

1. Corrosion casts of the cotton ear marmoset's oral microvasculature were used in the current study. These had been previously processed by **LEE** (1988). The surface gingival vascular morphology in the anterior region was initially examined in the SEM and recorded using stereopairs.

2. The palatal vasculature in the anterior region was similar to that described by **LEE** (1988). The palatal vasculature was not present in the mature animals due to incomplete casting. In the young animals simple hairpin capillary loops ran sagittally and formed a canopy over the palatal surface. Variation in height occurred between the rugal crests and troughs. From the maxillary canines, the rugae curved gently to extend into the midline of the palate. For the maxillary lateral incisors, small rugal crests extended from the nasopalatine foramen to the palatal side of the lateral incisors. No rugae were found associated with the maxillary central incisors.

3. The anterior mandibular lingual surface vasculature was also made up of simple hairpin capillary loops which were orientated from the tooth sockets towards the lingual sulcus and tongue. Deep to this canopy was a mainly venous network of postcapillary-sized venules and collecting-sized venules which appeared to drain from the tooth socket region towards the lingual sulcus. No differences were seen in the young and mature animals.

4. The terminology used by **LEE** (1988) to describe the gingival vasculature has been used in the current study. The circular plexus in the canine and incisor region consisted of a single vessel which encircled the tooth socket at the level corresponding to the epithelial attachment. Internal luminal diameter ranged from

10 to 30 μm, although the diameter was usually between 10 to 15 μm. Both arterioles and, more commonly, venules from the cervical PDL communicated with the circular plexus which suggested that blood flow to and from the circular plexus to the cervical PDL occured at different sites around the sockets.

5. Discontinuity of the circular plexus around the tooth sockets occurred with the vessel having either a straight or wavy appearance. Crevicular capillary loops could be seen emerging at the level of the circular plexus around some of the tooth sockets although no clear pattern was recorded.

6. Crevicular vessels were found coronal to the circular plexus. A large degree of animal variability was seen for these vessels. Loop patterns ranged from simple hairpin loop structures with similar diameter ascending and descending limbs which were commonly found in the young animals and on the palatal side of the sockets, to more complex loop structures that had a smaller diameter ascending limb and larger diameter postcapillary-sized venule descending limb.

7. More complex crevicular loop structures which the current author has termed "knot-like" were commonly seen in the mature animals although one of the young animals showed a proliferation of these vascular structures around the sockets and onto the labial gingival surface and interproximal papilla region. These vessels twisted around each other similar to a knot in a rope. They had an ascending and a descending limb that communicated with the limbs other adjacent knot-like crevicular loop structures.

8. A transition from the knot-like crevicular loops to loop structures having a bulb-like appearance resembling "renal glomeruli" appeared to occur. These glomerular-like crevicular loops were found only in the mature animals and were more common in the canine sockets. The initial site of formation was interproximally, either on the mesiolabial or distolabial surface. The loops tended to spread around towards the labial and palatal although they were absent on the palatal side of the

sockets. In the mature animals, knot-like and glomerular-like loops were seen extending over the gingival crest and onto the labial gingival surface. One of the young animals showed knot-like loops extending interproximally and onto the labial gingival surface. The formation of these loops was thought to be due to inflammation.

9. The labial gingival vasculature in the anterior region was also extremely variable. The vestibular gingival network was at the level of the free gingiva. In the young animals a band of capillaries ran around the labial crest of the sockets. In the mature animals showing proliferation of knot-like and glomerular-like loops onto the labial gingival surface, the vestibular gingival loops were arranged in bands which ran horizontally around the labial side below the labial crest of the socket. A distinct gap between the crevicular loops and the vestibular gingival loops could be seen although communication occurred at a deeper level.

10. Apical to the vestibular gingival network, were the labial gingival capillary loops. These ran occluso-apically and were at the level of the attached gingiva. Again considerable animal variability occurred with one of the young animals showing a complete absence of these vessels. This animal also showed extensive proliferation of knot-like crevicular loops around the tooth sockets as well as knot-like loops extending interproximally and onto the labial gingival surface. The attached gingiva may have been absent with this animal.

11. Gingival clefts (depressions) were seen in the lower anterior region at the level of the gingival capillary loops in one of the mature animals. These encircled the labial gingival region around the tooth sockets and extended interproximally. They were found around the labial surface of both the mandibular incisor and canine teeth.

12. Apical to the level of the gingival capillary loops were the alveolar mucosal vessels. The vessels here formed wide arcades which ran horizontally. Capillary

loops were absent in this region. The vascular morphology of these vessels was consistent with that described by **LEE** (1988) for the posterior segments.

13. Crevicular loops from adjoining sockets merged in the col region. The crevicular loops were orientated labio-lingually and a distinct gap between crevicular and col loops could not be seen. Again considerable animal and socket variability was seen depending on the type of crevicular loops present and on the width of the col region.

14. Sectioning of the corrosion casts using a mini-motor and safety razor blades through the tooth sockets has enabled the PDL to be viewed from the cervical third to below the apex. Vessels in the PDL generally had an occluso-apical orientation and intercommunication was frequent. As reported by **LEE** (1988) for the posterior segments, and using **RHODIN's** (1967, 1968) classification for vessel diameter, postcapillary-sized and collecting-sized venules were the most numerous in the cervical and middle thirds of the PDL. Venules with internal luminal diameters ranging from 50 to 100 μm, and which the current author could not classify as being either collecting venules or muscular venules, were also present in the PDL of the anterior sockets. Work by **PARLANGE** (1991) suggested that these larger venules may in fact be collecting venules.

15. The apical third of the PDL was more vascular with venous vessels forming a "basket-like" arrangement around the apex of the socket and with numerous communications being present. Vessel diameters were variable, with the collecting-sized venules being the most common. Numerous arterio-venous and venous-venous anastomoses were present. The arterial vessels supplying the PDL were considerably fewer in number and ran predominantly from the apex towards the cervical third although vessels did emerge from the bone and from the gingiva to supply the cervical third of the PDL.

16. Variability was observed in the cervical third of the PDL. Loop structures showing hairpin bends with one or two ascending limbs and a thickened descending limb were commonly seen in the palatal side of the tooth sockets. In one of the mature animals in the palatal cervical PDL region, large venules, 50 to 80 μm in diameter, were seen running occluso-apically. Smaller postcapillary-sized venules ran along the wall of these larger vessels and eventually drained into them.

17. Pulpal vessels below the apical foramen tended to fan out and ran apically. Direct communication between pulpal venules and PDL venules was observed. No communication was seen between pulpal arterioles and PDL arterioles although this may have occurred at a deeper level to the PDL.

18. Fanning of pulpal vessels below the apical foramen was not seen in all the sockets examined. In one example, a large collecting-sized venule was observed running below the apical foramen. Pulpal, as well as PDL venules could be seen draining into this larger venule which then ran both lingually and to a deeper level below the apical PDL vessels. Pulpal arterioles were seen running up along this collecting-sized venule to supply the pulpal tissues.

19. In the middle third of the pulp canal branching of the pulpal vessels occurred. An outer capillary network was seen with an inner core of larger diameter venules and arterioles being present. The capillaries emerged from the inner core of arterioles, ran outward towards the dentine layer and upwards towards the coronal portion. They curved back and drained into the central core of venules.

20. In the coronal portion of the pulp canal the pulpal capillary network was extensive. Capillaries ran coronally in an outer layer near the dentine and towards the pulp horn. They joined larger venules which ran mainly in the inner core region of the pulp canal and drained apically.

21. An arterial supply to the mandibular labial and lingual gingiva which originated in the apical PDL was observed. In this particular case an arteriole, 40 to 50 μm in diameter, was seen originating from larger vessels below the tooth apex. It ran up the mesial PDL wall and branched on numerous occasions until reaching the cervical third of the PDL. Branches then ran deep to the circular plexus to supply the crevicular loops and labial and lingual gingival tissues.

22. Groups of vessels were seen running between the mandibular labial PDL in the apical region and the labial alveolar mucosa. Studying the endothelial imprint pattern of these vessels and following their progress in the PDL and alveolar mucosa suggested an arterial supply to the mandibular PDL from the labial alveolar mucosa and venous drainage from the mandibular PDL to the labial alveolar mucosa.

23. Large venules, ranging up to 100 μm in diameter were observed to course down the mesial mandibular PDL, or in the bone directly adjacent to the mesial mandibular PDL in the anterior region. At the level between the middle and apical mesial PDL thirds, these venules merged to form a larger venule which appeared to drain through to the alveolar mucosa and labial sulcus. These venules were not seen on the labial and lingual sides. The distal side was not viewed in the current study nor was the apical region of the maxillary incisors. The possible variation in diameter of PDL vessels suggests that vessel type and vascular volume may vary around the tooth socket. Studies which have evaluated vessel type and vascular volume from one side of the tooth socket may not necessarily represent the other sides.

CHAPTER 8

APPENDICES

8.1 CHEMICAL REAGENTS AND SUPPLIERS

1. **DI-SODIUM HYDROGEN PHOSPHATE**
   (Ajax Chemicals, Sydney, N.S.W., Australia).

2. **GLUTARALDEHYDE**
   (Bio-Rad, P.O. Box 33, Hornsby, N.S.W., Australia).

3. **HEPARIN** (Heparin Sodium Injection B.P. Mucous)
   (Glaxo Australia Pty. Ltd., Mountain Highway, Boronia, Victoria, Australia).

4. **HYDROCHLORIC ACID**
   (BDH Chemicals Australia Pty. Ltd., Victoria, Australia).

5. **ILFORD FILM, PRINT DEVELOPER and FIXER**
   (Ilford Ltd., Mobberley, Cheshire, England, U.K.).

6. **MERCOX**
   (Vilene Hospital Ink and Chemical Co. Ltd. Tokyo, Japan).

7. **OSMIUM TETROXIDE**
   (Johnson Metthey Chemicals Ltd., Hertfordshire, England, U.K.).

8. **PANCREATIN**
   (Stansens Scientific and Surgical Divisions, 3 Percy Crt., Adelaide, Australia).

9. **PAPAVERINE HYDROCHLORIDE INJECTION** - 120 mgm./10 ml.
   (David Bull Laboratories Pty. Ltd., Victoria, Australia).

10. **POLYVINYLPYRROLIDONE** M.W. 40,000
    (Polysciences, Inc., Warrington, PA 18976, U.S.A.).

11. **POTASSIUM HYDROXIDE**
    (Analytical and Research Chemical Co., Adelaide, Australia).

12. **SAFFAN ANAESTHETIC INJECTION**
(Glaxovet, Glaxo Australia Pty. Ltd., Mountain Highway, Boronia, Victoria, Australia).

13. **SILVER DAG**
(Acheson Colloids Co., Prince Rock, Plymouth, England, U.K.).

14. **SODIUM CHLORIDE**
(Ajax Chemicals, Sydney, N.S.W., Australia).

15. **SODIUM DIHYDROGEN ORTHOPHOSPHATE**
(Ajax Chemicals, Sydney, N.S.W., Australia).

16. **SODIUM HYPOCHLORITE**
(Ajax Chemicals, Sydney, N.S.W., Australia).

17. **SODIUM NITRITE CRYSTAL**
(J.T. Baker Chemical Co., Phillipsburg, N.J., U.S.A.).

8.2 EQUIPMENT AND MATERIALS

1. **ILFORD FP4, BLACK and WHITE FILM**
(Ilford Ltd., Mobberley, Cheshire, England, U.K.).

2. **ILFORD ILFOSPEED PHOTOGRAPHIC PAPER**
(Ilford Ltd., Mobberley, Cheshire, England, U.K.).

3. **MEMBRA-FIL MEMBRANE FILTER**
(Johns-Manville, Canada).

4. **POLYETHYLENE TUBE, MEDICAL GRADE**
(Dural Plastics and Engineering, Dural, N.S.W., Australia).

	INNER DIAMETER (mm.)	OUTER DIAMETER (mm.)
SP 10	0.28	0.61
SP 45	0.58	0.96
SP 61	0.86	1.27
SP 95	1.20	1.70

5. SILASTIC TUBE, MEDICAL GRADE
(Dow Corning Corporation Medical Products, Midland, Michigan, U.S.A. 48640).

	INNER DIAMETER (mm.)	OUTER DIAMETER (mm.)
602-285	0.062	0.125
601-325	0.104	0.192

6. STEREOVIEWER "GEOSCOPE"
(Instrument Supply Co., 177 Payneham Road, St. Peters, S.A., Australia).

CHAPTER 9

BIBLIOGRAPHY

AHARINEJAD, S., FRANZ, P., FIRBAS, W., and **FAKHARI, M.** 1990.
Mandibular and molar vascularization in guinea pigs.
Anat. Rec. **228**, 471-477.

AHARINEJAD, S., LAMETSCHWANDTNER, A., FRANZ, P., and **FIRBAS, W.** 1991.
The vascularization of the digestive tract studied by scanning electron microscopy with special emphasis on the teeth, esophagus, stomach, small and large intestine, pancreas, and liver.
Scanning Microsc. **5**, 811-849.

ANDERSON, B.G. and **ANDERSON, W.D.** 1978.
Scanning electron microscopy of microcorrosion casts; intracranial and abdominal microvasculature in domestic animals.
Am. J. Anat. **153**, 523-536.

BARKER, J.H. and **SIMS, M.R.** 1981.
Endothelially lined lymphatics in human alveolar bone and periodontal ligament.
J. Dent. Res. **60**, 1074.

BENNETT, H.S., LUFT, J.H. and **HAMPTON, J.C.** 1959.
Morphological classification of vertebrate blood capillaries.
Am. J. Physiol. **196**, 381-390.

BERKOVITZ, B.K.B. 1990.
The structure of the periodontal ligament: an update.
Europ. J. Orthod. **12**, 51-76.

BERNICK, S. 1962.
Age changes in the blood supply to molar teeth of rats.
Anat. Rec. **144**, 265-274.

BEVELANDER, G. and **NAKAHARA, H.** 1968.
The fine structure of the human peridental ligament.
Anat. Rec. **162**, 313-326.

BIRN, H. 1966.
The vascular supply of the periodontal membrane.
J. Periodont. Res. **1**, 51-68.

BOUYSSOU, M., BADER, J., LODTER, P. and **DUFFAUT, M.** 1970.
Les Variations Fontionelles Des Glomi Artero-veineux Du Parodonte.
Actual. Odontostomatol. **92**, 456-477. (Cited by Weekes, 1983).

BOYDE, A. 1973.
Quantative photogrammetric analysis and qualitative stereoscopic analysis of S.E.M. images.
J. Microsc. **98**, 452-472.

BOYER, C.C. and **NEPTUNE, C.M.** 1962.
Patterns of blood supply to teeth and adjacent tissues.
J. Dent. Res. **41**, 158-171.

BRADLEY, J.C. 1972.
Age changes in vascular supply of the mandible.
Brit. Dent. J. **132**, 142-144.

BURTON, G.J., INGRAM, S.C. and **PALMER, M.E.** 1986.
The use of lead methacrylate 2-ethylhexanote to create a radio-opaque resin suitable for microvascular corrosion casting.
J. Microsc. **143**, 313-317.

BURTON, G.J. and **PALMER, M.E.** 1989.
The chorioallantoic capillary plexus of the chicken egg: a microvascular corrosion casting study.
Scanning Microsc. **3**, 549-557.

CARRANZA, F.A., ITOIZ, M.E., CABRINI, R.L. and **DOTTO, C.A.** 1966.
A study of periodontal vascularization in different laboratory animals.
J. Periodont. Res. **1**, 120-128.

CASLEY-SMITH, J.R. 1983.
The structure and functioning of the blood vessels, interstitial tissues and lymphatics. In: Lymphangiography. (eds: Foldi, M. and Casley-Smith J.R.), pp 27-164, F.K. Schattauer Verlag, Stuttgart-New York, .

CASLEY-SMITH, J.R. and **VINCENT, A.H.** 1978.
The quantitative morphology of interstitial tissue channels in tissues of the rat and rabbit.
Tissue and Cell **10**, 571-584.

CASTELLI, W. 1963.
Vascular architecture of the human adult mandible.
J. Dent. Res. **42**, 786-792.

CASTELLI, W. and **DEMPSTER, W.T.** 1965.
The periodontal vasculature and its responses to experimental pressures.
J. Am. Dent. Assoc. **70**, 890-905.

CASTENHOLZ, A. 1983a.
Visualization of periendothelial cells in arterioles and capillaries by scanning electron microscopy of ultrasound treated and plastoid injected brains in rats.
Scan. Electron Microsc., Part **I**, pp 161-170.

CASTENHOLZ, A. 1983b.
The outer surface morphology of blood vessels as revealed in scanning electron microscopy in resin cast, non-corroded tissue specimens.
Scan. Electron Microsc., Part **IV**, pp 1955-1962.

CASTENHOLZ, A. 1986.
Corrosion cast technique applied in lymphatic pathways.
Scan. Electron Microcs., Part **II**, pp 599-605.

CHATFIELD, E.J. 1978.
Introduction to stereo scanning electron microscopy. In: Principles and Techniques of Scanning Electron Microscopy. Biological Applications. (Ed: Hayat M.A.) Chp. **6**, 47-88. Van Nostrand Reinhold Co., New York.

CHRISTOFFERSON, R.H. 1988.
Angiogenesis as induced by trophoblast and cancer cells.
PhD. Thesis, University of Uppsala. pp 81.
(Cited by Lametschwandtner et al., 1990).

CIMASONI, G. 1983.
Gingival vasculature and crevicular fluid. In: Crevicular Fluid Updated, Monographs in Oral Science. (Ed. Myers H.M.) pp. 14-19. S. Karger Basel.

COHEN, L. 1960.
Further studies into the vasculature architecture of the mandible.
J. Dent. Res. **39**, 936-964.

COOK, W.R. and **TOMPSETT, D.H.** 1968.
Anatomical models prepared by corrosion casting.
Med. Biol. Illus. **18**, 183-188.

CROWE, P.R. 1989.
A T.E.M. stereological analysis of the marmoset periodontal ligament following incisor crown fracture, root canal therapy, and orthodontic extrusion.
M.D.S. Thesis, The University of Adelaide.

CUTRIGHT, D.E. and **HUNSUCK, E.E.** 1970a.
Microcirculation of the perioral regions in the *Macaca* rhesus. Part I.
Oral Surg., Oral Med., and Oral Path. **29**, 776-785.

CUTRIGHT, D.E. and **HUNSUCK, E.E.** 1970b.
Microcirculation of the perioral regions in the *Macaca* rhesus. Part II.
Oral Surg., Oral Med., and Oral Path. **29**, 926-934.

DE ALMEIDA, O.P. and **BOHM, G.M.** 1979.
Vascular permeability in the rat gingiva. A model of vessel response in chronic inflammation.
J. Pathol. **127**, 27-34.

DILLY, S.A. 1986.
Microcorrosion casting of the human respiratory acinus.
Scan. Electron Microsc., Part III, pp 1095-1101.

DOUVARTZIDIS, I. 1984.
A morphometric examination of the periodontal ligament vasculature of the marmoset molar.
M.D.S. Thesis, The University of Adelaide.

DUVERNOY, H.M., DELON, S., and **VANNSON, J.L.** 1981.
Cortical blood vessels of the human brain.
Brain Res. Bull. **7**, 519-579.

EGELBERG, J. 1966.
The blood vessels of the dento-gingival junction.
J. Periodont. Res. **1**, 163-179.

FAHRENBACH, W.B., BACON, D.R., MORRISON, J.C. and **VAN-BUSKIRK, E.M.** 1988.
Controlled vascular corrosion casting of the rabbit eye.
J. Electron Microsc. Tech. **10**, 15-26.

FOLKE, L.E.A. and **STALLARD, R.E.** 1967.
Periodontal microcirculation as revealed by plastic microspheres.
J. Periodont. Res. **2**, 53-63.

FORSSLUND, G. 1959.
The structure and function of the capillary system in the gingiva in man.
Acta. Odont. Scand. **17**, Suppl. 26 (Thesis).

FREEMAN, E. and **TEN CATE, A.R.** 1971.
Development of the periodontium. An electron microscopic study.
J. Periodontol. **42**, 387-395.

FREEZER, S.R. 1984.
A study of periodontal ligament mesial to the mouse mandibular first molar.
M.D.S. Thesis, The University of Adelaide.

FRYCZKOWSKI, A.W. 1987.
Vascular casting and scanning electron microscopy in diabetes.
Scanning Microsc. **1**, 811-816.

FRYCZKOWSKI, A.W., GRIMSON, B.S. and **PEIFFER, R.L.** 1985.
Vascular casting and electron microscopy of human ocular vascular abnormalities.
Arch. Ophthalmol. **103**, 118-120.

FRYCZKOWSKI, A.W., SHERMAN, M.D., HODES, B.L. and **SATO, S.E.** 1987.
Vascular casting and scanning electron microscopy in clinicopathologic correlations.
Arch Ophthalmol. **105**, 743-744.

GANNON, B.J. 1978.
Vascular casting. In: Principles and Techniques of Scanning Electron Microscopy. Biological Applications. (Ed. Hayat M.A.) Chp. **6**, 170-193. Van Norstrand Reinhold Co., New York.

GANNON, B.J. 1985.
Vascular Casting Workshop. 10th Congress of the New Zealand Electron Microscope Society.

GARFUNKEL, A. and **SCIAKY, I.** 1971.
Vascularization of the periodontal tissues in the adult laboratory rat.
J. Dent. Res. **50**, 880-887.

GASPARINI, F. 1949.
Sulla presenza di anastomosi arterovenose nel periostio alveolare.
Atti, Soc. Med. Chir. Padova **27**, 87-91.
(Cited by Kindlova, 1965, 1967b).

GATTONE, V.H. and **EVAN, A.P.** 1986.
Quantative renal vascular casting in nephrology research.
Scan. Electron Microsc., Part **I**, pp 253-262.

GATTONE, V.H. and **SALE, R.D.** 1986.
Quantitative vascular casting of the post-ischemic hydronephrotic kidney.
Scan. Electron Microsc., Part **II**, pp 549-556.

GAUDIO, E., PANNARALE, L. and **MARINOZZI, G.** 1985.
An S.E.M. corrosion cast study on pericyte localization and role in microcirculation of skeletal muscle.
Angiology **36**, 458-464.

GAUDIO, E., PANNARALE, L., CARPINO, F. and **MARINOZZI, G.** 1988.
Microcorrosion casting in normal and pathological biliary tree morphology.
Scanning Microsc. **2**, 471-475.

GLAVIND, L. and **LOE, H.** 1967.
Capillary microscopy of the gingiva in pregnant and non-pregnant individuals.
J. Periodont. Res. **2**, 74.

GRANT, D., and **BERNICK, S.** 1970.
Arteriosclerosis in periodontal vessels of aging humans.
J. Periodont. **41**, 170-173

HANAI, H., HANAI, T., OTSUKA, H. and **YAMANAKA, A.** 1975.
The arterial distribution of the lips in the crab-eating monkey by plastic injection method.
Okajimas Folia Anat. Jpn. **52**, 85-102.

HAYASHI, S. 1932.
Untersuchungen uber die arterielle Blutversorgung des Periodontiums.
Deutsche Monatsschrift fur Zahnheilkunde. **50**, 145-192. (Cited by Saunders and Rockert, 1967).

HILL, E.G. and **McKINNEY, W.M.** 1981.
The vascular anatomy and pathology of the head and neck: method of corrosion casting.
Adv. Neurol. **30**, 191-197.

HILL, W.C.O. 1957.
Primates: Comparative Anatomy and Taxonomy.
pp 115-116, University Press, Edinburgh.

HOCK, J. and **NUKI, K.** 1970.
Evidence for the abscence of vascular loops in non-inflamed gingiva.
J. Dent. Res. **49**, Special Issue, pp 200. IADR Abstract No. 607.

HOCK, J. and **NUKI, K.** 1971.
A vital microscopy study of the morphology of normal and inflammed gingiva.
J. Periodont. Res. **6**, 81-88.

HOCK, J. and **NUKI, K.** 1975.
Microvascular response to chronic inflammation in gingiva.
Bibl. Anat. No **13**, 186-187. Karger, Basel.

HODDE, K.C. 1981.
Cephalic vascular patterns in the rat. A scanning electron microscopic (SEM) study of casts.
Doctoral Thesis, University of Amsterdam.

HODDE, K.C. and **NOWELL, J.** 1980.
SEM of micro-corrosion casts.
Scan. Electron Microsc., Part **II**, pp 89-106.

HODDE, K.C., MIODONSKI, A., BAKKER, C. and **VELTMAN, W.A.M.** 1977.
Scanning electron microscopy of microcorrosion casts with special attention on artero-venous differences and application to the rat cochlea.
Scan. Electron Microsc., Part **II**, pp 477-484.

HODDE, F.E., STEEBER, D.A., and **ALBRECHT, R.M.** 1990.
Advances in corrosion casting methods.
Scan. Microsc., **4**, 693-704.

HOSSLER ,F.E., DOUGLAS, J.E. and **DOUGLAS, L.E.** 1986.
Anatomy and morphometry of myocardial capillaries studied with the vascular corrosion casting and scanning electron microscopy: a method for rat heart.
Scan. Electron Microsc., Part **IV**, pp 1469-1475.

HOSSLER, F.E. and **OLSON, K.R.** 1984.
Microvasculature of the avian eye: studies on the eye of the duckling with microcorrosion casting, scanning electron microscopy, and stereology.
Am. J. Anat. **170**, 205-221.

HOSSLER, F.E. and **OLSON, K.R.** 1990.
Microvasculature of the nasal salt gland of the duckling, Anas platyrhynchos: Quantative responses to osmotic adaptation and deadaptation studied with vascular corrosion casting.
J. Exp. Zool. **254**, 237-247.

HOSSLER, F.E. and **WEST, R.F.** 1988.
Venous valve anatomy and morphometry: Studies on the duckling using vascular corrosion casting.
Am. J. Anat. **181**, 425-432.

HOWELL, P.G.T. 1975.
Taking, presenting and treating stereo data from the SEM.
Scan. Electron Microsc., pp 697-704.

HUELKE, D.F. and **CASTELLI, W.A.** 1965.
The blood supply of the rat mandible.
Anat. Rec. **153**, 335-342.

HUIJSMANS, D.P., LAMERS, W.J., LOS, J.A. and **STRACKEE J.** 1986.
Towards computerized morphometric facilities: A review of 58 software packages for computer-aided three-dimensional reconstruction, quantification and picture generation from parallel serial sections.
Anat. Rec. **216**, 449-470.

ICHIKAWA, T., WATANABE, O. and YAMAMURA, T. 1977.
Vascular architecture in oral tissues by vascular casts method for scanning electron microscopy.
Bubl. Anat. **15**, 544-546.

INOKUCHI, T., YOKOYAMA, R., SATOH, H., HAMASAKI, M. and **HIGASHI, R.** 1989.
Scanning electron microscopic study of peri-endothelial cells of the rat cerebral vessels revealed by a combined method of corrosion casting and KOH digestion.
J. Electron Microsc. Tokyo **38**, 201-213.

IRINO, S., ONO, T. and **SHIMOHARA, Y.** 1982.
Microvascular architecture of the rabbit ventricular walls: a scanning electron microscopic study of corrosion casts.
Scan. Electron Microsc. Part **IV**, pp 1785-1792.

ISHIMITSU, K. 1960.
Beitrag zur Kenntnis der Morphologie und Entwick-lungsgeschichte der Glomeruli periodontii.
Yokohama Med. Bull. **11**, 415-432.
(Cited by Schroeder, 1986).

IWAKU, F. and **OZAWA, H.** 1979.
Blood supply of the rat periodontal space during amelogenesis as studied by the injection replica SEM method.
Arch. Histol. Jpn. **42**, 81-88.

JAMES, W.W. 1960.
The jaws and teeth of primates.
Pitman Medical Publishing Co. Ltd., London.

JASINSKI, A. and **MIODONSKI, A.** 1978.
Model of skin vascularization in Rana esculenta L.: scanning electron microscopy of micrcorrosion casts.
Cell Tissue Res. **191**, 539-548.

JASINSKI, A. and **MIODONSKI, A.** 1979.
Light and scanning microscopy of the taste organs and vascularization of the tongue of the spotted salamander, Salamandra salamandra (L.).
Z. Mikrosk. Anat. Forsch. **93**, 780-792.

KAI, K. 1989.
SEM study of vascular architecture of periodontal ligament under chronic marginal periodontitis.
Kanagawa-Shigaku **24**, 273-289.

KAJIHARA, H., NAKAGAMI, K. and **IIJIMA, S.** 1983.
Vascular arrangement of the mammalian spleen as revealed by injection replica scanning electron microscopy.
Hiroshima J. Med. Sci. **32**, 433-442.

KAJIHARA, H., YAMAHARA, M., MALLIWAH, J.A. and **MAEDA, Y.** 1985.
Three-dimensional vascular architecture of the dog heart as revealed by injection replica scanning electron microscopy.
Hiroshima J. Med. Sci. **34**, 165-171.

KAWATO, F. 1989.
Changes of the periodontal vascular network, periodontal fiber and alveolar bone incident to tooth extrusion.
Kanagawa-Shigaku **24**, 117-138.

KENNEDY, J. 1969.
Experimental ischemia in monkeys.
II. Vascular response.
J. Dent. Res. **48**, 888-894.

KENNEDY, J. 1974.
Effects of inflammation in collateral circulation of the gingiva.
J. Periodont. Res. **9**, 147-152.

KIKUTA, A. and **MURAKAMI, T.** 1989.
Three-dimensional vascular architecture of the Malpighi's glomerular capillary beds as studied by vascular corrosion casting-SEM method.
Prog. Clin. Biol. Res. **295**, 181-188.

KINDLOVA, M. 1963.
Blood circulation in pulp and periodontium of rat incisors and molars.
Dental Abstracts **8**, 106.

KINDLOVA, M. 1965.
The blood supply of the marginal periodontium in *Macacus* rhesus.
Archs. Oral Biol. **10**, 869-874.

KINDLOVA, M. 1967a.
Vascular supply of the periodontium in periodontitis.
Int. Dent. J. **17**, 476-489.

KINDLOVA, M. 1967b.
Glomerular vascular structures in the periodontium. In: The Mechanism of Tooth Support. A Symposium. (Eds. - Anderson D.J., Eastoe J.E., Melcher A.H. and Picton D.C.A.) pp 76-79. Wright, Bristol.

KINDLOVA, M. 1968.
Development of vessels in the marginal periodontium in rats.
J. Dent. Res. **47**, 507.

KINDLOVA, M. 1970.
The development of the vascular bed of the marginal periodontium.
J. Periodont. Res. **5**, 135-150.

KINDLOVA, M. and **MATENA, V.** 1959.
Blood circulation in the rodent teeth of the rat.
Acta. Anat. **37**, 163-192.

KINDLOVA, M. and **MATENA, V.** 1962.
Blood vessels of the rat molar.
J. Dent Res. **41**, 650-660.

KINDLOVA, M. and **TRNKOVA, H.** 1972.
The vascular arrangement beneath the sulcular and junctional epithelium in different degrees of cellular infiltration of dog gingiva.
J. Periodont. Res. **7**, 323-327.

KISHI, Y. and **TAKAHASHI, K.** 1977.
A scanning electron microscope study of the vascular architecture of the periodontal membrane.
(In Japanese). Jpn. J. Oral Biol. **19**, 192-207.
(Cited by Weekes, 1983).

KISHI, Y., WANG, T., SO, S., YOSHIZAKI, E. and **TAKAHASHI, K.** 1986.
A scanning electron microscope study of the capillary loops of oral epithelial papillae using corrosive resin casts. Part I. Gingiva, alveolar mucosa, buccal mucosa.
Jpn. J. Oral Biol. **28**, 247-252.

KISHI, Y., SHIMOZATO, N., and **TAKAHASHI, K.** 1989.
Vasculature architecture of cat pulp using corrosive resin cast under scanning electron microscope.
J. Endodont. **15**, 478-483.

KONERDING, M.A., STEINBERG, F. and **STREFFER, C.** 1989.
The vasculature of xenotransplanted human melanomas and sarcomas on nude mice. I. Vascular corrosion casting studies.
Acta Anat. Basel **136**, 21-26.

KRATKY, R.G. and **ROACH, M.R.** 1984.
Shrinkage of Batson's and its relevance to vascular casting.
Atherosclerosis **51**, 339-341.

KRATKY, R.G., ZEINDLER, C.M., LO, D.K. and **ROACH, M.R.** 1989.
Quantitative measurement from vascular casts.
Scanning Microsc. **3**, 937-942.

KUS, J., MIODONSKI, A., OLSZEWSKI, E. and **TYRANKIEWICZ, R.** 1981.
Morphology of arteries, veins, and capillaries in cancer of the larynx: scanning electron-microscopical study on microcorrosion casts.
J. Cancer Res. Clin. Oncol. **100**, 271-283.

LAHSTEINER, F., LAMETSCHWANDTNER, A., PATZNER, R.A. and **ADAM, H.** 1988.
Vascularization of male gonads in Blennius pavo (Teleostei, Blenniidae) as revealed by scanning electron microscopy of vascular corrosion casts.
Scanning Microsc. **2**, 2077-2086.

LAMETSCHWANDTNER, A., LAMETSCHWANDTNER, V. and **WEIGER, T.** 1984.
Scanning electron microscopy of vascular corrosion casts - technique and applications.
Scan. Electron Microsc. Part **II**, pp 663-695.

LAMETSCHWANDTNER, A., LAMETSCHWANDTNER, V. and **WEIGER, T.** 1990.
Scanning electron microscopy of vascular corrosion casts - technique and applications: Updated Review.
Scan. Electron Microsc. Part **IV**, pp 889-941.

LAMETSCHWANDTNER, A., MIDONSKI, A. and **SIMONBERGER, P.** 1980.
On the prevention of specimen charging in scanning electron microscopy of vascular corrosion casts by attaching conductive bridges.
Mikroskopie **36**, 270-273.

LEE, D. 1988.
S.E.M. study of the marmoset palate and periodontium microvasculature.
M.D.S. Thesis, The University of Adelaide.

LEE, D., SIMS, M.R., SAMPSON, W.J. and **DRYER, C.W.** 1990.
Stereo-pair three-dimensional imaging of microvascular architecture in primate dental tissues.
Aust. Orthod. J. **11**, 251-255.

LEE, D., SIMS, M.R., DRYER, C.W. and **SAMPSON, W.J.** 1991.
A scanning electron microscope study of microcorrosion casts of the microvasculature of the marmoset palate, gingiva and periodontal ligament.
Archs oral Biol. **36**, 211-220.

LEISER, R., LUCKHARDT, M., KAUFMANN, P., WINTERHAGER, E., and **BRUNS, U.** 1985.
The fetal vascularisation of term human plancental villi.
Anat. Embryol. **173**, 71-80.

LEISER, R., DANTZER, V. and **KAUFMANN, P.** 1989.
Combined microcorrosion casts of maternal and fetal placental vasculature. A new method of characterizing different placental types.
Prog. Clin. Bilo. Res. **296**, 421-433.

LENZ, P. 1968.
Zur Gefasstruktur des Parodontiums.
Dtsch. zahnaerztl. Z. **23**, 357-361.
(Cited by Edwall, 1982).

LEVY, B.M. 1971.
The nonhuman primate as an analogue for the study of periodontal disease.
J. Dent. Res. Suppl. No. 2, **50**, 246-253.

LEVY, B.M., DREIZEN, S. and **BERNICK, S.** 1972a.
The Marmoset Periodontium in Health and Disease. In: Monographs on Oral Science. (Ed. Myers H.M.), Vol **1**, S. Karger, Basel.

LEVY, B.M., DREIZEN, S. and **BERNICK, S.** 1972b.
Effect of aging on the marmoset periodontium.
J. Oral Pathol. **1**, 61-65.

LEVY, B.M., DREIZEN, S., BERNICK, S. and **GRANT, D.** 1970.
Comparative study of the periodontium of aged marmosets and humans.
J. Dent. Res. **49**, 199. Special Issue, IADR abstract No. 604.

LOW, F.N., OLSON, G.E., PERSKY, B. and **VAN RYBROEK, J.J.** 1981.
Technical aspects of stereoprojection for electron microscopy. In: Three Dimensional Microanatomy of Cells and Tissue Surfaces. pp 1-20. (Eds. Allen D.J., Motta P.M. and DiDio L.J.A.) Proceedings of the Synposium on Three Dimensional Microanatomy held in Mexico City, Mexico, August 17-23, 1980. Elsevier/North-Holland, New York.

MACPHEE, P.J., SCHMIDT, E.E., KEOWN, P.A. and **GROOM, A.C.** 1988.
Microcirculatory changes in livers of mice infected with murine hepatitis virus. Evidence from microcorrosion casts and measurements of red cell velocity.
Microvasc. Res. **36**, 140-149.

MIODONSKI, A. and **JASINSKI, A.** 1979.
Scanning electron microscopy of microcorrosion casts of the vascular bed in the skin of the spotted salamandra, Salamandra salamandra L.
Cell Tissue Res. **196**, 153-162.

MIODONSKI, A., KUS, J. and **TYRANKIEWICZ, R.** 1981.
SEM Blood Vessel Cast Analysis. In: Three Dimensional Microanatomy of Cells and Tissue Surfaces. pp 71-87. (Eds. Allen D.J., Motta P.M. and DiDio L.J.A.) Proceedings of the Synposium on Three Dimensional Microanatomy held in Mexico City, Mexico, August 17-23, 1980. Elsevier/North-Holland, New York.

MORMANN, W., MEIER, C. and **FIRESTONE A.** 1979.
Gingival blood circulation after experimental wounds in man.
J. Clin. Period. **6**, 417-424.

MOTTI, E.D.F., IMHOF, H.G., GARZA, J.M. and **YASARGIL, G.M.** 1987.
Vasoplastic phenomena on the luminal replica of rat brain vessels.
Scanning Microsc. **1**, 207-222.

MOTTI, E.D.F., IMHOF, H.G., JANZER, R.C., MARQUARDT, K. and **YASARGIL, G.M.** 1986.
The capillary bed in the choroid plexus of the lateral ventricles: a study of luminal casts.
Scan. Electron Microsc. Part **IV**, pp 1501-1513.

MOXHAM, B.J. 1979.
Recording the eruption of the rabbit incisor using a device for continuously monitoring tooth movements.
Archs oral Biol. **24**, 889-899.

MOXHAM, B.J. and **BERKOVITZ, B.K.B.** 1982.
The periodontal ligament and physiological tooth movements. In: The Periodontal Ligament in Health and Disease. (Eds. - Berkovitz B.K.B., Moxham B.J. and Newman H.N.). Chp **10**, pp 221-225. Pergamon Press, London.

MURAKAMI, T. 1971.
Application of the scanning electron microscope to the study of the fine distribution of the blood vessels.
Arch. Histol. Jpn. **32**, 445-454.

MURAKAMI, T. 1972.
Vascular arrangement of the rat renal glomerulus. A scanning electron microscope study of corrosion casts.
Arch. Histol. Jpn. **34**, 87-107.

MURAKAMI, T. 1975.
Pliable methacrylate casts of blood vessels: Use in scanning electron microscope study of the micro-circulation in the rat hypophysis.
Arch. Histol. Jpn. **38**, 151-168.

MURAKAMI, T. 1976.
Double afferent arterioles of the rat renal glomerulus as studied by the injection replica scanning electron microscopic method.
Arch. Histol. Jpn. **39**, 327-332.

MURAKAMI, T., ITOSHIMA, T. and **SHIMADA, Y.** 1974.
Peribiliary portal system in the monkey liver as evidenced by the injection replica scanning electron microscope method.
Arch. Histol. Jpn. **37**, 245-260.

MURAKAMI, T., UNEHIRA, M., KAWAKAMI, H. and **KUBOTSU, A.** 1973.
Osmium impregnation of methyl methacrylate vascular casts for scanning electron microscopy.
Arch. Histol. Jpn. **36**, 119-124.

NAKAMURA, M.T. 1985.
Scanning electron microscopic observations of vascular system of rat molar periodontium.
J. Jpn. Orthodont. Soc. **44**, 251-276. (In Japanese).

NAKAMURA, M.T., KIYOMURA, H., NAKAMURA, T.K. and **HANAI, H.** 1983.
Scanning electron microscopy of vascular system of rat molar periodontium.
J. Dent. Res. Vol **62**. Special Issue, pp 651, Abstract No. 16.

NAKAMURA M.T., NAKAMURA, T.K., YOSHIKAWA, M., KANEMATSU, J. and **KIYOMURA, H.** 1987.
Scanning electron microscopic study of rat molar periodontium.
Microcirculation **2**, 133-135.

NELSON, A.C. 1987.
Study of rat lung alveoli using corrosion casting and freeze fracture methods coupled with digital image analysis.
Scanning Microsc. **1**, 817-822.

NERANTZIS, C., ANTONAKIS, E. and **AVGOUSTAKIS, D.** 1978.
A new corrosion casting technique.
Anat. Rec. **191**, 321-325.

NOBUTO, T., TOKIOKA, T., IMAI, H., SUWA, F., OHTA, Y., and **YAMAOKA, A.** 1987.
Microvascularization of gingival wound healing using corrosion casts.
J. Periodontol. **58**, 240-246.

NOBUTO, T., TANDA, H., and **YANAGIHARA, K.** 1989a.
The relationship between connective tissue and its microvasculature in the healthy dog gingiva.
J. Periodont. Res. **29**, 45-53.

NOBUTO, T., YANAGIHARA, K., TERANISHI, Y., MINAMIBAYASHI, S., IMAI, H., and **YAMAOKA, A.** 1989b.
Periosteal microvasculature in the dog alveolar process.
J. Periodont. **60**, 709-715.

NOPANITAYA, W., AGHAJANIAN, J.G. and **GRAY, L.D.** 1979.
An improved plastic mixture for corrosion casting of the gastrointestinal microvascular system.
Scan. Electron Microsc. Part **III**, pp 751-755.

NOWELL, J.A. and **LOHSE, C.L.** 1974.
Injection replication of the microvasculature for SEM.
Scan. Electron Microsc. Part **I**, pp 267-274.

NOWELL, J.A. and **TYLER, W.S.** 1974.
SEM of LM-oriented injection replicas.
8th Int. Congr. El. Microsc., Canberra, pp 152-153.
(Cited by Hodde and Nowell, 1980).

NOWELL, J.A., PANGBORN, J. and **TYLER, W.S.** 1970.
SEM of the avian lung.
Scan. Electron Microsc., pp 249-256.

NUKI, K. and **HOCK, J.** 1974.
The organization of the gingival vasculature.
J. Periodontol. Res. **9**, 305-313.

OHASHI, Y., KITA, S. and **MURAKAMI, T.** 1976.
Microcirculation of the rat small intestine as studied by the injection replica scanning electron microscope method.
Arch. Histol. Jpn. **39**, 271-282.

OHTANI, O. and **MURAKAMI, T.** 1978.
Peribiliary portal system in the rat liver as studied by the injection replica scanning electron microscope method. In: Scanning Electron Microscopy. (Eds. Becker R.P., Johari O.) AMF O'Hare, I11., Scanning Electron Microscopy, Inc. Chp **20**, 241-244.

OHTANI, O. 1983.
Microcirculation of the pancreas: a correlative study of intravital microscopy with scanning electron microscopy of vascular corrosion casts.
Arch. Histol. Jpn. **46**, 315-325.

OHTANI, O., KIKUTA, A., OHTSUKA, A., TAGUCHI, T. and **MURAKAMI, T.** 1983.
Microvasculature as studied by the microvascular corrosion casting/scanning electron microscope method. I. Endocrine and digestive system.
Arch. Histol. Jpn. **46**, 1-42.

OLSON, K.R. 1980.
Application of corrosion casting procedures in identification of perfusion distribution in a complex microvasculature.
Scan. Electron Microsc., Part **III**, pp 357-364, 372.

OLSON, K.R., FLINT, K.B. and **BUDDE, R.B.** 1981.
Vascular corrosion replicas of chemo-baroreceptors in fish: the carotid labyrinth in Ictaluridae and Clariidae.
Cell Tissue Res. **219**, 535-541.

PARLANGE, L.M. 1991.
A TEM stereological analysis of blood vessels and nerves in marmoset periodontal ligament following orthodontic extrusion.
M.D.S. Thesis, The University of Adelaide.

PANNARALE, L., GAUDIO, E., and **MARINOZZI, G.** 1986.
Microcorrosion casts in the microcirculation of skeletal muscle.
Scan. Electron Microsc., Part **III**, pp 1103-1108.

PHILLIPS, I.R. and **GRIST, S.M.** 1975.
Clinical use of CT 1341 anaesthetic alphaxalone acetate in marmosets. (Callithrix jacchus).
Lab. Anim. **9**, 57-60.

PROVENZA, D.V. 1964.
Oral Histology. Inheritance and Development.
J.B. Lippincott Company, Philadelphia, pp 338-341.

PROVENZA, D.V., BIDDEX, J.C. and **CHENG, T.C.** 1960.
Studies on the etiology of periodontosis. II. Glomera as vascular components in the periodontal membrane.
Oral Surg., Oral Med., and Oral Path. **13**, 157-164.

REISS, G. and **REALE, E.** 1989.
Osmium impregnation and micromanipulation. Their association in studies using secondary backscattered electrons.
Prog. in Clinical and Biol. Res. **295**, 563-570.

RHODIN, J.A.G. 1967.
The ultrastructure of mammalian arterioles and precapillary sphincters.
J. Ultrastruct. Res. **18**, 181-223.

RHODIN, J.A.G. 1968.
Ultrastructure of mammalian venous capillaries, venules and small collecting veins.
J. Ultrastruct. Res. **25**, 452-500.

RHODIN, J.A.G. 1973.
Dimensions and geometry of the microcirculation: Introductory remarks.
Microvasc. Res. **5**, 313-315.

ROGERS, P.A. and **GANNON, B.J.** 1983.
The microvascular cast as a three-dimensional tissue skeleton: visualization of rapid morphological changes in tissues of the rat uterus.
J.Microsc. **131**, 241-247.

SAUNDERS, R.L. de C.H. 1967.
Microangiographic studies of periodontic and dental pulp vessels in monkey and man.
Can. Dent. Assoc. J., **33**, 245-252.

SAUNDERS, R.L. de C.H. and **ROCKERT, H.O.E.** 1967.
Vascular supply of dental tissues, including lymphatics. In: Structural and Chemical Organization of Teeth. Vol. 1, Chp. 5, pp 199-245.
(Ed. Miles A.E.W.), Academic Press, N.Y.

SCHENKMAN, D.I., BERMAN, D.T. and **ALBRECHT, R.M.** 1985.
Use of polymer casts or metal particle infusion of ducts to study antigen uptake in the guinea pig mammary gland.
Scan. Electron Microsc., Part III, pp 1209-1214.

SCHMIDT, E.E., MACDONALD, I.C. and **GROOM, A.C.** 1982.
Direct arteriovenous connections and the intermediate circulation in dog spleen, studied by scanning electron microscopy of microcorrosion casts.
Cell Tissue Res. **225**, 543-555.

SCHMIDT, E.E., MACDONALD, I.C. and **GROOM, A.C.** 1983a.
Luminal morphology of small arterial vessels in the contracted spleen, studied by scanning electron microscopy of microcorrosion casts.
Cell Tissue Res. **228**, 33-41.

SCHMIDT, E.E., MACDONALD, I.C. and **GROOM, A.C.** 1983b.
Circulatory pathways in the sinusal spleen of the dog, studied by scanning electron microscopy of microcorrosion casts.
J. Morphol. **178**, 111-123.

SCHMIDT, E.E., MACDONALD, I.C. and **GROOM, A.C.** 1983c.
The intermediate circulation in the nonsinusal spleen of the cat, studied by scanning electron microscopy of microcorrosion casts.
J. Morphol. **178**, 125-138.

SCHMIDT, E.E., MACDONALD, I.C. and **GROOM, A.C.** 1988.
Microcirculatory pathways in normal human spleen, demonstrated by scanning electron microscopy of corrosion casts.
Am. J. Anat. **181**, 253-266.

SCHOUR, I. and **MASSLER, M.** 1971.
The teeth. In: The rat in laboratory investigation. (eds. - Farris E.J. and Griffith J.Q.) Chp **6**, 104-160.
Hafner Publishing Company, New York.

SCHRAUFNAGEL, D.E. 1987.
Microvascular corrosion casting of the lung. A state-of-the-art review.
Scanning microsc. **1**, 1733-1747.

SCHRAUFNAGEL, D.E. and **SCHMID, A.** 1988a.
Microvascular casting of the lung: effects of various fixation protocols.
J. Electron Microsc. Tech. **8**, 185-191.

SCHRAUFNAGEL, D.E. and **SCHMID, A.** 1988b.
Microvascular casting of the lung: vascular lavage.
Scanning Microsc. **2**, 1017-1020.

SCHROEDER, H.E. 1986.
The Periodontium. Handbook of Microscopic Anatomy.
Vol. V/5, Springer-Verlag, Berlin.

SCHWIETZER, G. 1909.
Uber die Lymphgefasse des Zahnfleisches und der Zahne bei Menschen und bei Saugetieren. IV. Feinerer Bau bei Saugetieren, nebst Beitragen zur Kenntnis der feineren Blutgefassverteilung in der Zahnpulpa und Zahnwurzelhaut.
Arch. mikr Anat., **74**, 927-999.
(Cited by Kindlova, 1965).

SCHENKMAN, D.I., BERMAN, D.T., ALBRECHT, R.M. 1985.
Use of polymer casts or metal particle infusion of ducts to study antigen uptake in the Guinea pig mammary gland.
Scan. Electron Microsc. Part **III**, pp 1209-1214.
(Cited by Lametschwandtner et al. 1990).

SEYNK, J., MALM, A. and **OHLSSON, M.E.** 1971.
Comparison of coronary angiography and vascular corrosion casts in evaluation of the results of myocardial revascularization.
Vasc. Surg. **5**, 88-93.

SHAW, J.H. and **AUSKAPS, A.M.** 1954.
Studies on the dentition of the marmoset.
Oral Surg., Oral Med., and Oral Path. **7**, 671-677.

SIMIONESCU, M. and **SIMIONESCU, N.** 1984.
Ultrastructure of the microvascular wall: functional correlations. In: Handbook of Physiology. (ed. Renkin E.M. and Michael C.C.) Vol. **IV**, pp 41-100. American Physiological Society, Bethesda, Maryland.

SIMS, M.R., SAMPSON, W.J., LEPPARD, P.I. and **DREYER, C.W.** 1992.
Ageing changes in the periodontal ligament microvascular bed - luminal volumes.
I.A.D.R., Australian and New Zealand Division, 32nd Annual Meeting, Adelaide. 28th-30th Sept. 1992.

SIMS, M.R., SAMPSON, W.J. and **FUSS, J.M.** 1988.
Glomeruli in the molar gingival microvascular bed of germ-free rats.
J. Periodont. Res., **23**, 248-251.

SOBIN, S.S. and **TREMER, H.M.** 1980.
Methods for the determination of three-dimensional microvascular geometry. In: Microcirculation. Vol III, Chap. **15**, pp 303-310. (Eds. Kaley G. and Altura B.M.). University Park Press, Baltimore.

STEINHARDT, G. 1935.
Die Gefassversongung des gesunden, kranken und zahnlosen Kiefer.
Dtsch. Zahn-, Mund- u., Kieferheilkd. **2**, 265-339.
(Cited by Schroeder, 1986).

STEWART, L., PELLEGRINI, C.A. and **WAY, L.W.** 1988.
Chlorangiovenous reflux pathways as defined by corrosion casting and scanning electron microscopy.
Am. J. Surg. **155**, 23-28.

TAKEMORI, K., OKAMURA, H., KANZAKI, H., KOSHIDA, M. and **KONISHI, I.** 1984.
Scanning electron microscopy study on corrosion cast of rat uterine vasculature during the first half of pregnancy.
J. Anat. **138**, 163-173.

TANG, M.P.F. and **SIMS, M.R.** 1992.
A TEM analysis of tissue channels in normal and orthodontically tensioned rat molar periodontal ligament.
Europ. J. Orthod. **14**, 433-444.

TOMPSETT, D.H. 1976.
New polyester resins for corrosion casting and block embedding.
Ann. R. Coll. Surg. Engl. **58**, 243-244.

TORISU, H. 1989.
Changes of periodontal vasculature and alveolar bone on the occlusal trauma.
Kanagawa-Shigaku **24**, 358-383.

VAN-BUSKIRK, E.M., BACON, D.R. and **FAHRENBACH, W.F.** 1990.
Replication of ciliary vasomotor effects with controlled intravascular corrosion casting.
Trans. Am. Ophthalmol. Soc. **87**, 125-140.

WEDL, C. 1881.
Ueber Gefassknauel im Zahnperiost.
Virchows. Arch. Pathol. Anat., **84**, 175-177.
(Cited by Kindlova, 1965).

WEEKES, W.T. 1983.
Vascular morphology of rat molar periodontium.
M.D.S. Thesis, The University of Adelaide.

WEEKES, W.T. and **SIMS, M.R.** 1986a.
The vasculature of the rat molar periodontal ligament.
J. Periodont. Res., **21**, 186-194.

WEEKES, W.T. and **SIMS, M.R.** 1986b.
The vasculature of the rat molar gingival crevice.
J. Periodont. Res., **21**, 177-185.

WEEKES, W.T. and **SIMS, M.R.** 1986c.
Gingival vascular architecture of the common marmoset (Callithrix jacchus).
J. Dent. Res., **65**, 755. Abstract No. 267.

WEIDEMAN, M.P. 1984.
Architecture. In: Handbook of Physiology.(Volume editors: E.M. Renkin and C.C. Michel) Section 2: The Cardiovascular System.Volume IV, Microcirculation., Part **I**, Chp. 2, pp 11-40. Am. Physiol. Soc., Bethesda, Maryland.

WEIGER, T., LAMETSCHWANDTNER, A. and **STOCKMAYER, P.** 1986.
Technical parameters of plastics (Mercox CL-2B and various methylmethacrylates) used in scanning electron microscopy of vascular corrosion casts.
Scan. Electron Microsc., Part **I**, pp 243-252.

WEIR, A.P. 1990.
The marmoset periodontal ligament: A T.E.M. analysis following incisor crown fracture, endodontic therapy, orthodontic extrusion and long term retention. Morphometric and stereological data.
M.D.S. Thesis, The University of Adelaide.

WERGIN, W.P. and **PAWLEY, J.B.** 1980.
Recording and projecting stereo pairs of scanning electron micrographs.
Scan. Electron Microsc., Part **I**, pp 239-249.

WILSON, N.H.F. and **GARDNER, D.L.** 1982.
The postnatal development of the temporomandibular joint of the common marmoset (Callithrix jacchus).
J. Med. Primatol., **11**, 303-311.

WONG, R.S.T. 1983.
Vascular morphology of the mouse molar periodontium.
M.D.S. Thesis, The University of Adelaide.

WONG, R.S.T. and **SIMS, M.R.** 1987.
A scanning electron microscopic, stereo-pair study of methacrylate corrosion casts of the mouse palatal and molar periodontal microvasculature.
Archs. Oral Biol., **32**, 557-566.

YAMAMOTO, I., YANAGAWA, T. and **ARAI, A.** 1974.
On the nutrient arterial branches of the mandibular ramus in the dog by the plastic injection method.
Okajimas Folia Anat. Jpn. **50**, 377-392.

YOSHIDA, S., OHSHIMA, H., DOMON T., and **WAKITA, M.** 1986.
Microdissection of methylmethacrylate vascular casts in the scanning electron microscope.
J. Electron Microsc. **35**, 276-279.

YOSHIDA, S., OHSHIMA, H. and **KOBAYASHI, S.** 1988.
Development of the vascular supply in the dental pulp of rat molars - scanning electron microscope study of microcorrosion casts.
Okajimas Folia Anat. Jpn. **65**, 267-281.

YOSHIDA, S., OHSHIMA, H. and **KOBAYASHI, S.** 1989.
Vascularization of the enamel organ in developing molar teeth of rats: scanning electron microscope study of corrosion casts.
Okajimas Folia Anat. Jpn. **66**, 99-111.